MARINE PROPELLER DESIGN, TESTS AND MANUFACTURE

THOMAS HOFMANN

ISBN 0-315-82613-4

Marine Propeller Design,

Tests and Manufacture

by

©Thomas Hofmann, B.Eng.

A Thesis Submitted to the School of Graduate Studies

in Partial Fulfillment of the Requirements for the Degree of

Master of Engineering

Faculty of Engineering and Applied Science

Memorial University of Newfoundland

October 1991

St. John's, Newfoundland, Canada

Abstract

This thesis presents three aspects of marine propeller technology. 1) the theoretical design of small propellers; 2) some aspects of manufacturing, in particular, propeller casting; and 3) tests on full scale vessels. Although this work was done in the context of small fishing vessels, most of it is applicable to ships' propellers in general.

Two lifting line theory propeller design programs were written and tested. Their usefulness was demonstrated by using test cases which involved real vessels and experimental test results. Through development of lifting surface corrections, results can be produced, from the lifting line theory which closely approximate experimental test data; also, propellers for specific vessels have been designed using the new programs. The lifting line methods for propeller design, as used here, are useful methods for designing propellers for small vessels for which few propulsive or resistive data are available and for preliminary design of other subcavitating propellers.

A 1/5 scale model of the vessel *"MV SUGAR"* was constructed to do a set of model tests: resistance tests; open water propeller and self propulsion tests; and hot film anemometer wake measurements. Although the model was designed and constructed by the author, the tank testing was done by a visiting post-doctoral

fellow, Dr. Shukai Wu. The testing program was done to determine the propulsion and resistance data required for lifting line propeller design and to compare model and full scale results. A graph of the Taylor wake fraction and thrust deduction fraction as measured from the model are given in the appendix. Complete test results are given in the reference.

Sea trials were performed to determine vessel propulsive performance of the *"MV SUGAR"* and the *MV BECKY A.* by using a purpose designed and instrumented propeller stub shaft. Results from both full scale trials were analysed. These tests confirm previous claims of very poor propulsive efficiency for these vessels.

A method for commercially producing a propeller casting was developed. This method did not require the use of a solid pattern to produce the mould. A strickle gear was designed and built to construct propeller moulds for propellers up to 24 inches in diameter. An expert system was developed to ensure that casting quality could be maintained through information access on mould design. The system was tested by producing a prototype propeller mould and casting for a model propeller.

Acknowledgements

The author thanks Dr. Neil Bose for his support and guidance throughout the project; Chester J. McPherson, President of Avalon Propulsion Systems Ltd. for making available shop facilities and time for the construction of the model and testing of the strickle gear; Mr. Max Clarke for volunteering his vessel, *MV SUGAR*, for testing as one of the case-study vessels at no charge and spending hours at sea operating the vessel while testing was ongoing; Mr. Ron Alcock, the owner of the *MV BECKY A.*; Dr. Shukai Wu for performing the model tests on the *MV SUGAR*; Dr. Awad Hanna for his enthusiasm on the application of expert systems to foundry practice; and the personnel at the Memorial University Centre for Computer Aided Engineering for the many runs to the printer for computer output; Prof.J.E. Kerwin of the Massachessets Institute of Technology, for making available at a substantially reduced cost, the lifting surface propeller design and analysis software MIT-PBD10 and MIT-PSF-2 for research purposes. Finally, the author would like to thank the following for their support of the project: the Canadian Centre for Fisheries Innovation and Seabright Corp. ; National Research Council of Canada (Institute for Marine Dynamics); Natural Sciences and Engineering Research Council; and Faculty of Engineering and Applied Sciences and Technical Services, Memorial University of Newfoundland.

Contents

List of Figures

List of Tables

List of symbols

Chapter 2	
Γ	circulation
$\bar{\Gamma} = \frac{d\Gamma}{dr} dr$	circulation differential of a vortex line
R	propeller radius
r	blade section radius
v	relative inflow velocity
ω	rotational velocity
w^*	resultant induced velocity
w_a, w_t, w_r	axial, tangential and radial induced velocity components
g, NB	number of propeller blades
β_i	hydrodynamic pitch angle
(z, ψ, r)	cylindrical coordinates
ϕ_i, ϕ_e	internal and external velocity potentials
i_a, i_t	axial and tangential induction factors
$I_n^{t,a}$	tangential or axial induction factor Fourier coefficients
G	non-dimensional circulation
P	propeller pitch
D	propeller diamater
C_p	power coefficient
C_t	thrust coefficient
η	propeller efficiency
T	propeller thrust
$w(x)$	local wake fraction
$t(x)$	local thrust deduction fraction
β	advance angle
C_l	lift coefficient of section
C_d	drag coefficient of section
ϵ	lift/drag ratio
K_T, K_Q	thrust and torque coefficients
λ	advance ratio
J	advance coefficient

Chapter 2	(continued)
κ	Goldstein coefficient
a'	interference velocity
α	angle of incidence
m/c	section camber/chord ratio
t/c	section thickness/chord ratio
C_f	flat plate friction coefficient
Chapter 3	
E	Young's modulus
τ	shear stress
ν	Poisson's ratio
J	polar moment of inertia
R	resistance
V	voltage
S_g	gauge factor
ϵ_a	strain
σ_a	axial stress
A	cross-sectional area
P	axial load
V_a	speed of advance
n	shaft revolutions per minute
Chapter 4	
W_t	total casting weight
t	section thickness
d	shell thickness
q	constant
V	volume
A	surface area
L	characteristic length
W	width
T	time
M	casting modulus

Chapter 1

Introduction

Propeller design has evolved very quickly over the past thirty years. Much of this development is a direct result of the advances in digital computers. Techniques used for design have become more powerful with improvements in the hardware. The object of screw propeller design is to determine the propeller geometry such that certain conditions of operation are met; the main requirement is to convert the power from an engine to produce thrust to propel a vessel. The primary requirements which must be met by a propeller design can be described in the following terms. The most important criterion is that the propeller and the primemover are properly matched. That is, the diameter and pitch should be chosen to absorb all

the power available at the correct operating speed of the vessel and propeller shaft rpm (revolutions per minute). Engine and machinery choices should be optimized for the highest possible efficiency based on reliable hull and propeller performance predictions. This usually means that the propeller itself must have the highest possible efficiency, but in some applications where cavitation and radiated noise reduction are important, a lower propeller efficiency may be deemed acceptable. Also, the propeller must have adequate strength over its lifetime; this is governed by the initial blade thickness and material selection. Finally, from the perspective of the manufacturer it must be possible to economically produce the design.

When propellers were first used for propulsion, very little was known about the operation of the screw propeller and why it worked. Early designs were the product of trial and error, and imagination. These were followed by formalized empirical methods which produced workable propellers when used correctly. Momentum theory was applied to propellers in the late nineteenth century; it explained the action produced by the propeller, but it did not give any insight into why these things happened. Diameters were chosen more or less arbitrarily at first and then through the use of the well known B_p-δ charts derived from model series tests (Burtner 1953). Cavitation inception was controlled to some extent by using charts, such as Burrill's cavitation diagram, to determine the minimum required blade area of a standard propeller blade (Burrill 1965). Blade strength was based largely on

experience, and then later on simple beam theory, to determine the minimum root thickness and thickness distribution along the blade span. Today, finite element analysis is used to analyse blade strength in great detail.

Theoretical analysis was first applied to propellers in the form of momentum theory. This helped to explain the operation of a propeller in basic energy terms, but it could not be used as a direct design method. Today, theoretical methods for propeller design consist primarily of different treatments of circulation theory of aircraft wings for operation in water. Wu (1965), Kerwin (1986), Glover (1987) and the Propulsor Committee of the 19th ITTC 1990 (International Towing Tank Conference) give a good review of these methods to date. Several of the different methods will be discussed in general terms so that their basic approaches are outlined.

In his dissertation of 1910, Betz, a student of the theoretical hydrodynamicist, Prandtl, first formally formulated the circulation theory of aircraft wings for use with screw propellers (Betz 1910). The vortex theory of propellers was developed on the basic assumption that certain geometric qualities of the flow in which a propeller operates must exist if the energy losses are to be minimized. That is, the sheets of vortices shed at the trailing edge of the blades must be of true helical shape. Goldstein (1929) developed this theory to account for the physical characteristics of propellers - the most important being a finite number of blades. He showed that

the (potential) flow past a vortex sheet could be calculated by relating the two theoretical cases of a propeller with a finite number of blades and a propeller with an infinite number of blades. This produced the "Goldstein factor" for periodicity of flow under conditions of optimum circulation. However, he neglected the effects of the propeller hub.

The problem of flow analysis consists of determining the induced velocities at the propeller blades. The large number of numerical calculations involved in the implementation of the theories were a major obstacle during early development, but have now mostly been overcome by high speed digital computers. Lerbs (1952) simplified the calculations by introducing the concept of induction factors. This concept amounts to factoring the theoretical induced velocities into components and expressing them in terms of ratios with respect to the speed of advance. Rigorously calculated, the induction factors depend only on helix geometry and therefore can be calculated independent of loading; they are as a result, valid under all loading conditions even when circulation is non-optimum. To achieve this, Lerbs made certain assumptions: 1) The radial induced velocity was assumed to be negligible in the cases of light to moderate loading; this however, is not the case for heavily loaded propellers such as towing propellers. 2) The calculated hydrodynamic pitch approximates the shape of the streamlines in the wake. These are assumed to depend only on the axial and tangential velocity components. Lerbs' method became

known as the lifting line method for marine pr ›pellers because the forces produced by the circulation are assumed to act along radial lines in place of the blades as in the similar theory of airscrews. Kerwin (1986) explains that Prandtl (1918-19) deduced that the three dimensional problem could be solved by concentrating the circulation around high aspect ratio blades on individual lifting lines. These lines produce vortices in the streamwise direction, to account for changes in circulation along the blade span.

Before high speed computers became readily available, Eckhardt and Morgan developed an "engineering" approach to the lifting line method. They assumed an optimum distribution of circulation, and a reduced thrust, proportional to the Goldstein factor due to the number of blades - and proceeded to calculate the induced velocities. This greatly reduces the amount of calculation involved. They showed that their method produces only small errors under light and moderate loading conditions and therefore is a very useful design tool (Eckhardt and Morgan 1955). The author has shown that, by writing an appropriate computer code, this method is actually very useful for fishing vessel propeller design and sizing. These computer programs are in use at a local propeller servicing firm (Hofmann 1989b, 1989c).

Classical momentum theory, as applied to propellers, forms the background to the major assumptions used in the theoretical velocity field analyses. In general,

certain relationships can be shown to be true under various degrees of propeller loading. That is, the relationships between the components of the induced velocities, their effect on the slipstream and the degree of loading. Induced velocities are the components of the velocity increase experienced by the fluid and imparted to it by the propeller. Kruppa (1967) gives a good explanation of momentum theory. He concludes with a definition of propeller loading in terms of the induced velocities. The axial component of the induced velocity is assumed to be: 1) much smaller than the advance velocity for lightly loaded propellers; and 2) approximately equal to the advance velocity for heavily loaded propellers. Furthemore the ratio of the squares of the axial induced velocity and advance velocity is small in moderately loaded propellers.

Goldstein (1929) first formulated Betz's (1910) vortex theory for propellers for the real case of a propeller with a finite number of blades. He showed that the velocity characteristics changed substantially by removing the assumption of infinite blade number. His analysis was done for the case of optimum circulation distribution of a propeller with minimum energy loss. By calculating the ratio of the circulation with infinite and finite numbers of blades, the Goldstein coefficients, κ, for periodicty of flow were derived.

Glauert (1947) showed that the individual airfoil sections along the blade span, having certain characteristics of lift and drag, could be included directly into a

lifting line calculation to design a propeller. However, he used momentum theory to determine the average induced velocity at the lifting line.

Lerbs (1952) produced a rigorous method for calculating the induced velocities under non-optimum conditions of circulation. He then extended Glauert's methods to calculate elemental contributions to thrust and torque along the blade span. These results were then integrated over the propeller blades to give overall performance of the propeller. He effectively produced the first practical numerical propeller design method which could be applied under various non-optimum conditions of loading. Lerbs' methods were extended later to include corrections for the effects of treating a three dimensional problem in two dimensions - lifting surface corrections (Kerwin 1986).

Lifting line methods are very useful for conventional propeller design and are used extensively by leading propeller manufacturers and naval authorities for preliminary work (Paulson et al. 1982; private communication, J.L.Kennedy, Department of National Defense, DND, Ottawa). The circulation distribution and hydrodynamic pitch are determined, before three-dimensional lifting surface methods are applied (Kerwin 1986). The required pitch distribution can be constant or varied (wake adapted). Blade cross-sectional characteristics are incorporated by using detailed airfoil section data and lift-drag relationships. A strength analysis can also be included by incorporating simple beam theory directly into the calculation to

obtain the primary stresses (Muckle 1941; Morgan 1954). Although this method has been very successful, it does not directly account for three-dimensional effects such as rake, skew, cross flow and flow curvature (Kerwin 1986). For many propeller designs, these are of secondary importance, but they do play a larger role in special propellers with wide, unsymmetric or highly skewed blades, where strength and vibratory considerations are much more important. To help account for three-dimensional effects the results of many lifting surface calculations are applied in the form of lifting surface pitch and camber corrections (Cox 1961, Morgan et al. 1968). These corrections at one time formed part of ongoing work in lifting surface theory which were applied primarily to refine and optimize designs produced by using the lifting line design method. However, ongoing work today focuses primarily on using pure lifting surface theory and panel methods for design. These methods are now used for the design of large propellers using input data from lifting line theory. Lifting surface theory is used for a three dimensional analysis of the propeller flow which takes into account the width of the blades. It can also account for blade thickness effects by using source distributions on the camber surface. Panel methods are used for detailed analysis of particular regions of interest such as flow around the blade root fillets or accounting for the effect of blade thickness on the flow field.

Lifting surface and panel methods used for propeller design are the topics of

ongoing research in this field. However, due to the very limited data available, in general, for small fishing vessels, the input data required for these techniques would be difficult to obtain in the vast majority of cases. Lifting line techniques on the other hand do not require as much detail and still yield useful results. By using lifting line design and analysis programs, large advances in the design of fishing vessel propellers can be made without the detailed numerical input required for more sophisticated methods. Experience gained using lifting line methods could lead to further development and the application of lifting surface methods to fishing propeller design.

WAOPTPROP is the author's core computer program for determining the ideal, wake adapted, hydrodynamic design of a propeller. By using the inputs: advance ratio, assumed induced velocity and number of blades, the actual induced velocity components are calculated and the thrust, torque, ideal efficiency and pitch diameter ratios are calculated by using Lerbs' induction factor method. WAOPTPROP was written keeping in mind the design approaches used in previous design programs based on Eckhardt and Morgan's (1955) methods (Hofmann, 1989b, 1989c).

The second program written was for the analysis of propeller performance over its operating range. This computer program (PPT2) combined Eckhardt and Morgan's (1955) design method with airfoil theory to evaluate the thrust, torque and efficiency of a propeller at conditions other than the design condition. Following an

approach previously used by the author (Hofmann 1990a), a lift and drag model for airfoils was used to determine the operating angles of attack of the blade sections. Hence, the thrust and torque values could be determined. The two programs, WAOPTPROP and PPT2, together form a design tool which allow the complete evaluation and design of a propeller under arbitrary loading conditions limited only to sub-cavitating operation.

Fuel costs are the second highest variable cost to the small vessel operator (besides crew). By making available more efficient propellers which can help to reduce fuel costs, fishermen and other operators can benefit from the immediate savings. The aim of this work was to develop a capability for the detailed design of marine propellers of higher efficiency for smaller vessels such as fishing vessels. Although the technology exists within the larger marine propeller manufacturers, it is not in general available to small vessel operators. A consequence of custom designed propellers is the difficulty and high cost of purchasing non-stock propellers. To this end the question of manufacturing was also addressed.

The most economical way of producing a complicated shape is by casting. Traditional methods of casting require wooden (or other materials) solid patterns which are used to create a cavity in the casting mould. These are inherently expensive and time consuming to produce. By being able to produce a mould without the need for a solid pattern, production costs can reduced substantially. The process can

also be applied to make patterns for stock or standard propellers. A strickle gear was designed, built and used to make a casting mould (Hofmann 1990c) without requiring a pattern. A crude reverberatory furnace was built to melt a charge of metal and a propeller casting was manufactured to demonstrate the viability of the system for propellers.

As most of the know-how required to produce sound castings is based on experience, an expert system, PROCASTER, was developed to guide the user in choosing the correct feeding and gating system for a particular case (Hofmann 1990d). The system was written in the EXSYS PROFESSIONAL expert system shell, a unique information access and storage tool for the foundry was devloped. It uses a rule-based inductive reasoning process to determine appropriate riser and gating system dimensions and to retrieve non-numerical technical information through user interactive menus.

To better understand the limitations of the design systems developed here, test case vessels were equipped with a purpose designed thrust and torque measurement system inserted into the propeller shaft. By comparing the behind the vessel performance curves as measured during seatrials, with those calculated by using the performance analysis program PPT2, the validity of the program could be gauged. By using the results from calculations, model tests and sea trials, a new more efficient propeller could be designed for a given vessel.

Chapter 2

Custom propeller design

2.1 Propeller Design

The first step in powering a given vessel is to determine the variation of hull resistance within the operating speed range. This will determine the thrust power required and hence the thrust the propeller must produce, taking into account the thrust deduction fraction. The engine power can then be determined from the total thrust requirement at speed, and the losses of all the components in the system. Other allowances for power take-off for auxiliary machinery and service allowances for unsteady operating conditions and performance in rough seas must also be made. Although there are many ways to deal with these problems for large ships, the emphasis of this work was to apply some of these engineering techniques to

smaller vessels such as fishing boats. With large ships, there exist many methods for resistance prediction; wake data for single or twin or even triple screw ships are readily available in the literature. Thrust deduction measurements have been completed from countless self-propulsion tests by many towing tanks. For small, heavy, full form fishing vessels, these data are rare and those that are available are not generally applicable. Therefore, highly complex methods for propeller design are not practical and will not give better or more reliable results than simpler methods. By applying methods such as the lifting line methods for propeller design, very good results are achievable with much less sophistication than lifting surface or panel methods.

The object of propeller design is to determine the overall geometric characteristics such as diameter, blade pitch, blade shape and area, cross-section shape and to ensure adequate strength. The design must produce the required thrust at the design condition and yet not overload the engine at off-design conditions. Propeller design involves the detailed analysis of the performance of the propeller. That is, over its entire operating speed range the torque and thrust characteristics must be determined so that the off-design performance of the vessel can be predicted and optimizated within the parameters dictated by the vessel design (Gerr 1989).

2.1.1 Lifting line theory - Lerbs' induction factor method

This section is a review of Lerbs' (1952) paper outlining the method. An introduction is given to the design program which was written in this study and which was based on this approach.

As has been stated previously, the blades are replaced by lifting lines whose circulation, Γ, varies over the radius, r. Variation of Γ across the span requires free vortices to be shed between r and $(r + dr)$, of strength $\bar{\Gamma} = \frac{d\Gamma}{dr}dr$ from Stokes law. The direction of the free vortex line is assumed to coincide with the direction of the resultant motion relative to the lifting system, therefore, for a propeller, the free vortex lines shed from the trailing edge of the blades are helices. The combination of all the vortex lines can be regarded as vortex sheets. The flow induced by the free vortex sheets can be found from Biot-Savart's Law. A difficulty arises in that the shape of the free vortex sheets depends on the induced velocity and the induced velocity depends on the shape of the free vortex sheets, therefore, certain assumptions must be made. These are: 1) for a lightly loaded propeller the induced velocity influence can be neglected, which gives a true helical shape (ie. shape of the vortex sheet is determined by inflow velocity v, the radius r and the rotational velocity ω); 2) for moderately loaded propellers the induced velocity is taken into account but the effects of centrifugal forces on the slipstream and from contraction are neglected; 3) for heavily loaded propellers the effects of slipstream contraction

and centrifugal forces must be included in the analysis (Heavily loaded propellers were not considered in this study); and 4) the vortex sheets are not uniform helical sheets. That is, the hydrodynamic pitch is not radially uniform.

The vortex sheets considered in the following are of true helical shape, consisting of cylindrical vortex lines of constant diameter and constant pitch in the axial direction. However, unlike previous work (Schubert 1940; Guilloton 1949) Lerbs avoided any *a priori* assumptions with respect to pitch. The problem then became the independent calculation of the individual axial and tangential velocity components w_a and w_t.

In developing this method, the relationships between the geometry and the flow needed to be determined so that expressions for the velocity field of a symmetrical helical vortex system could be found. In addition the influence of the hub cylinder on the velocity field needed to be established.

The velocity field can be found by using two approaches. Using Laplace's equation in the potential flow outside the vortex, leads to a boundary value problem of a partial differential equation. The other approach is to apply the Biot-Savart law which reduces the problem to an integration along a vortex line. Both approaches give the same result. The former approach is used here.

Lerbs uses the analytical expression for the velocity potential as given by Moriya [1]

[1]While researching this subject, it was discovered that this reference as cited by Lerbs (1952) was incorrect. The author was T. Moriya and not Kawada, according to the University of Tokyo.

to avoid the elaborate numerical integration of the Biot-Savart surface integrals required for other methods (Moriya 1933). Moriya's expression is valid for a vortex system which is infinitely long in both directions. A system of g helical tip vortices is considered corresponding to a propeller with g number of blades. The potential of the hub vortex is subtracted from Moriya's potential function - a potential of an infinitely long symetrical system of g helical vortices of constant radius, r_o, and constant pitch angle, β_{io}. For cylindrical coordinates the potential may be written as follows (Lerbs 1952, equations 1a, 1b):

a) for internal points $r<r_o$

$$\phi_i = \frac{g}{2}\bar{\Gamma} + \frac{g}{2\pi}\bar{\Gamma}[\frac{z}{k_o} + \frac{2r_o}{k_o}\Sigma_{n=1}^{\infty} I_{ng}(\frac{ng}{k_o}r)K'_{ng}(\frac{ng}{k_o}r_o)\sin ngv] \qquad (2.1)$$

b) for external points $r>r_o$

$$\phi_e = \frac{\Gamma}{2\pi}[g\psi - 2\pi\Sigma_{m=1}^{g}(\frac{m-1}{g}) + 2g\frac{r_o}{k_o}\Sigma_{n=1}^{\infty} K_{ng}(\frac{ng}{k_o}r)I'_{ng}(\frac{ng}{k_o}r_o)\sin ngv] \qquad (2.2)$$

where, (z, ψ, r) are cylindrical coordinates; z=0 at propeller disc, positive in direction of flow; ψ=0 at the first lifting line; k_o=$r_o \tan\beta_{io}$ is proportional to the pitch of the vortex lines; and $v = \psi - z/k_o$. The I, K and I', K' are modified Bessel functions and their derivatives with respect to their argument. $\bar{\Gamma}$ is the infinitesimal circulation of one of the g vortex lines $\bar{\Gamma} = \frac{d\Gamma}{dr}dr$, and Γ is the circulation at one of the lifting lines.

The object was to determine the induced velocities, not in the entire field, but

at the lifting lines. In the expressions ϕ_i and ϕ_e the velocities at the lifting line were found corresponding to locations z=0 and ψ=0. These corresponded to a vortex system extending from $-\infty$ <z< $+\infty$ in two dimensional flow while the vortex system of the propeller extended from z=0 to z=$+\infty$ in three dimensional flow. The potentials were written extending from $-\infty$ to $+\infty$ with the halves ahead and behind the propeller being equal by the Biot-Savart relations. It followed that the axial and tangential components of the induced velocity at the lifting line and the bisectors were obtained from $\frac{1}{2}\phi_i$ and $\frac{1}{2}\phi_e$. However, ϕ_i and ϕ_e did not consider the radial component of the induced velocity of the vortex system, therefore, if the radial component is needed the Biot-Savart integral must be used. Hence, the analysis is restricted to lightly and moderately loaded propellers.

By differentiating the velocity potential for the internal and external flows with respect to the axial and tangential direction, the induced velocities are found (Lerbs 1952, equations 5a, 5b):

internal points: $\bar{w_{ai}} = \frac{1}{2}\frac{\partial \phi_i}{\partial x}$ and $\bar{w_{ti}} = \frac{1}{2r}\frac{\partial \phi_i}{\partial \psi}$

external points: $\bar{w_{ae}} = \frac{1}{2}\frac{\partial \phi_e}{\partial x}$ and $\bar{w_{te}} = \frac{1}{2r}\frac{\partial \phi_e}{\partial \psi}$

and under conditions of light to moderate loading, the radial components were assumed to be zero:

$\bar{w_{ri}} = \frac{\partial \phi_i}{\partial r}$ and $\bar{w_{re}} = \frac{\partial \phi_e}{\partial r}$=0 at the lifting line.

The previously mentioned Bessel functions are replaced by Nicholson's asymptotic

approximations which yield the final results for the induced velocities at the lifting line as written below (Lerbs 1952 page 82).

The internal and external axial components were given by,

$$\bar{w_{ai}} = \frac{1}{k_o}\frac{g\bar{\Gamma}}{4\pi}(1+B_2) \tag{2.3}$$

$$\bar{w_{ae}} = -\frac{1}{k_o}\frac{g\bar{\Gamma}}{4\pi}B_1 \tag{2.4}$$

and the internal and external tangential components were given by,

$$\bar{w_{ti}} = -\frac{1}{r}\frac{g\bar{\Gamma}}{4\pi}B_2 \tag{2.5}$$

$$\bar{w_{te}} = \frac{1}{r}\frac{g\bar{\Gamma}}{4\pi}(1+B_1) \tag{2.6}$$

where the constants $B_{1,2}$ and $A_{1,2}$ are defined as,

$$B_{1,2} = (\frac{1+y_o^2}{1+y^2})^{1/4}[\frac{1}{e^{gA_{1,2}}-1} \mp \frac{1}{2g}\frac{y_o^2}{(1+y_o^2)^{3/2}}\ln(1+\frac{1}{e^{gA_{1,2}}-1})] \tag{2.7}$$

$$A_{1,2} = \pm[\sqrt{1+y^2}-\sqrt{1+y_o^2}] \mp \ln\frac{(\sqrt{1+y_o^2}-1)(\sqrt{1+y^2}+1)}{(\sqrt{1+y_o^2}+1)(\sqrt{1+y^2}-1)} \tag{2.8}$$

$$y_o = \frac{r_o}{k_o} = \frac{1}{\tan\beta_{io}} \tag{2.9}$$

$$y = \frac{r}{k_o} = \frac{x}{x_o\tan\beta_{io}} \tag{2.10}$$

where β_{io} is the pitch angle, $x = r/R$ is the radius fraction on the propeller blade and x_o is the radius of the helical vortex line.

Upon consideration of these equations, it is apparent that as $y \to y_o$ then the induced velocity components tend to infinity. To avoid this difficulty, Lerbs introduces the *induction factors*, i_a and i_t, which are defined by (Lerbs 1952, equations

6),

$$\bar{w}_t = \frac{\bar{\Gamma}}{4\pi(r - r_o)} i_t$$
$$\bar{w}_a = \frac{\bar{\Gamma}}{4\pi(r - r_o)} i_a.$$

These induction factors are the non-dimensional parts of the induced velocities which are related by $\bar{\Gamma}/4\pi(r - r_o)$. They relate the velocity induced at r by a fictitious *straight line* potential vortex at r_o parallel to the axis extending from z=0 to z=∞. Through this mathematical manipulation, a function (the induction factors) was found that did not tend to infinity as the section radius approached the vortex radius (ie. the induction factors remain finite, as $r \rightarrow r_o$). Hence, the induction factors are written explicitly as follows (Lerbs 1952, equations 7),

$$i_{ai} = g\frac{x}{x_o \tan\beta_{io}}\left(\frac{x_o}{x} - 1\right)(1 + B_2) \tag{2.11}$$

$$i_{ae} = -g\frac{x}{x_o \tan\beta_{io}}\left(\frac{x_o}{x} - 1\right)B_1 \tag{2.12}$$

$$i_{ti} = g\left(\frac{x_o}{x} - 1\right)B_2 \tag{2.13}$$

$$i_{te} = -g\left(\frac{x_o}{x} - 1\right)(1 + B_1). \tag{2.14}$$

These factors depend only on geometric characteristics of the helix and not on the circulation (that is, on the relative position of the reference x to the point x_o at which the vortex is shed and on the pitch angle of the vortex line). Therefore, these factors are valid under any type of circulation, or in other words, under any loading conditions.

Hub Influence

The propeller hub imposes certain boundary conditions on the circulation at the lifting line and on the induced flow. The circulation at the hub must be zero. (Intuitively, the hub does not produce any lift, so this must be true.) By imposing the condition that the circulation must be zero when approaching the hub surface, a discontinuous change in circulation occurs. This would mean that no equalizing pressure would be possible at the hub, but in real terms, a flow between adjacent blades produces an equalization in pressure between the pressure side of one blade and suction side of the next blade. A continuous change in circulation is therefore possible at $x_h = r_h/R$, the (non-dimensional) hub radius. The hub also requires that the radial component of the induced velocity be zero from the impermeability condition on the hub surface. This condition does not enter into the present analysis because the radial velocity component is neglected.

The Velocity Field

The velocity components induced by g equally spaced helical vortex lines are obtained by integrating over the respective elementary components of the vortex lines. Integrating the free vortices at a station x of a lifting line gives the components in terms of the speed of advance. From i_t and i_a and the non-dimensional circulation

$G=\Gamma/\pi Dv$, the following integrals can be written (Lerbs 1952, equations 12),

$$\frac{w_t}{v} = \frac{1}{2}\int_{x_h}^{1} \frac{dG}{dx_o}\frac{1}{x-x_o} i_t dx_o \tag{2.15}$$

$$\frac{w_a}{v} = \frac{1}{2}\int_{x_h}^{1} \frac{dG}{dx_o}\frac{1}{x-x_o} i_a dx_o. \tag{2.16}$$

These integrals represent the induced velocity components and correspond to integrals which occur in the theory of airfoil sections of finite span.

It is convenient to introduce a new variable ϕ (not the same ϕ used to define velocity potential in the previous discussion) such that at the hub, x_h, ϕ=0 and at the tip of the blade, x=1, $\phi=\pi$. ϕ_o is also defined in this way, but it locates the corresponding point on the vortex line and references the influence of the other positions of ϕ to the location under consideration. The general expression for the reference radius is, therefore, given by (Lerbs 1952, equation 14),

$$x = \frac{1}{2}(1+x_h) - \frac{1}{2}(1-x_h)\cos\phi. \tag{2.17}$$

The circulation G, across the span, is replaced by a Fourier series approximation of the form (Lerbs 1952, equation 15),

$$G = \Sigma_{m=1}^{\infty} G_m \sin m\phi. \tag{2.18}$$

Introducing this into the expression for w_t/v gives the complete component of the induced velocity as the circulation is continuous.

The induction factors depend on both ϕ and ϕ_o in addition to the number of blades and the pitch angle of the vortex lines. The induction factors are also

expanded into a Fourier series (Lerbs 1952, equation 16),

$$i_{a,t}(\phi,\phi_o) = \Sigma_{n=0}^{\infty} I_n(\phi)\cos n\phi_o. \tag{2.19}$$

When these are inserted into the respective expressions for axial and tangential induced velocity ratios, the following expressions are obtained (Lerbs 1952. equation 17).

$$\frac{w_t}{v} = \frac{1}{1-x_h}\Sigma_{m=1}^{\infty} m G_m h_m^t(\phi) \tag{2.20}$$

$$\begin{aligned} h_m^t(\phi) &= \int_0^{\pi} \frac{i_t(\phi,\phi_o)\cos m\phi_o}{\cos\phi_o - \cos\phi} d\phi_o \\ &= \frac{1}{2}\Sigma_{n=0}^{\infty} I_n^t(\phi)\left[\int_0^{\pi} \frac{\cos(m+n)\phi_o}{\cos\phi_o - \cos\phi} d\phi_o + \int_0^{\pi} \frac{\cos(m-n)\phi_o}{\cos\phi_o - \cos\phi} d\phi_o\right] \end{aligned} \tag{2.21}$$

Glauert (1947) solved the integrals $\int_0^{\pi} \frac{\cos\mu\phi_0}{\cos\phi_0 - \cos\phi} d\phi_0 = \pi\frac{\sin\mu\phi}{\sin\phi}$, so the equation for h_m^t is written in series form, suitable for numerical evaluation (Lerbs 1952, equation 17a).

$$h_m^t = \frac{\pi}{\sin\phi}\left[\sin m\phi \Sigma_{n=0}^{m} I_n^t(\phi)\cos n\phi + \cos m\phi \Sigma_{n=m+1}^{\infty} I_n^t \sin n\phi\right] \tag{2.22}$$

Similarly for the axial component (Lerbs 1952, equations 18, 18a),

$$\frac{w_a}{v} = \frac{1}{1-x_h}\Sigma_{m=1}^{\infty} m G_m h_m^a(\phi) \tag{2.23}$$

$$h_m^a = \frac{\pi}{\sin\phi}\left[\sin m\phi \Sigma_{n=0}^{m} I_n^a(\phi)\cos n\phi + \cos m\phi \Sigma_{n=m+1}^{\infty} I_n^a \sin n\phi\right]. \tag{2.24}$$

h_m becomes indefinite at the endpoints where ϕ equals 0 or π radians. L'Hospital's rule was applied to get the limits at these two end points (Lerbs 1952, equations

19):

$$h_m^{t,a}(0) = \pi[m\Sigma_{n=0}^{m} I_n^{t,a}(0) + \Sigma_{n=m+1}^{\infty} n I_n^{t,a}(0)] \quad (2.25)$$

$$h_m^{t,a}(\pi) = -\pi\cos(m\pi)[m\Sigma_{n=0}^{m} I_n^{t,a}(\pi)\cos(n\pi) + \Sigma_{n=m+1}^{\infty} n I_n^{t,a}(\pi)\cos(n\pi)] \quad (2.26)$$

Hence, the induced velocities were related to the circulation distribution and the induction factors. Therefore, the induced velocities could be calculated for any given distribution of circulation. Successive approximations were necessary to meet the condition that the vortex sheets and the relative stream lines coincide at the lifting line, since, the induction factors depend on the direction of the sheets and therefore on the induced velocities.

2.1.2 Hydrodynamic propeller design - WAOPTPROP

How were the expressions derived in the previous section used to design a propeller? The first step was to determine the design conditions under which the propeller was expected to operate. Once these had been established, the hydrodynamic design could be initiated.

The characteristics of interest were the diameter, the pitch required to produce a certain thrust while consuming a specified amount of power and the propeller efficiency. The required thrust or the available power are often the governing criteria. The diameter is determined by the aperture size or by calculating the optimum diameter from empirical results such as the Wageningen B_p-δ screw series results

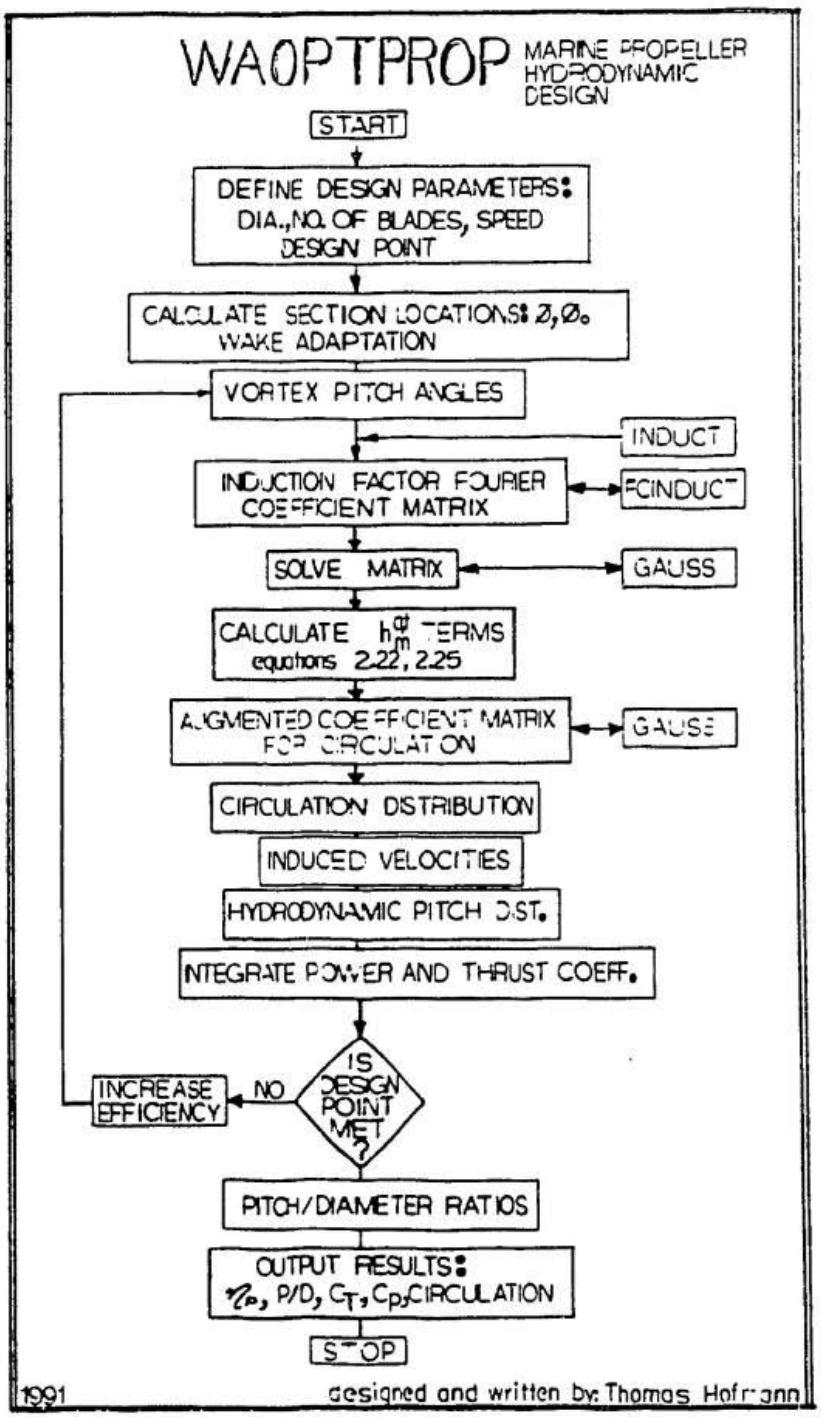

Figure 2.1: Propeller design program flow chart.

(Burtner 1953). The final diameter will often be optimized for best efficiency, low noise and tip-cavitation free operation on large ships. For smaller vessels the preliminary design process is not so detailed and is limited to a selection of diameter according to aperture size and a check on the likelihood of cavitation occurring by using Burrill's chart, for example (Burrill 1944).

The thrust and power (or torque) coefficients were calculated in non-dimensional form for convenience and were used to determine the final results - propeller specifications. The Lerbs lifting line method forms the basis of the program, OPTPROP, that was written as part of this study. It was then modified to include wake adapted propeller capability; WAOPTPROP is the modified version. The program was written using VAX FORTRAN, but as the intended use is for personal computers, no standard routines are used. All the subroutines were written in a form which will allow compiling using a simple PC FORTRAN compiler.

Refer to figure 2.1 for the following explanations. The blade radius fractions were defined in terms of the angle ϕ as outlined in equation (17). The benefits of this type of definition, instead of the conventional method of a percent of the radius of the propeller, was that the mathematics can be handled more easily in polar form. This format also resulted in a concentration of stations at the hub and tip where the circulation distribution varied more rapidly than around the centre of the span.

Given the number of blades, the hub radius ratio and the advance ratio (non-dimensional speed), the program WAOPTPROP calculated the ratios of the reference location x_o and the locations of the other reference points of influence to the vortex. The subroutine INDUCT then calculated the corresponding induction factors, equations (2.11), (2.12), (2.13), (2.14), which are the solutions to the left-hand side of the Fourier series as given by equation (2.19). Equation (2.19) could be written in matrix form, (7X7 because, there are seven blade sections, at each of which the corresponding equation has six Fourier coefficiencts and a solution), which was then solved by using the Gaussian matrix inversion technique in the subroutine GAUSS. GAUSS was written to avoid the use of mainframe library routines which could hinder transfer of the program to a personal computer. To avoid the accumulation of excessive rounding errors, double precision computations were used throughout. Having found the Fourier coefficients of the induction factor series, the $I_n(\phi)$ values, the program proceded to calculate the various parts for the $h_m^{a,t}$ factors which were used to calculate the non-dimensional circulation.

To calculate the circulation distribution in the form of a Fourier series with a limited number of terms, the following system of equations was set up in the form of an augmented matrix (Lerbs 1952, equation 23). Having calculated $h_m^{a,t}$ previously using equations (2.21) and (2.23)

$$\Sigma_{m=1}^{p} m G_m [h_m^a(\phi) + \frac{\lambda_i}{x} h_m^t(\phi)] = (1 - x_h)\frac{w^*}{v}. \qquad (2.27)$$

The factors h_m, λ_i and x were calculated and a value of ideal efficiency was assumed to initiate the calculation. The system of p linear equations were solved using the subroutine GAUSS to find the coefficients G_m of the circulation series expansion. Hence, the circulation distribution could be calculated by summing the Fourier series at each location x_o/x.

$$circulation = \Sigma_{m=1}^{p} G_m \sin j\phi \tag{2.28}$$

where, j=number of locations, p=number of coefficients.

Given the coefficients G_m the axial and tangential velocity components were calculated as ratios of the advance velocity as the following sums:

$$\frac{w_t}{v} = \Sigma \frac{1}{1 - x_h} j G_m h_t \tag{2.29}$$

$$\frac{w_a}{v} = \Sigma \frac{1}{1 - x_h} j G_m h_a. \tag{2.30}$$

The hydrodynamic pitch angle was then calculated according to the relation derived from section geometry,

$$\tan \beta_i = \frac{1 + \frac{w_a}{v}}{\frac{x}{\lambda} - \frac{w_t}{v}} \tag{2.31}$$

followed by the hydrodynamic pitch-diameter ratio

$$\frac{P}{D} = \pi x \tan \beta_i. \tag{2.32}$$

Finally, the ideal thrust and power coefficients were calculated by integrating the elemental thrust and power coefficients across the span of the blade by using

the trapezoidal rule. The elemental thrust and power coefficients are,

$$C_P = \int 4Gx\Gamma\frac{1+\frac{w_a}{v}}{\lambda} \tag{2.33}$$

$$C_T = \int 4G\Gamma\frac{x}{\lambda}-\frac{w_t}{v} \tag{2.34}$$

which lead to the propeller ideal efficiency $\eta = C_T/C_P$.

The assumed value of ideal efficiency made at the beginning would not necessarily correspond to the actual value required in the design condition. Therefore, it was necessary to iterate for a range of values and determine the correct induced velocity according to the required thrust or power coefficient.

These results were for the ideal case since frictional effects were not yet taken into account. Frictional effects were incorporated into the formulation by superimposing the empirical data from airfoil sections and accounting for the losses in thrust through adjustments in pitch. A strength of the method was that it could account for non-uniform flow in the wake by allowing for a radial variation of wake (ie. wake adapted). Other effects not accounted for in this method stem from neglecting the blade width. Therefore, it could be stated that as the propeller blades move away from straight, high aspect ratio configurations, the accuracy of the method decreases. However, this method is used by most leading designers and manufacturers of marine propellers for preliminary design of large or special application propellers, especially wake adapted propellers, or for designing conventional propellers where extensive analysis is not required.

Wake adapted propellers

The wake behind the vessel in the region of the propeller disc is assumed to vary radially, and is assumed to be constant over the circumference at each radius. To determine the useful thrust of a propeller operating in the wake, the circulation distribution must be determined by taking into account the wake variations. To express these characteristics mathematically, Lerbs (1952) defined the following terms: the non-dimensional circulation distribution $G = \frac{\Gamma}{\pi D v_s}$, the advance ratio $\lambda_s = \frac{v_s}{\pi n D}$, the resistance augmentation $dT = dR_t + \Delta(dR_t) = dR_t + tdT$ where, $dR_t = dT(1 - t(x))$, and the wake fraction $w(x)$ such that $v = v_s(1 - w(x))$. Both t and w are considered functions of x and are assumed to consist of two parts relating potential flow (subscript p) and viscous flow (subscript f).

$$w(x) = w_p(x) + w_f(x)$$

$$t(x) = t_p(x) + t_f(x)$$

With these definitions, Lerbs obtained the power input and useful power coefficients on the basis of the Kutta-Joukowski law (Lerbs 1952, equations 24, 25):

$$C_{pi} = \frac{P_i}{\frac{\rho}{2}R^2\pi v_s^3} = \frac{4g}{\lambda_s}\int_{x_h}^{1} G[(1-w) + \frac{w_a}{v_s}x\,dx \tag{2.35}$$

$$C_{pu} = v_s\int_{x_h}^{1}\frac{dT(1-t)}{\frac{\rho}{2}R^2\pi v_s^3}dx = 4g\int_{x_h}^{1} G(\frac{x}{\lambda_s} - \frac{w_t}{v_s}(1-t)dx \tag{2.36}$$

The induced velocity ratios are related to the circulation by the integrals (Lerbs 1952, equations 26); these are similar to equations 2.16 and 2.17 except that ship

speed is substituted for speed of advance:

$$\begin{aligned}\frac{w_a}{v_s} &= \frac{1}{2}\int_{x_h}^{1}\frac{dG}{dx_o}\frac{1}{(x-x_o)}i_a dx_o \\ &= \frac{1}{(1-x_h)}\Sigma_{m=1}mG_m h_m^a \qquad (2.37)\\ \frac{w_t}{v_s} &= \frac{1}{2}\int_{x_h}^{1}\frac{dG}{dx_o}\frac{1}{(x-x_o)}i_t dx_o \\ &= \frac{1}{(1-x_h)}\Sigma_{m=1}mG_m h_m^t \qquad (2.38)\end{aligned}$$

The non-dimensional circulation, G, was again expressed as a Fourier series as in equation (2.18). The optimization problem to be solved was to maximize the output thrust power, C_{pu}, given a constant input power, C_{pi}, requiring that the incremental change in input power equals the output power (Lerbs 1952, equation 28):

$$\frac{\partial C_{pu}}{\partial G_m} = -k\frac{\partial C_{pi}}{\partial G_m} \qquad (2.39)$$

where k is a constant independent of x, and the wake and thrust deduction are assumed to be known.

Substitution of equations (2.17), (2.35), (2.36) into both (2.33) and (2.34) will enabled the integrals to be calculated. Equations (2.33) and (2.34) will have been transformed into sums of polynomials of G_m and a system of m equations in m unknowns (G_m values).

Lerbs discovered several difficulties when he attempted to apply these equations to actual propeller design. Firstly, these equations are not linear in G_m; secondly, the multiplier k could not be eliminated, requiring several solutions to be found so

that k could be interpolated from C_{pi}; thirdly, the thrust deduction was not known with sufficient accuracy to justify the laborious calculations.

Dickman (1938) developed a relationship between wake fraction and thrust deduction fraction analytically, but it gives only the potential part of the increased resistance obtained from self-propulsion test analysis, particularly when there is a large variation in wake (Lerbs 1952).

Van Manen (1952) gives an approximate relationship between thrust deduction fraction and wake fraction based on calculations and experiments. The ratio of the local value and global value of each is related as follows:

$$\frac{1-t'}{1-t} \approx (\frac{1-w'}{1-w})^{\frac{1}{4}}.$$

Van Manen states that this relationship is justified as $t(x)$ varies little over the outer blade sections and it also implies a lower blade loading at the inner radii where $t(x)$ is greatest.

In previous work, Lerbs derived the optimum condition in terms of the wake fraction, thrust deduction fraction and the ideal propeller efficiency (Lerbs 1952).

$$\frac{\tan\beta}{\tan\beta_i} = \eta\sqrt{\frac{(1-t_o)}{(1-t(x))}\frac{(1-w(x))}{(1-w_o)}}. \tag{2.40}$$

He then assumed that the variation of thrust deduction could be neglected to get the approximate optimum condition (Lerbs 1952, equation 31):

$$\frac{\tan\beta}{\tan\beta_i} \approx \eta\sqrt{\frac{1-w(x)}{1-w_o}} = f(x). \tag{2.41}$$

$f(x)$ is assumed to be known from efficiency diagrams (for example, Kramer 1938), or from wake measurements. For a free-running propeller, Betz's general optimum condition expressed as, $tan\beta/tan\beta_i$, is independent of radius. That is, the efficiency of an increment of circulation is independent of radius. Van Manen (1952) deduced a similar relation as (2.41), but in his case, the exponent was set at 0.75 instead of 0.5.

Modifying equation (2.30) slightly to account for a variable wake gives,

$$\tan \beta_i = \frac{[1 - w(x)] + \frac{w_a}{v_s}}{\frac{x}{\lambda_s} - \frac{w_t}{v_s}} \tag{2.42}$$

Manipulation of equations (2.37), (2.38) and substituion into (2.35) and (2.36) gives an integral equation for the variation of circulation with position along the span (Lerbs 1952, equation 32). This integral is rewritten in Fourier series form to give a system of linear equations in m unknowns. This is solved as before at m stations to obtain the coefficients G_m for the circulation. The induced velocities are then calculated using the expansions (2.37) and (2.38). The input power coefficient is calculated and checked against the required value to refine the estimated ideal efficiency assumed in equation (2.41). Once the induced velocities were calculated, the lift coefficient/chord length ratio could be calculated according to the relation as given by Lerbs,

$$\frac{C_L l}{D} = \frac{G \cos \beta_i}{\frac{x}{\lambda_s} - \frac{w_t}{v_s}} 2\pi \tag{2.43}$$

which determines the section characteristics and hence the basic propeller blade geometry.

Given the computer program WAOPTPROP, the propeller design procedure is straight forward. The wake distribution is measured or estimated for the given design speed and the required input power coefficient is calculated using equation number (2.35). The program then iterates from an assumed low value of ideal efficiency to a solution by progressively closer approximations to the required C_{pi} based on increments of assumed ideal propeller efficiency. The final results of the program are the power and thrust power coefficients as calculated, the hydrodynamic pitch distribution is given in terms of the pitch diameter ratio. Figure 2.2 gives a sample output from the program for a single iteration. The circulation distribution gives the distribution of loading along the blade span. The induced velocity ratios are printed out next followed by the design results. C_{pi} is the required value of power coefficient; C_T and C_P are the calculated values of thrust and power coefficients; d is the propeller diameter; *pitch*, is the mean pitch in uniform flow; and EFF is the propeller ideal efficiency. For wake adapted analysis these would be followed by the radial pitch distribution. Appendix B gives the FORTRAN listing of the program including all the subroutines.

```
CIRCULATION WITH INTERMEDIATE POINTS

        1RADX=  0.2000000     CIRC2=  0.0000000E+00
        2RADX=  0.2136297     CIRC2=  1.1169008E-02
        3RADX=  0.2535899     CIRC2=  2.0585597E-02
        4RADX=  0.3171573     CIRC2=  2.7182156E-02
        5RADX=  0.4000000     CIRC2=  3.0876445E-02
        6RADX=  0.4964724     CIRC2=  3.2321583E-02
        7RADX=  0.6000000     CIRC2=  3.2284081E-02
        8RADX=  0.7035277     CIRC2=  3.1085309E-02
        9RADX=  0.8000001     CIRC2=  2.8484998E-02
       10RADX=  0.8828428     CIRC2=  2.4026178E-02
       11RADX=  0.9464102     CIRC2=  1.7510720E-02
       12RADX=  0.9863704     CIRC2=  9.2493016E-03
       13RADX=   1.000000     CIRC2= -2.6780986E-09
       14RADX=  0.9863704     CIRC2= -9.2493081E-03

INDUCED VELOCITIES

WTV(          1 )=  0.2327480     WAV(          1 )=  0.1689280
WTV(          2 )=  0.2137835     WAV(          2 )=  0.2055833
WTV(          3 )=  0.1646722     WAV(          3 )=  0.2444799
WTV(          4 )=  0.1125691     WAV(          4 )=  0.2472781
WTV(          5 )=  8.3773755E-02 WAV(          5 )=  0.2439426
WTV(          6 )=  7.0740819E-02 WAV(          6 )=  0.2422469
WTV(          7 )=  6.7371733E-02 WAV(          7 )=  0.2430193

88888888888888888888888888888888888888888888888888888888888888888
iterations required          0
CPI=  0.7840000000000000
diameter=    1.000000000000000    pitch=  0.7448814712329811
CT=  0.7355737    CP=  0.9658955
EFF=  0.7615458
88888888888888888888888888888888888888888888888888888888888888888
```

Figure 2.2: Sample output from WAOPTPROP.

2.1.3 Results from propeller design

The design program WAOPTPROP was tested by reproducing the published calculation results in Lerbs' (1952) paper. It was then used to address a typical case of engine and propeller mis-matching.

As the various sections of the program were written, they were tested by reproducing the examples given by Lerbs (1952). Invariably, the calculated values differed only in the third or fourth decimal place. Lerbs' original calculations were done by hand while the encoded calculations were done in double precision to avoid rounding and truncation errors. However, there was still some doubt as to how well the program could predict the required pitch distribution on an actual propeller.

The opportunity to use the program on a specific vessel arose during the spring of 1991. The owner of a 75 ft. (23 m) long, steel, shelter deck stern trawler, *MV BEAR COVE POINT*, consulted with the local propeller firm Avalon Propulsion Systems Limited, (APS), about reconditioning the vessel's propeller. During discussions the owner complained of poor performance at sea. The vessel had apparently never performed to specifications even though it had a large amount of installed power. The trawler was a lengthened 65 ft (about 20 m) design and had a fully enclosed processing deck installed. These modifications increased the displacement substantially. No other structural changes were made to the original design except that the main engine power was increased. The result was a vessel that could

not achieve the design speed of about 10 knots. The maximum speed recorded was about 7 knots in port departure condition. The original propeller supplier attempted to correct the problem, but failed. Some time later another attempt was made by another propeller company which also failed. Through consultation with APS, it was surmised that the poor vessel performance at sea was attributable to the existing propeller. The vessel was inspected while in drydock at St.John's. It was found that the single chine, steel hull exhibited a very full midship section and that the maximum propeller diameter was very restricted for the installed power and shaft speed (rpm). As with most vessels of this type in the region, very few vessel performance data were available. A uniform steady flow design calculation was carried out using WAOPTPROP to determine the correct pitch/diameter ratio. A similar calculation was carried out by using WAP (Hofmann 1989d) and by using the slip method for determining pitch (Gerr 1989 and appendix A). From experience, the installed power was considered sufficient for propelling the vessel at 10 knots in the fully loaded condition. There were no values for wake or true slip available for this or similar vessels. Again, from experience with full form fishing vessels in Newfoundland, the wake fraction was estimated to be about 0.40 (see for example, Wu and Bose 1991) and the true slip about 0.45 (Gerr 1989 and appendix A). All three of these calculations yielded essentially the same result: a pitch to diameter ratio, P/D=0.84.

WAP uses the Eckhardt and Morgan (1955) design method. The design condition to be specified in this case was the required thrust. This presented a problem because resistance data do not exist for this vessel; therefore, an estimate was made based on model tests on a very full form 20m vessel done by Nordco Ltd. (1990). This program led to a pitch/diameter ratio of 0.825. From experience of previous use at Avalon Propulsion Systems Ltd. (APS), WAP tends to underestimate pitch; this is borne out by the comparison with other methods as shown in table 2.1.

WAOPTPROP was used in this case to calculate a range of power and thrust coefficients. By incrementing the assumed ideal propeller efficiency, the dependence of thrust coefficient, C_T, and power coefficient, C_P, on hydrodynamic pitch was calculated and plotted. Figure 2.3 shows a plot of the thrust and power coefficients as a function of the hydrodynamic pitch. Which curve is used to determine the required pitch depends on the chosen design point; either the required thrust, to propel the vessel at a certain speed; or the available power for propulsion. The design coefficients were determined from the following relationships which correspond to equations 2.35 and 2.36 for useful and input power, respectively.

$$C_T = \frac{T}{\rho \pi R^2 V_A^2}$$
$$C_P = \frac{\omega Q}{\rho \pi R^2 V_A^3} \tag{2.44}$$

where T is the required thrust; Q is the shaft torque at rotational velocity ω; V_A

Table 2.1: Comparative results for P/D: *MV BEAR COVE POINT.*

design method	P/D
WAP	0.825
slip method	0.845
WAOPTPROP	0.839

is speed of advance; R is the propeller radius; and ρ is the water density. The propeller efficiency was defined as $\eta = C_T/C_P$. These values are related to the usual K_t and K_q by:

$$K_t = \frac{C_T}{V_A}$$
$$K_q = \frac{C_P}{\omega}$$

The curves were used to determine the required propeller pitch by drawing a vertical line through the design point power or thrust coefficient and reading off the corresponding pitch. In this case the design point chosen was a power coefficient equal to 1.141 which gave a pitch of 1.45 m.

Another problem foreseen in this case was inadequate blade area. Due to the restricted diameter and increased power output, the standard propeller installed was ineffective in converting all of the power. Inspection of the blade surfaces indicated a substantial amount of surface cavitation on the suction side which would have led to a reduction in thrust. It was also reported by ship's personnel that the engine fuel rack position did not reach full throttle except when auxiliary loads were high. The

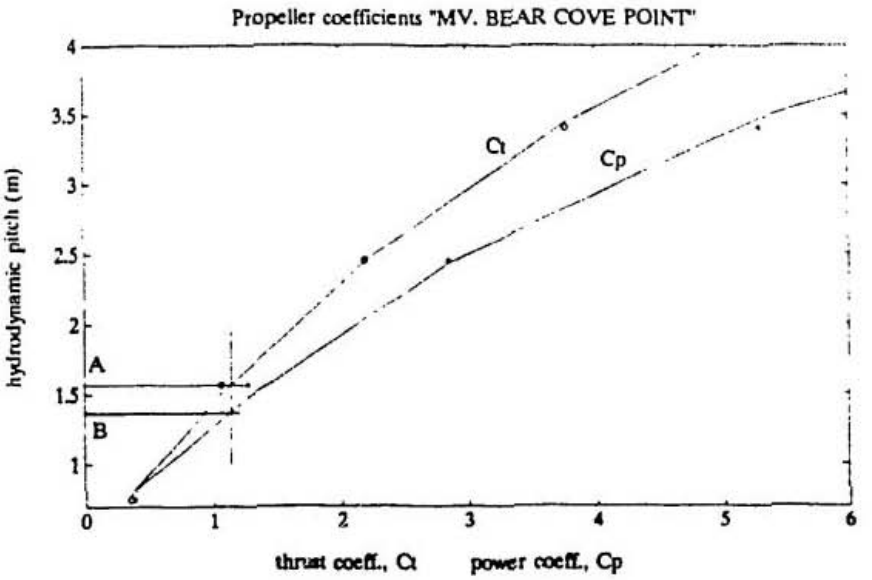

Figure 2.3: *MV BEAR COVE POINT* pitch determination.

thrust loads were estimated and found to be high; average blade loading was around 18 pounds per square inch (psi) (a value of 6 psi is suggested as a maximum mean pressure, Burrill 1943-44). It was necessary to increase the expanded blade area ratio to lower the mean loading and to avoid thrust break-down due to cavitation.

A solution was recommended which involved a major alteration to the existing propeller. The diameter was increased by two inches to 1.778 m (70 inches) in diameter. This was the maximum diameter allowed by aperture size plus clearance. The pitch was altered to 1.525 m (60 inches) and the blade area was increased by 20%, from 0.54 to 0.68 to reduce the mean blade loading to below 6 psi. To help increase the propeller efficiency the tip loading was increased by altering the distribution of area toward the tips. That is, the tips were squared-off more from

the standard elliptical design of the original propeller. Vibration was not a concern with this vessel.

The work was done as suggested by APS. The owner reported back after his first three voyages with the altered propeller. There was no appreciable change in the noise levels experienced in the work area of the shelterdeck. Therefore, the reduction in tip clearance had not increased the propeller induced hull vibration. The design speed had now been achieved in port departure condition (usually a full load of ice and fuel and provisions for ten days at sea). The transit speed had increased from 7 to about 9-9 1/2 knots under full load. The owner was quite pleased with the results. The gain in speed had reduced his steaming time to and from the fishing grounds by 8 to 10 hours. This saved him fuel and other costs because of quicker turn-around and fewer hours at sea.

A new propeller was subsequently purchased (after the skeg was lowered to allow a further increase in diameter) which had nominal dimensions: 1.830 m (72 inches) in diameter; the pitch was equal to 1.525 m (60 inches) as before; and an expanded blade area ratio of 0.70. The altered propeller was retained as a spare.

The level of confidence in the results from the new program increased substantially because this case was successful. The results described show that by applying sound engineering to difficult propeller problems, workable solutions can be found. The use of the program as an independent design tool looks very promising. The

wake adapted propeller feature has as yet not been used for actual design cases. It should be noted that although it can potentially produce a better design, the detailed wake information required is usually not available. The program is expected to become more useful when more detailed wake and resistance data become available.

2.2 Hydrodynamic propeller performance

The propeller designer is interested in the performance of a propeller operating under off-design conditions for several reasons. These include the need to optimize propeller designs for particular applications (e.g. towing); the avoidance of "over-pitching", and hence engine overloading; and to ensure compliance with design and performance specifications such as bollard pull and trial or design speed.

Initially, an attempt was made to write a computer program as suggested by Lerbs (1952) using the induction factor method previously explained. However, after considerable effort it became apparent that the complexity of the numerical procedures, required to simultaneously solve two interdependent sets of equations iteratively, far outweighed the potential gains in accuracy. This may be the reason why no refer ces were found in the literature in which Lerbs' suggested method was used in computations. In cases where high accuracy is required, a lifting surface program can be used (Greely and Kerwin 1982). Therefore, based on previous experience (Hofmann 1990a) and on published material by Kerwin (1959), Burrill (1943-44) and Bose (1983), a new program was written to analyse the hydrodynamic performance of a propeller throughout its range of operation. The method used was from the propeller design method by Eckhardt and Morgan (1955); this is a lifting line method which assumes that circulation is optimum. The method was developed to avoid the complex calculations required by Lerbs' method for design

so that reasonble results could be obtained by hand. It makes use of Goldstein's factors for periodicity of flow for a finite number of blades. The authors showed that by avoiding high propeller loading, only small errors were incurred at the design condition.

The question could be asked: why was this work justified when there were much more sophisticated methods available for propeller analysis? The primary reasons were simplicity and scarcity of specific information.

During the course of this work the lifting surface steady flow analysis program produced by Greely and Kerwin (1982), MIT-PSF-2, was used for verification of the new program's results. Six test propellers from the Wageningen B-series were analysed: two 3 bladed, two 4 bladed and two 5 bladed propellers (van Lammeran et al. 1969). It quickly became apparent that PSF-2 was quite cumbersome to use. For each advance coefficient of interest, a new data file needed to be written. For a minimum of three values of advance coefficient on the thrust and torque coefficient curves for the six test cases, the 18 runs required took two days to complete.

The performance analysis program written as a part of this project is called PPT2. Using PPT2 and another program, BKTKQ, written to calculate the regression polynomials of the B-series experimental results, a full range of points were calculated for all the propellers in about one and one half hours. A half of a day was required to plot all the results. These are substantial savings in time;

firstly, of computer time required to run the programs; and secondly, of time spent by a qualified (and expensive) designer. This is a major consideration for a commercial enterprise. Other considerations include the awkward way in which the program must be run (using data files etc.) and the possibility of transferring the programs to micro-computers or personal computers. The MIT program is difficult to use on a micro-computer because of large memory requirements, while the present programs have only a limited memory requirement which makes them ideal for micro-computer use. As they were written without using library programs such as those for matrix inversion, they can be easily compiled for the appropriate FORTRAN system with only minor adaptations. Finally, the user keyboard input makes PPT2 much more user-friendly and does not implicitly require a good understanding of propeller design or of lifting surface techniques. For conventional propellers MIT-PSF-2 is in general too sophisticated; it produces very detailed output that would rarely be used for day to day work on small propellers. Its high commercial purchase and operating costs cannot be justified in a smaller commercial setting; the programs were available at a reduced rate with the restriction that they could only be used for university research.

A serious drawback of previous analysis programs (for example, Kerwin 1959, Burrill 1943-44) was that they assumed an ideal lift curve for the blade sections without allowing for stall. Stall was allowed for by Bose (1983), in his windmill anal-

ysis program, by implementing an idealized lift and drag model which extends well beyond the stall region of airfoil section operation. Bose's approach was adapted to marine propeller performance analysis as part of earlier work (Hofmann 1990a). In the latest version of the program, PPT2, this method was refined by taking into account different types of airfoils and their specific lift characteristics. Also, by using an improved modular programming technique the correct angle of attack of an individual section could be more accurately determined. The lift model and methods are explained in the subsequent sections.

After running the MIT-PSF-2 program for the B-series propellers it was found that in some cases the results produced at low advance coefficient differed greatly from the experimental results. These discrepancies were possibly due to limitations in the potential lifting surface theory which cannot account for flow separation, because there is no viscosity by definition; although viscous drag is included by using a constant drag value. PPT2 however, accounts for flow separation by modelling the stall region of the sections and therefore produces a more rational result at low advance coefficients. This was an important feature because many small vessels operate at relatively low advance coefficients (less than about 0.5). By developing appropriate corrections for PPT2, the differences in the calculated thrust and torque coefficients could be reduced so that the program re-produces B-series data.

2.2.1 Propeller performance analysis program - PPT2

The propeller performance analysis program PPT2 calculated the thrust and torque coefficients and the propeller efficiency over the full range of operation of a propeller. The numerical design method of Eckhardt and Morgan (1955) was adapted to calculate the airfoil section lift at a radial blade location. To determine the appropriate angle of attack at which individual sections operate, the calculated lift was compared with the lift possible from the section (as given by a lift model). When the correct value was determined, the lift of the section was recalculated. The thrust and torque for the whole blade was found by integrating the recalculated values at the blade sections.

2.2.2 Main program

PPT2 is a FORTRAN program written on a VAX 8530 computer. Again library programs were not used so as to make transfer to other computers and micro's as simple as possible. The main program handles the data input and controls the function of the various subroutines and outputs the results. The following paragraphs describe in detail the program operation. Figure 2.4 gives the flow chart of the program PPT2.

The title and acknowledgements pages were followed by data input from the keyboard. The data which were required as input to run the program were as

follows: propeller diameter, number of blades (3,4,5, or 6), expanded blade area ratio, propeller shaft revolutions per minute, and the overall (Taylor) wake fraction. Wake adapted analysis could be chosen if the data were available. The pitch diameter ratio was then typed in at the prompts. The option for specifying the type of airfoil section followed. The current version of PPT2 had three options: NACA a=1.0 mean line, NACA a=0.8 mean line and circular arc sections with flat face. The geometric properties of the propeller : chord/diameter, thickness/chord and camber/chord ratios were incorporated into the geometry subroutine GEO explicitly. GEO took the geometric properties at arbitrary locations and through a second order regression procedure calculated the properties at the required radial locations.

The actual calculations were initiated by setting the first value of advance coefficient, J. At each blade section the advance angle and pitch angle were determined. An angle of attack was assumed initially. The subroutine NUMLFT was called to calculate the theoretical lift coefficient, C_l. At the same angle of attack another subroutine , TRULFT, was called to calculate the lift, C_{lt}, at that angle according to a lift model. These two values were compared by finding the difference between them. As the value of C_l was always greater than C_{lt} when the iteration was begun (Hofmann 1990a), by stepping up the angle of attack and recalculating C_l and C_{lt}, the point at which the difference became zero or negative could be determined.

The subroutine ATTACK was then called to determine the angle accurately. 0.05 degrees was found to be sufficiently accurate to produce a smooth K_T output curve. When the angle of attack for that section was determined, the ideal incremental thrust and torque coefficients were calculated using the following equations:

$$K'_{Ti} = \pi^3 x^3 \kappa a'(1 - a')$$

$$K'_{Qi} = \frac{1}{2} x K'_{Ti} \tan \beta$$

where x is the radius fraction; κ is the Goldstein factor; a' is the rotational interference factor; and β is the advance angle.

The subroutine DRAG was called to calculate the section drag coefficient at the angle of attack. The drag/lift ratio, ϵ, was calculated to account for viscous flow.

$$K'_T = K'_{Ti}(1 - \epsilon \tan \beta_i)$$

$$K'_Q = K'_{Qi}(1 + \frac{\epsilon}{\tan \beta_i}) \tag{2.45}$$

where β_i was the hydrodynamic pitch angle of the section.

The total thrust and torque coefficients, K_T and K_Q, of the blades were found by integrating the incremental values across the span by using Simpson's rule. A simple lifting surface correction to K_T and K_Q was then applied to better approximate the experimental results. After calculating the propeller efficiency, the next value of J was chosen and the entire procedure repeated. The program output was in table form where the K_T, K_Q, and efficiency value are printed out corresponding to ship

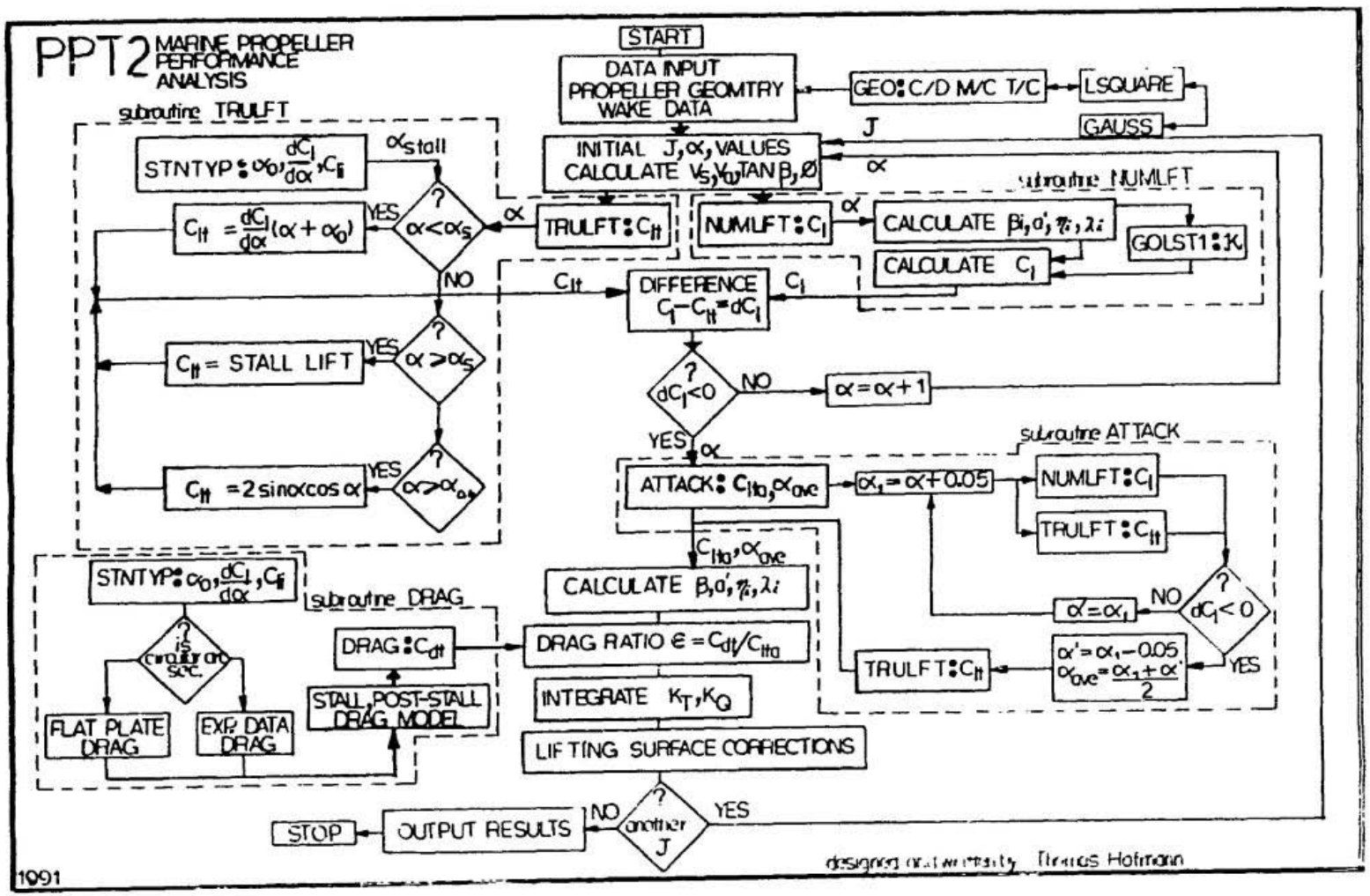

Figure 2.4: Flow chart of PPT2.

speed and J value. Figure 2.5 shows the output from PPT2 for the analysis of the existing propeller on the *MV SUGAR*.

The useful operating range of the propeller can be read off at a J value corresponding to where the thrust coefficient changes sign to negative. Negative thrust means the propeller is water milling and is therefore not useful for propulsion beyond that value of J. Plotting the value of thrust, torque and efficiency with respect to J gives the propeller curves.

2.2.3 The subroutines

NUMLFT

This subroutine was used to calculate the theoretical lift coefficient according to the Eckhardt and Morgan propeller design method (Eckhardt and Morgan 1955, Bose 1983, Hofmann 1990a).

The lift coefficient is given by:

$$C_l = \frac{4\kappa a' \pi x}{nb\frac{c}{D}(1-a')\sqrt{1+\tan^2\beta_i}}$$

where as before, κ is the Goldstein factor; a' is the rotational interference factor; x is the radius fraction; n is the revolution per second; b is the number of blades; c/D is the chord/diameter ratio of the section; and β_i is the hydrodynamic pitch angle.

```
PROPELLER PERFROMANCE DATA:
---------------------------
OPERATING CONDITIONS:
          DIAMETER :                          0.56    m
          PITCH RATIO:                        0.44
          NUMBER OF BLADES :                  3
          SHAFT RPM:                          1326.00
          MAXIMUM SHIP SPEED:                   21.35   KNOTS
          OVERALL WAKE FRACTION:               0.400

PERFORMANCE CHARACTERISTICS:
          Vs              J              Kt              Kq              eff
 1.334230      3.3333335E-02  9.2949018E-02  5.1667136E-03  9.543975
 2.668460      6.6666670E-02  9.3736432E-02  5.8262111E-03  17.07069
 4.002689      0.1000000      9.0417132E-02  6.1535467E-03  23.38543
 5.336920      0.1333333      8.4391870E-02  6.4949649E-03  27.57291
 6.671149      0.1666667      7.5357854E-02  6.2855203E-03  31.80213
 8.005379      0.2000000      6.4933285E-02  6.1565619E-03  33.57215
 9.339608      0.2333333      5.3078841E-02  5.8659194E-03  33.60332
 10.67384      0.2666667      4.0312979E-02  5.9066443E-03  28.96630
 12.00807      0.3000000      2.5980230E-02  7.4703521E-03  16.60517
 13.34230      0.3333333      1.2659688E-02  4.1861678E-03  16.04373
 14.67653      0.3666667     -2.8156661E-03  3.7533133E-03  -4.377820
 16.01076      0.4000000     -2.0289032E-02  3.3978035E-03  -38.01397
 17.34499      0.4333333     -4.0042102E-02  2.8871584E-03  -95.65076
 18.67922      0.4666667     -6.3114293E-02  2.2053584E-03  -212.5570
 20.01345      0.5000000     -9.1633849E-02  1.5743456E-03  -463.1759
 21.34768      0.5333334     -0.1268936      9.7573374E-04  -1103.893
```

Figure 2.5: Sample output from PPT2.

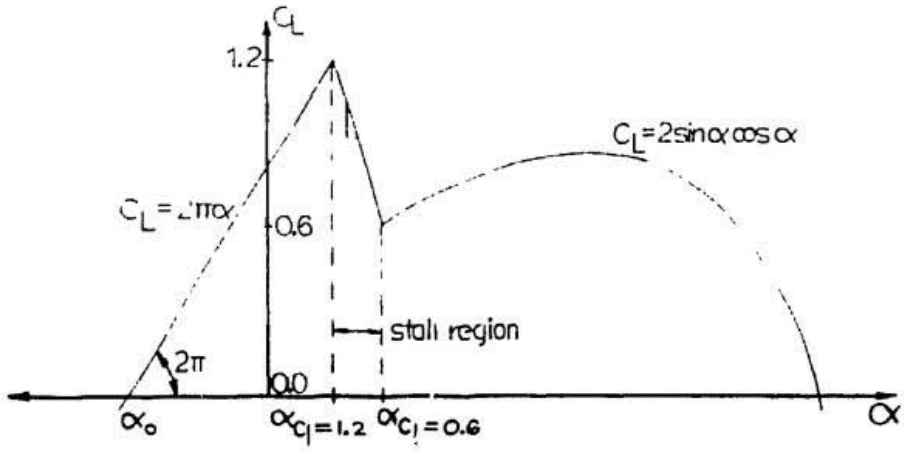

Figure 2.6: Ideal lift model.

TRULFT

The idealized lift model was represented in this subroutine. Figure 2.6 shows the lift curve of this model.

The lift model was idealized to incorporate reasonable lift characteristics for a wide range of lift curves corresponding to varying angles of incidence. From thin airfoil theory it is known that the pre-stall lift curve has a slope of about 2π for airfoil shaped sections. The stall region generally varies considerably with angle of attack while the post-stall region of the curve for thin airfoils can be approximated by the equation $C_l = 2\sin\alpha\cos\alpha$ (Hoerner and Borst 1985, Abbott and von Doenhoff 1945, 1959). As an upper limit on lift Bose (1983) chose $C_l = 1.2$ as a conservative average value. The initial section lift is linear according to thin

airfoil theory and varies from some negative value (if the angle of attack is less than the zero lift angle) to the maximum value with a slope approximately equal to 2π. From analysis of experimental data for circular arc airfoil sections, the lift slope for these sections was actually found to be less than this value: 1.58π (see section on subroutine STNTYP). The stall region was then defined as between the angles of attack corresponding to $C_l = 1.2$ and $C_l = 0.6$. The lift in the stall region is taken as a straight line between these two values with a negative slope. The post-stall region is as defined above. This region begins where the angle corresponds to $C_l = 0.6$.

The subroutine STNTYP is called from within TRULFT to give the zero lift angle, α_o, and the lift slope, $dC_l/d\alpha$, depending on the section type chosen during the input stage. The type of section chosen can be varied along the span.

The stall angle for the section is calculated,

$$\alpha_{stall} = \frac{C_{l\ stall}}{2\pi} + \alpha_o$$

and together with the zero lift angle sets the position of the model. Therefore, having determined the appropriate lift model for the section, the lift coefficient is calculated at the current angle of attack.

STNTYP

The user has a choice of three airfoil section types. In this subroutine, the characteristic zero lift angle, α_o, the ideal lift coefficient, C_{li}, and the lift slope $\frac{dC_l}{d\alpha}$ are defined. The first two choices are NACA meanlines commonly used in propeller design: NACA a=1.0 and a=0.8 (Abbott and von Doenhoff 1945, 1959). The third choice is circular arc sections. Although the circular arc sections are obsolete for aircraft, they are still used extensively for standard propellers. For example, the B-series propellers have airfoil sections on the inner radii and circular arc sections on the outer radii. Very little published data were available for circular arc sections.

During the first quarter of the 1900's a large number of systematic and arbitrary airfoil sections were tested at Göttingen, Germany. Among these was a series of roundback sections which were tested under varied cavitation numbers. Riegels (1961) published the compiled results of many tests. These sections, the Gö xx K circular back sections, included data in tabular and graphical form. These data were not useful for programming purposes in their published form and incompatible with standard ways of representing airfoil data for design purposes.

By first plotting the experimentally measured lift coefficients with respect to the angle of attack and fitting a second order curve to them, the lift curves were found for each section type in the series. Figure 2.7 shows some typical lift curves for these sections.

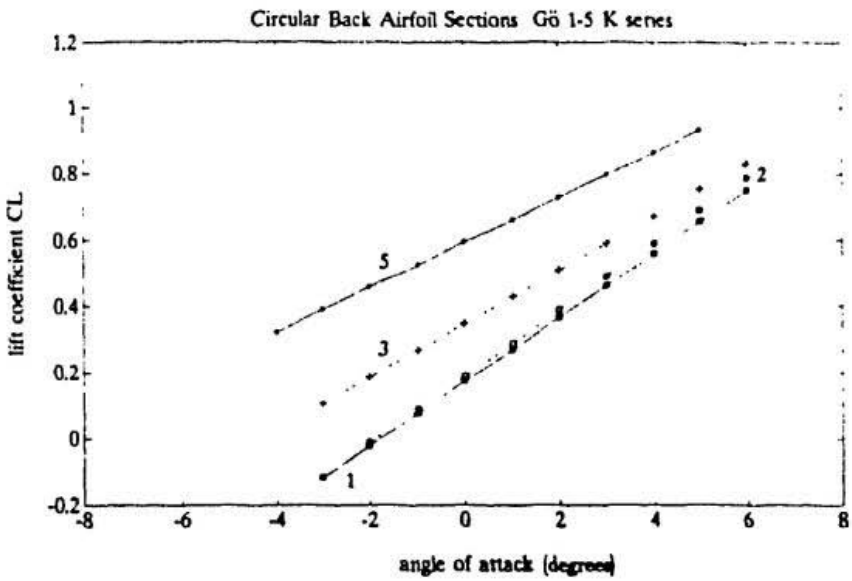

Figure 2.7: Experimental lift curves for typical Göttingen circular arc airfoil sections.

The zero lift angle was then determined with respect to the camber/chord ratio and plotted as shown in figure 2.8. A linear relationship was found between the zero lift angle and the camber/chord ratio for these sections.

The lift corresponding to an angle of incidence equal to zero was termed the design lift coefficient, C_{l_i}, for propellers, as propellers are usually designed for shockless entry. By plotting C_{l_i} with respect to camber/chord ratio, m/c, for all the sections in the series (omitting the "fat" sections with rounded off ends) and then fitting a straight line to the data through a regression routine, a linear relationship was established between C_{l_i} and m/c. This could be expected since thin airfoil theory assumes a linear variation of lift with camber. The actual values are plotted along with the straight line through them in figure 2.9 for thin and thick sections.

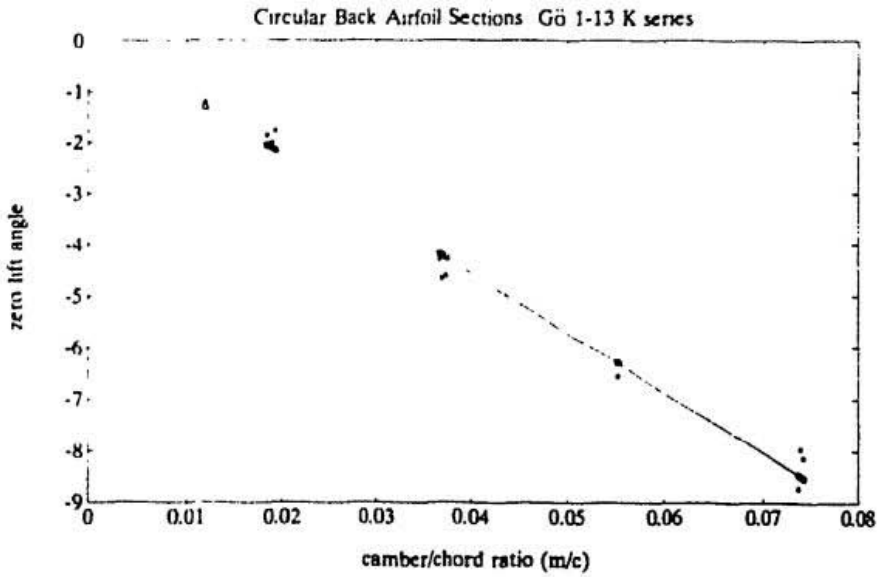

Figure 2.8: Zero lift angle varies linearly with camber ratio.

The first straight line is for thin sections and the second line with a lower slope is for thick sections as defined below.

This subroutine uses published data directly for the NACA sections, but for the circular arc sections, it uses the following equations: the zero lift angle in degrees is,

$$\alpha_o = -115.6622\frac{m}{c} + 0.0635.$$

For thin sections (m/c < 0.055) the ideal lift coefficient is,

$$C_{li} = 9.7942\frac{m}{c} + 0.0077,$$

while for thick sections (m/c > 0.055) it is,

$$C_{li} = 5.6046\frac{m}{c} + 0.2292$$

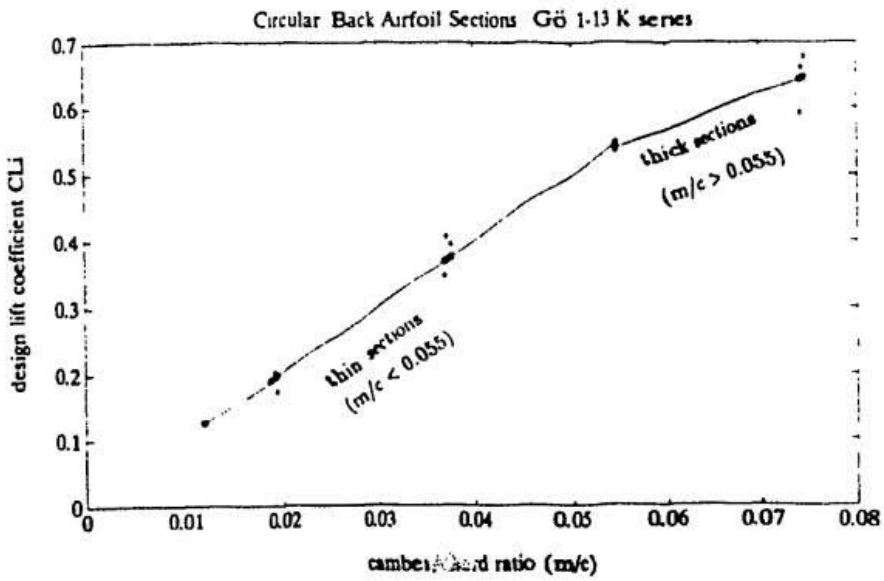

Figure 2.9: Design lift coefficient variation with camber ratio.

where m/c is the section camber ratio.

ATTACK

Once the interval has been determined where the model and the theoretical lift coefficients are similar, the subroutine ATTACK is called to determine the angle more accurately and then calculate the corresponding lift coefficient.

The procedure used was as follows. Having found the one degree interval within which the sign of the difference changed to negative, the angle for which the last positive difference was calculated was taken as the starting point. The angle was then stepped-up by 0.05 degrees and the lift coefficients re-calculated by calling NUMLFT and TRULFT subroutines. At each increment the difference was used

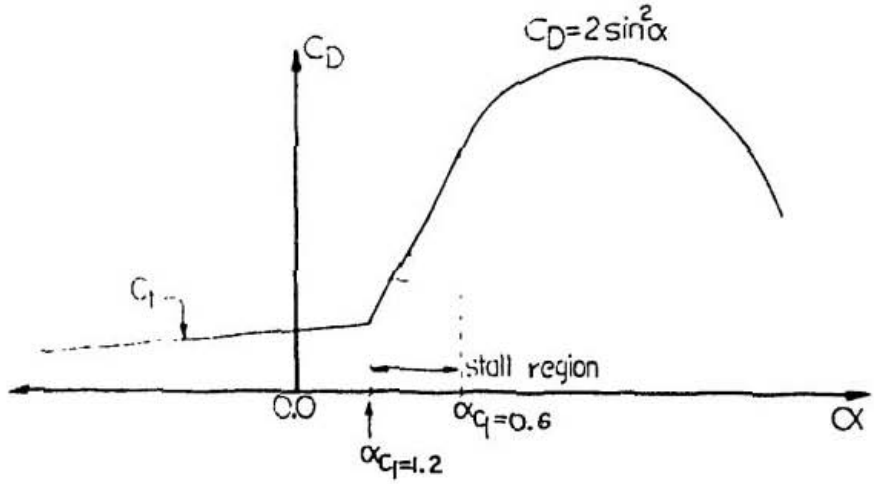

Figure 2.10: Thin airfoil drag model.

to find the crossing point. The exact angle of attack was taken as the average of the two values bracketing the step where the difference again went negative. The final lift coefficient, C_{lta}, was then calculated for that angle. Therefore, the angle of attack was determined within 0.05 degrees along with the corresponding lift coefficient.

DRAG

This subroutine calculated the drag of an airfoil section. For the NACA thin airfoils an idealized model was used (Bose 1983). This model is shown in figure 2.10.

The initial drag, up to the angle where stall occurs, was taken as the Prandtl-

Schlichting flat plate friction which depends on Reynold's number.

$$C_f = \frac{0.455}{(log\ R_e)^{2.58}}$$

In the stall region, the drag is approximated by a straight line between the stall angle and the beginning of the post-stall region at an angle of attack corresponding to C_d=0.6. In the post-stall region, the drag curve is given by $C_d = 2\sin^2\alpha$ (Hoerner and Borst 1985, Bose 1983).

For circular arc sections, data published by Riegels (1961) was used. The usual way C_d is represented for airfoils is an equation of the form

$$C_d = 2C_f(1 + a\frac{t}{c}) + b(C_{l_i} - C_l)^2 \qquad (2.46)$$

where a,b,and c are constants. The first term is the drag due to section thickness and the second is that due to lift and angle of attack. Figure 2.11 shows the drag coefficient variation with angle of attack form the first four sections in the series. These curves are typical for the entire series of airfoils.

The published data in Riegels does not state at which Reynold's number the tests were done. Therefore, Reynold's number could not be scaled. The C_d for Göttingen series airfoils was plotted with respect to thickness/chord ratio, t/c. Figure 2.12 shows the linear dependence of the minimum drag coefficient on the section thickness/chord ratio. A linear equation was derived by regression analysis

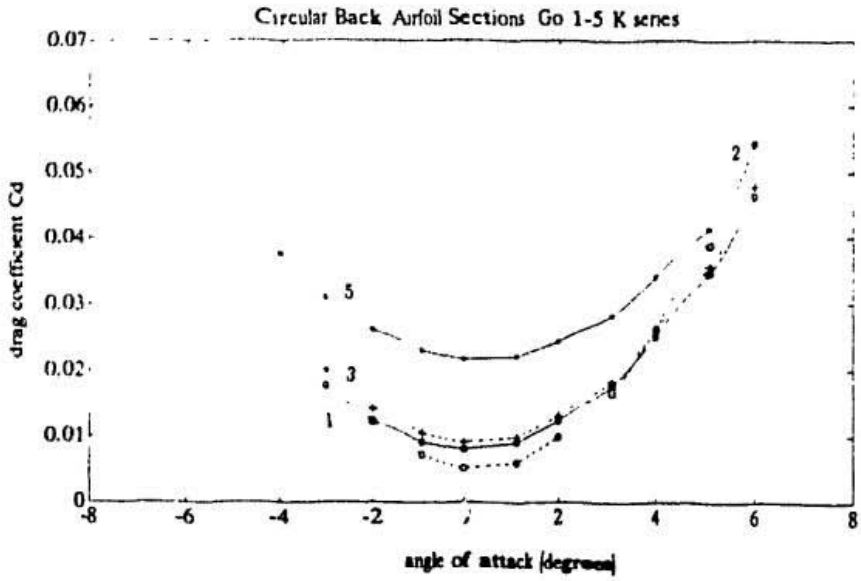

Figure 2.11: Gö xx K circular arc section drag data.

to fit the data so that the drag could be calculated directly.

$$C_d = 0.0800\frac{t}{c} + 0.0024$$

By calculating and plotting the difference in lift coefficient and design lift coefficient with respect to the incremental increase in drag, a quadratic relationship was found.

$$\Delta C_d = 0.0786(C_L - C_{Li})^2 + 0.0162(C_L - C_{Li}) + 0.0004$$

The total drag coefficient due to both thickness and variation of angle of attack for Göttingen circular arc airfoil sections was derived as:

$$C_D = 0.0028(1 + 28.57\frac{t}{c}) + 0.078(C_L - C_{Li})^2 + 0.0162(C_L - C_{Li})$$

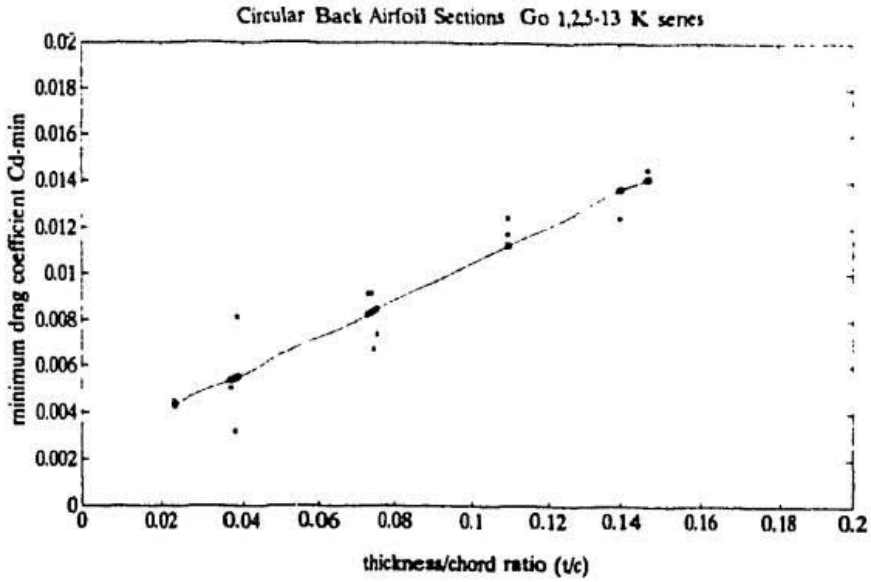

Figure 2.12: Drag variation with thickness ratio.

The form of this equation was the same as for standard thin sections, but it contained an extra term in $(C_L - C_{Li})$. This implied that the circular arc section drag is more sensitive to changes in angle of attack than the streamline airfoil sections.

This equation was applied in place of the flat plate formulation in the pre-stall operating condition and was assumed for all circular arc airfoils. The rest of the drag curve was defined as for the NACA sections.

GOLST1

This subroutine is called whenever the Goldstein factors, κ, for periodicity of flow are required. They are calculated as a function of blade number, advance ratio and radial location of the section. The κ values are published in the form of curves on

a graph for easy reference during hand calculations (see for example, Eckhardt and Morgan 1955). To make these curves more useful numerically, regression analysis was done on the curves to produce second order equations of the form,

$$\kappa = a + b\lambda_i^{-1} + c\lambda_i^{-2}$$

for blade numbers 3,4,5 and 6 and radius fractions 0.3 to 0.9 (a,b and c are constants).

GEO,LSQUARE,GAUSS

The propeller blade geometry could be supplied to the program at arbitrary radial locations in the form of camber/chord, chord/diameter and thickness diameter ratios. The subroutine GEO took these values and using the least squares regression routine LSQUARE redefined them at the appropriate section radii. LSQUARE used the subroutine GAUSS to solve the system of equations which produced, for each set of data, a second order polynomial from which the desired values were calculated.

2.2.4 Results of propeller analysis

To evaluate the accuracy of PPT2 results, a series of six B-series propellers were analysed by using the program. The six propellers were: B3.50, B4.40, B5.60 with pitch/diameter ratios equal to 0.8 and 1.0. The same six propellers were also anal-

ysed by using a program, BKTKQ, written to calculate the propeller coefficients for the B-series propellers from the multiple regression polynomials of the experimental results (Lewis 1988). The thrust and torque curves were plotted by using MATLAB software produced by The Math Works Inc. All results for a particular propeller were plotted on the same graph for easy comparison. It was readily apparent that the lifting line theory used in PPT2 under-estimated the experimental results. To verify that the differences could be attributed to lifting line and blade width effects, the same six propellers were analysed at three values of advance coefficient using the MIT-PSF-2 lifting surface program. These results were also plotted on the same graph for each propeller. In most cases the lifting surface program results coincided very closely with the experimental results. At low advance coefficient (J=0.15), the PSF-2 results differed from the experimental results for both the B3.50, P/D=0.8 case and the B5.60, P/D=1.0 case. Appendix H gives the performance curves for all the propellers analysed. However, at higher calculation points, J=0.4 and 0.8, the PSF-2 points fell very close to the curves for K_t and K_q. The two four bladed propellers showed the best agreement between the PSF-2 and the experimental results; the data points coincided almost exactly (Appendix H). These plots showed that the errors in the PPT2 results were primarily attributable to differences in the two theories. Figures 2.15 and 2.16 show the results of all three programs on the same graph. The solid curves with the stars show the experimental results while the cir-

cles show the points calculated by using the MIT-PSF-2 program. The broken line curves show the lifting surface corrected results of the PPT2 calculations. These calculations were done for all six propellers. The results from B4.40, P/D=1.0 and B5.60, P/D=0.8 demonstrate the best and worst cases, in figures 2.15 and 2.16, respectively.

An attempt was made to generate a set of lifting surface corrections for PPT2. These corrections would also be valid for the lifting line design program, but in the design case these would be applied as a pitch and/or section camber correction. The approach taken to find suitable corrections was to first compute the differences for all the thrust and torque coefficient data points available from the analysis of the six propellers. These differences were normalized by dividing them by the value calculated from PPT2 (called difference factors). These difference factors were then plotted with respect to the advance coefficient. For thrust, figure 2.13 shows the grouping of the factors for P/D=0.8 and P/D=1.0. These curves clearly imply some relationship dependent on advance coefficient and pitch/diameter ratio. The thrust differences between experimental and PPT2 results tended to increase with higher J values. Propeller blade loading increases with advance coefficient; therefore, it could be expected that the lifting line approximation will be affected more under higher loading conditions. That is, the rotational effects have a larger influence; the radial induced velocities, which are assumed zero in lifting line theory, have larger

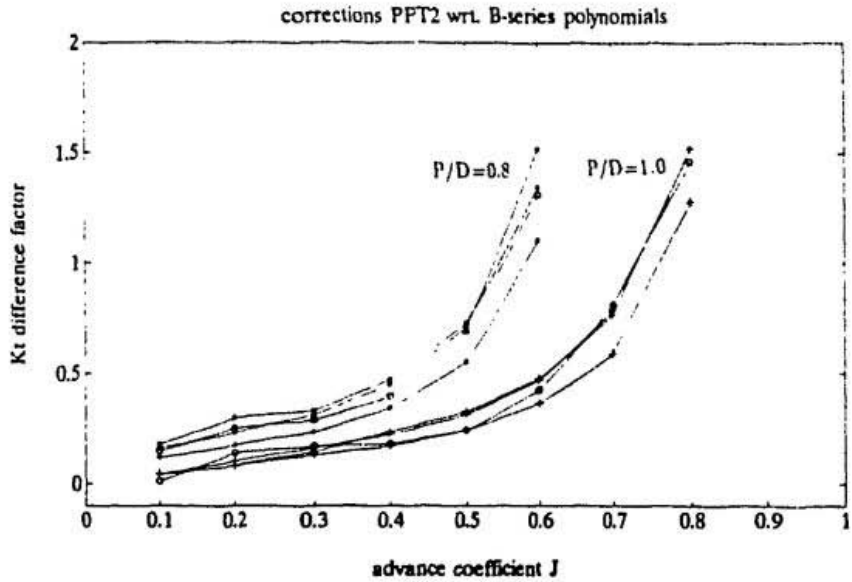

Figure 2.13: Thrust difference factors.

values. The cubic nature of the difference factor curves were produced by dividing the differences by increasingly small values of thrust coefficient during normalizing.

As the difference factor curves were grouped by P/D, varying a maximum amount of about 15-20%, the curves for all the propellers with the same P/D were combined. This produced a single relationship which could be used in direct calculations to correct the thrust coefficient of PPT2, depending essentially on blade loading.

As a first approximation, the thrust differences were averaged for each group of P/D curves and curve fitted in a least squares sense to a third order polynomial. These were then applied as two equations which modified the PPT2 thrust

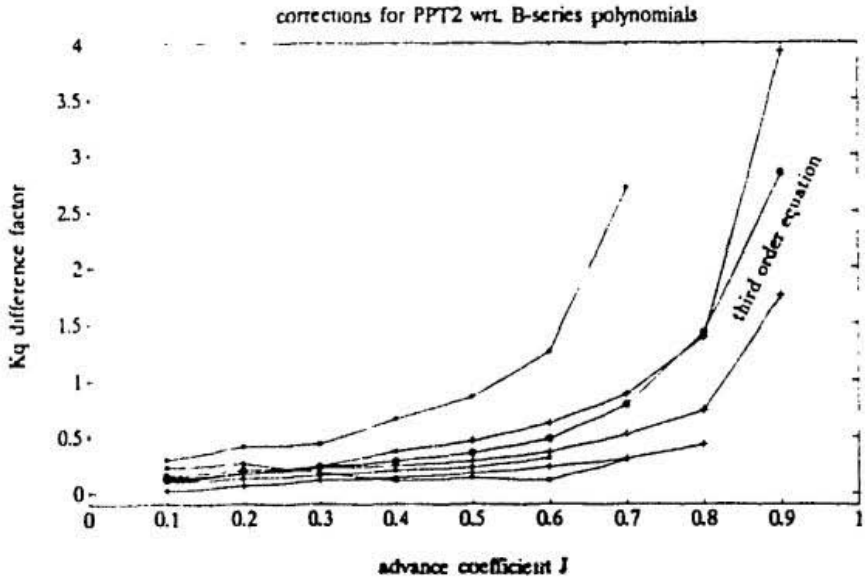

Figure 2.14: Torque difference factors

coefficients. For P/D=0.8 the difference factor is given by:

$$\Delta K_t = 21.6241J^3 - 16.2785J^2 + 4.4236J - 0.1558$$

and for P/D=1.0 the factor is given by:

$$\Delta K_t = 12.1919J^3 - 12.0786J^2 + 4.0395J - 0.2838$$

where the difference factor ΔK_t is defined as

$$\Delta K_t = \frac{K_t^{B-series} - K_t^{PPT2}}{K_t^{PPT2}}$$

and the corrected value of Kt was found from

$$K_{t\ corrected} = \Delta K_t \times K_t + K_t$$

The torque factors did not show any obvious classification. Figure 2.14 shows the variation of the torque factors. It was not clear from the results of the six propellers, in what way the lifting surface corrections for torque should be formulated. Torque is largely dependent on the component of drag which varies with angle of attack (the $(C_{L_t} - C_L)$ terms in equation 2.46). The drag component due to thickness has a smaller effect over the operating range of a propeller. A much larger number of propellers need to be analysed to determine the best way these corrections and their dependence can be formulated.

As a first attempt, the torque correction was taken as the mean of the difference factors for all the propellers, producing a single third order equation

$$\Delta K_q = 17.0107J^3 - 18.3133J^2 + 6.1630J - 0.3628$$

which was applied to the calculated values of torque in the same way as for thrust.

The results of these calculations showed a substantial improvement in the thrust estimates. Figure 2.15 and 2.16 show the results for B4.40, P/D=1.0 and the B5.60, P/D=0.8 propellers.

The thrust corrections reduced the errors between the K_t curves of the experimental results and PPT2 points. In all cases tested, the thrust coefficient curves were under estimated with PPT2. The differences varied from about 5% (B5.60, P/D=1.0) to over 30% (B3.50, P/d=0.8). The largest errors occurred at high advance coefficient and the smallest errors at low advance coefficient. The error

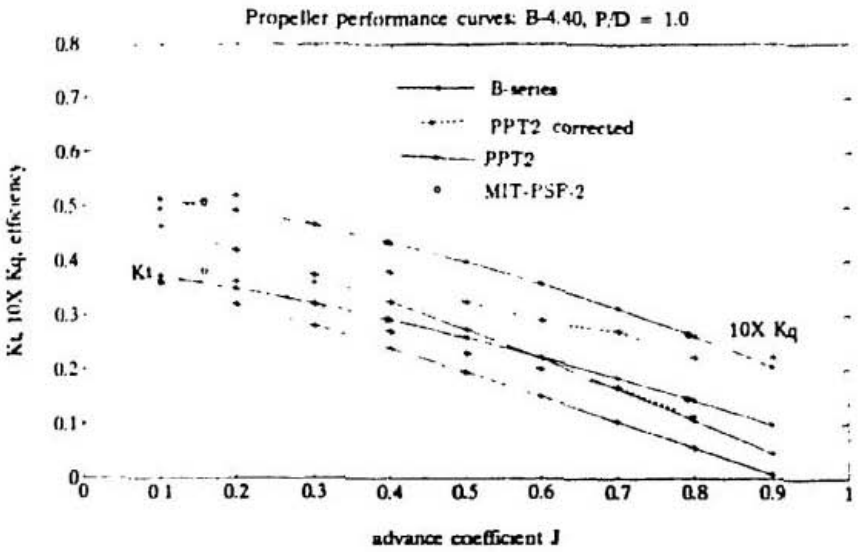

Figure 2.15: K_t, K_q and η curves for propeller B4.40, P/D=1.0 .

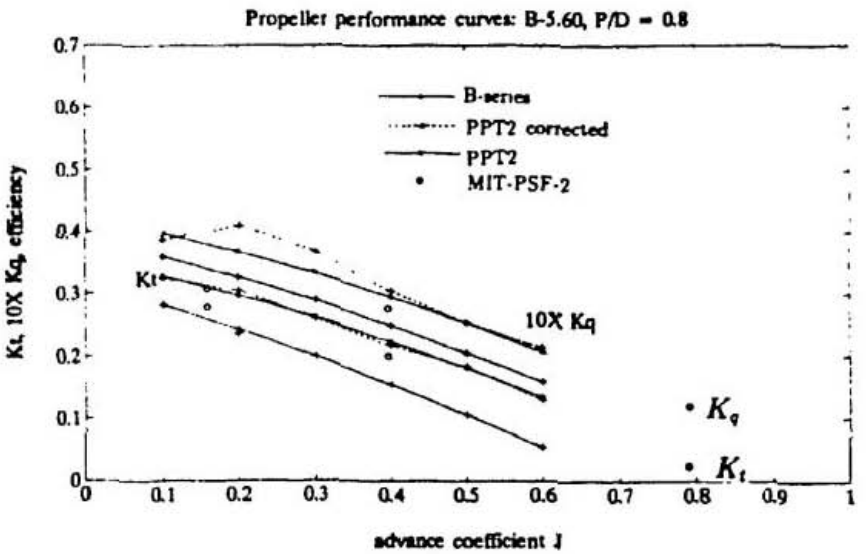

Figure 2.16: K_t, K_q and η curves for propeller B5.60, P/D=0.8 .

distribution increased with J values in some cases. By applying the lifting surface corrections as described, the errors were reduced to between 0% and about 10%. However, the lifting surface corrected thrust curves produced were not smooth curves. It may be possible to produce smooth curves, which better approximate the experimental curves by least squares fitting the difference factors directly instead of their average values. This approach may produce better results if a much larger set of data points were available. Alternatively, the corrected results could be approximated by fitting a curve to produce a smoothed result. This may help reduce some of the arithmetic inconsistencies in the numerical work.

The torque curves showed similar trends as the thrust curves between the experimental and the PPT2 results. The differences increased with J value. The smallest differences, occurring at low J, were about 3% (under-estimate) and the largest differences at high J values were about 100% in the best and worst cases respectively (B4.40, P/D=0.8 and P/D=1.0). The crude correction to torque was applied to the PPT2 results. The points produced now over estimated the B-series $K' - q$ curves in all the propellers tested except for B4.40, P/D=0.8. This could be expected because the difference factor curve in figure 2.14 for this propeller is substantially different from the others which were loosely grouped together. As is apparent in figures 2.15 and 2.16, the lifting surface corrections formulated in this way do not produce as good agreement as did the thrust corrected curves. The

torque curves now over-estimated the B-series results by about 10-15 % for the B5.60, P/D=0.8 propeller, and under-estimated the torque by as much as 40% for the B4.40, P/D=1.0 propeller at high advance ratios. However, as the propellers under consideration usually do not operate at advance coefficients above 0.5, say, it could be argued that the errors may be accepted as conservative engineering estimates when taken as a first approximation in the context of conventional propellers for fishing vessels.

This approach to lifting surface corrections seems promising for thrust, but a much enlarged body of data is needed to produce a comprehensive set of corrections for general work. Lifting surface corrections for torque require further work on a much larger series of propellers.

2.2.5 Discussion

Lifting line performance analysis of a propeller introduces another level of complexity over initial design in that the propeller blades, while usually being designed for shockless entry, do not necessarily operate under shockless conditions. That is, they usually have some angle of attack which will vary along the span. The performance of the airfoil sections and their individual contributions to the propeller thrust and torque must be accounted for. The lifting surface approach on the other hand considers the entire "wing" at once. This is the fundemental difference between the

two approaches. Each has its limitations.

By introducing the airfoil lift and drag models, and by allowing a variation in the type of section across the span, a better estimate of section performance is achieved over the entire operating range of the propeller.

The program PPT2 was shown to produce reasonable results for conventional propellers. It calculated the thrust and torque coefficients and the propeller efficiency by taking into account the type of airfoil sections, the geometric properties of the sections and viscous flow. By calculating the angle of attack at which individual sections operate, the lift and stall characteristics were accurately predicted. The discrepancies between lifting line and lifting surface theories were approximately accounted for by deriving appropriate corrections. Hence, the propeller performance was calculated over its entire useful range.

Chapter 3

Propeller tests

3.1 Scale model construction

The *MV SUGAR* was built in 1986 by Jackson's Boatbuilders at Whiteway, Trinity Bay, Newfoundland. It is a typical inshore fishing boat hull of about 10m (36'-0") in overall length built with some minor adjustment of the frame templates to reduce the deadweight capacity of the boat. The owner, Mr. Max Clarke intended the vessel for pleasure use only; therefore, he did not require the displacement normally found in these vessels. It was built of spruce planking over sawn frames in the typical robust Newfoundland tradition. The engine was a 65 HP Kubota marine diesel driving a three bladed bronze propeller through a rigidly connected shaft and a reversing reduction gear. For further details about the vessel see Appendix E.

As part of an undergraduate workterm project the author measured the hull of the vessel while it was hauled out for the winter (Hofmann 1989b). A lines and body plan was drawn from these measuremnts to 1/2"=1'-0" scale to determine the basic hull characteristics and estimate resistance. The original lines plan was expanded to 1/5 scale during the fall of 1990 and re-faired by hand. It proved to be a difficult task to fair the larger scale lines and still maintain the characteristic shape of the hull. This was due to inaccuracies in the measurements of the offsets from the small scale lines plan and the magnification of these errors.

A 1/5 scale model was constructed from pine laths over plywood frames and covered in glass reinforced plastic (GRP) in the spirit of cold moulded boat building (see the photographs at the end of the section). To facilitate the setup and construction of the model, a common datum for all frames was chosen in line with the stemhead. The frames were then cut out and chamfered according to the sections from the bodyplan. They were precut leaving tabs so that the centres of the frames could be removed after completion of the hull leaving the skeleton in place (photo 1). The frames were set into the keel about 3/4" and then located and screwed to the work table. The plywood laminated keel was slotted to receive the copper stern tube. Once the copper tube was in place the slot was filled in with epoxy filler. The resulting skeleton was lathed over by glueing and stapling the pine lathes to the edges of the frames (photo 2). The staples were removed after

the glue had dried and the surface then hand-planed to remove exposed edges and sawcut roughness (photo 3). The rough lathe surface was filled and smoothed with filler and then covered with a single layer of woven glass fibre cloth and wetted out with polyester resin. The hardened shell was again filled with autobody filler and the entire surface sanded to a very smooth surface (photo 4). When everything had cured, the hull was released from the table and set into the cradle. The centres of the frame panels were removed by cutting out the tabs holding them in place (photo 5). The interior was cleaned and sealed with thinned resin. It was found that the hull was very fragile to puncture, so a layer of GRP was applied on the inside panels between frames to strengthen them. The top edges of the hull were strengthened and finished by laminating a wooden rubbing bar on the outside along the edge and fitting a gunwale around the top along the inside edge. These were then also fibreglassed into place. This helped to stiffen the hull and provided surfaces for mounting the towing gear. The model was then spray painted to a glossy smooth finish with four coats of white *CENTURI* epoxy paint by an autobody shop (photo 6,7 and 8).

There was some difficulty in obtaining a good scale propeller for the self propulsion tests. However, it was possible to borrow a four bladed propeller from the NRC - Institute for Marine Dynamics. This propeller was a crude one intended for use by hobbyists. It was reconditioned to improve its performance. Reconditioning

Table 3.1: Model propeller characteristics.

Diameter	90 mm
Pitch/diameter ratio (P/D)	0.82
Expanded area ratio	0.62
number of blades	4
blade outline shape	elliptical
turbulence stimulation	1.5 mm strips along L.E. both sides of blade

consisted of trimming the blades as required to make them reasonably uniform in size and shape. The pitch was adusted on two of the blades so that all of the blades had a uniform pitch. The propeller was reworked so the thickness of the blades were approximately the same and then statically balanced. A cloth wheel was used to polish the propeller to a high gloss.

To help in scaling the Reynolds number by inducing turbulence at the leading edges, a 1.5 mm wide strip of fine grained white sand was glued to the leading edges of the blades on both the pressure and suction sides extending from the hub to about the 0.95R radius. The two part epoxy used in the bonding of the sand to the blade worked quite well; however, the sand needed to be renewed after about two weeks of testing. The reconditioning work was done by the author by using the facilities at Avalon Propulsion Systems Ltd., St. John's. Model propeller characteristics after reconditioning were as given in table 3.1:

Both open water propeller tests and self propulsion tests and resistance tests on the

MV SUGAR model were done by Dr. Shukai Wu, a post doctor fellow (WU 1991). Photographs 9 and 10 show the model in the towing tank at Memorial University undergoing tests.

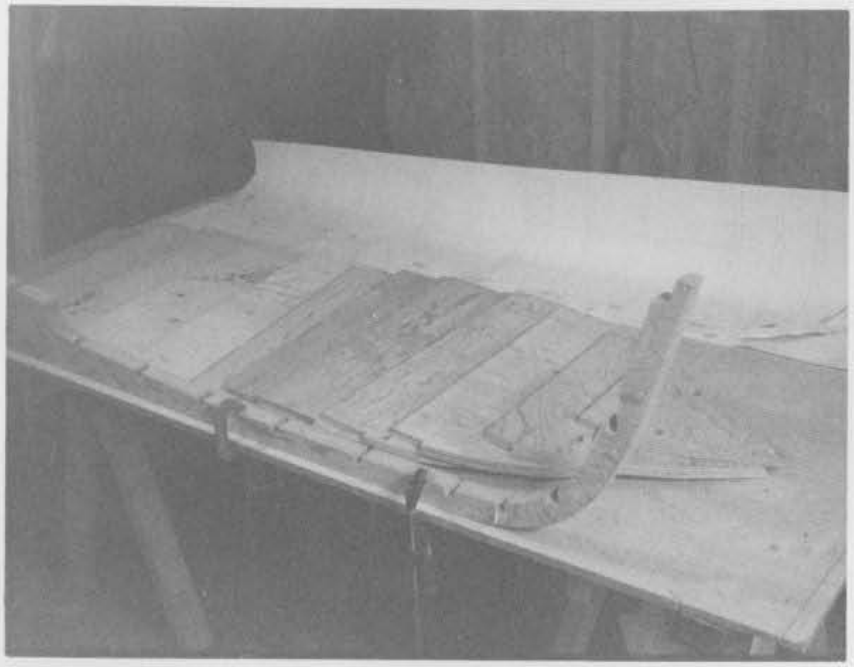

photo 1

photo 2

photo 3

photo 4

photo 5

photo 6

photo 7

photo 8

photo 9

photo 10

3.2 Existing propeller analysis

An analysis was done on the existing propeller of the *MV SUGAR* to determine its performance charcteristics by using the performance program PPT2. The propeller was a standard Osborne Propellers Ltd. design for small craft and was measured in detail so that accurate section profiles could be drawn and the required relationships for program inputs could be determined. The sections of the propeller blades were measured and drawn. The propeller characteristics and section profiles are given in Appendix F. The peculiar shapes of the profiles is apparent. The maximum thickness lies well back from the mid-chord instead of ahead of the mid-chord as would be expected for many airfoil sections or at mid-chord for circular arc sections. A possible explanation could be as follows. The pattern from which this propeller was cast was an aluminum, three bladed one. It originally had circular sections with maximum thickness near or at mid-chord. However, at some point a propeller was required with a lower blade area, so the pattern was trimmed at the trailing edge. This left the odd section shapes. Although this is standard practice, because it is much cheaper to alter patterns where possible than make new ones, it underlines the lack of understanding often encountered in the small vessel equipment industry. A much better approach would have been to trim the leading edge. This would have resulted in a better airfoil shape and may even have improved performance (or at least not reduced it).

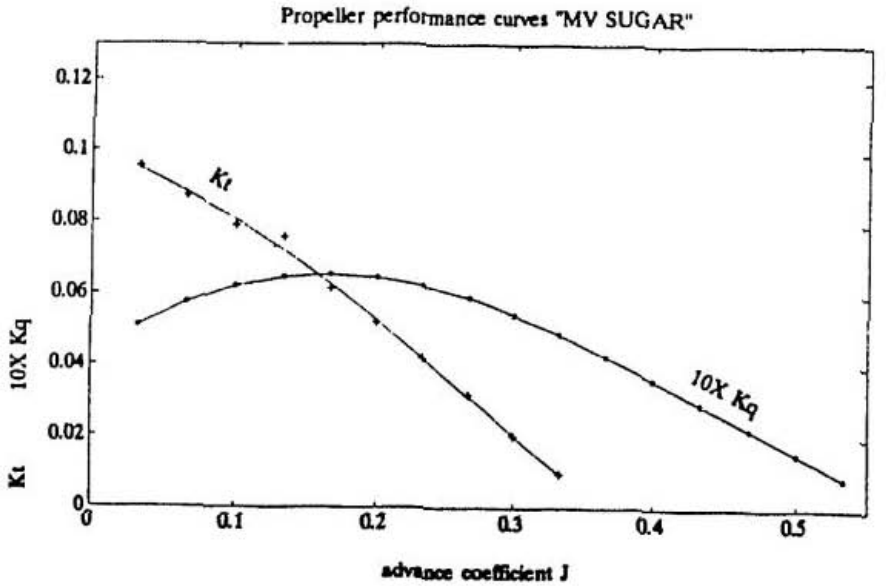

Figure 3.1: *MV SUGAR* propeller curves.

The basic section data were used as inputs to the computer program to generate the performance curves in open water (zero wake). These performance curves were generated using the program PPT2 (figure 3.1).

The propeller curves shown in figure 3.1 are the uncorrected PPT2 results as no lifting surface corrections are yet available for pitch ratios other than 0.8 and 1.0.

3.3 Instrumentation of the propeller shaft

To enable the measurement of thrust and torque on a full scale vessel, a propeller stub shaft was designed and manufactured. In the the case of the *MV SUGAR* a new propeller shaft with a removable section was also manufactured and installed while on the *MV BECKY A*. the stub shaft was inserted into the existing shaft line.

The stub shaft contained strain gauges; therefore, the average propeller thrust and torque could be measured directly while the vessel was under way. The signals from the Wheatstone bridge circuits were transmitted to amplifiers through slip rings so that the variations of thrust and torque with shaft revolutions (rpm) and ship speed could be recorded. From a series of trial runs at different speeds, the performance curves of the propeller in operation behind the vessel could be generated and plotted. These results could then be compared with the calculated values.

A short hollow stub shaft was designed, to which the strain gauges were bonded. As space was very restricted on board, a set of slip rings were fabricated to fit over the instrumentated segment of shaft to form a compact removable unit (see Appendix D). The final design used two independent Wheatstone bridge circuits each of which was made up of two strain gauge rosettes (four rosettes in total). Each bridge was therefore made up of four single strain gauge legs. The bridges were excited using a Vishay Measurements Group 2100A strain gauge conditioner and amplifier system. The signals were transmitted through eight copper slip rings via sixteen modified carbon machine tool brushes. The thrust and torque data were recorded on a two channel pen recorder. The whole system was powered on board the vessel by a HONDA EX650 portable generator supplying 120 VAC at 60 Hz with a 550 VA output rating.

3.3.1 Strain gauges for torque measurement

The Wheatstone bridge for torque measurement consisted of two 2-element 90° rosettes (Micromeasurements type CEA-06-187-UV-350) mounted 180° apart on the hollow bored section of shaft. The shaft section was dimensioned to give adequate shear strain due to angular deflection under load. Drawing number 994290-23 in Appendix D shows the arrangement. The inside and outside diameters of the hollow shaft section were determined iteratively by using the direct surface stress equation derived from Mohr's circle analysis of a cylindrical section under torsional load. The total strain was determined from the relation

$$E\epsilon = 2(1+\nu)\tau$$

where, $\tau = TR/J$, is the shear stress; E is Young's modulus; ϵ is the strain; ν is Poisson's ratio; T is the applied torque; R is the radius to the outer surface; and J is the polar moment of inertia of the section.

For a Wheatstone bridge where all legs have equal resistance, the following relationship can be derived for the change in output voltage in terms of the supplied voltage (Dally and Riley 1965).

$$\Delta E = \frac{V}{2}\left(\frac{\Delta R_1}{R_1} - \frac{\Delta R_2}{R_2} + \frac{\Delta R_3}{R_3} - \frac{\Delta R_4}{R_4}\right)$$

As the strains can be assumed to be equal,

$$\epsilon = \epsilon_1 = \epsilon_2 = \epsilon_3 = \epsilon_4$$

and therefore the changes in resistance of the strain gauges are equal,

$$\frac{\Delta R_1}{R_1} = -\frac{\Delta R_2}{R_2} = \frac{\Delta R_3}{R_3} = -\frac{\Delta R_4}{R_4}$$

then the output to input voltage ratio is,

$$\frac{\Delta E}{V} = S_g \epsilon$$

where, S_g, the gauge factor, has a value of approximately 2.

The ratio $\Delta E/V$ is called the sensitivity. This value was used to determine the signal amplification required to achieve an acceptable full scale output signal, which was then recorded. Figure 3.2 shows the Wheatstone bridge wiring of the measuring and recording system.

3.3.2 Strain gauges for thrust measurement

Thrust was measured from the compressive or tensile axial strain in the hollow shaft section by using a Wheatsone bridge circuit similar to the one shown in figure 1. However, in this case two 2-element 90° 'tee' rosettes were used (Micromeasurements type CEA-06-125-UT-350). These also, were mounted 180° apart on the same section of shaft as the torque gauges. The correct shaft dimensions were determined such that sufficient strain could be produced at the operating thrust values according to the formula for axial stress,

$$\sigma_a = E\epsilon_a = \frac{P}{A}$$

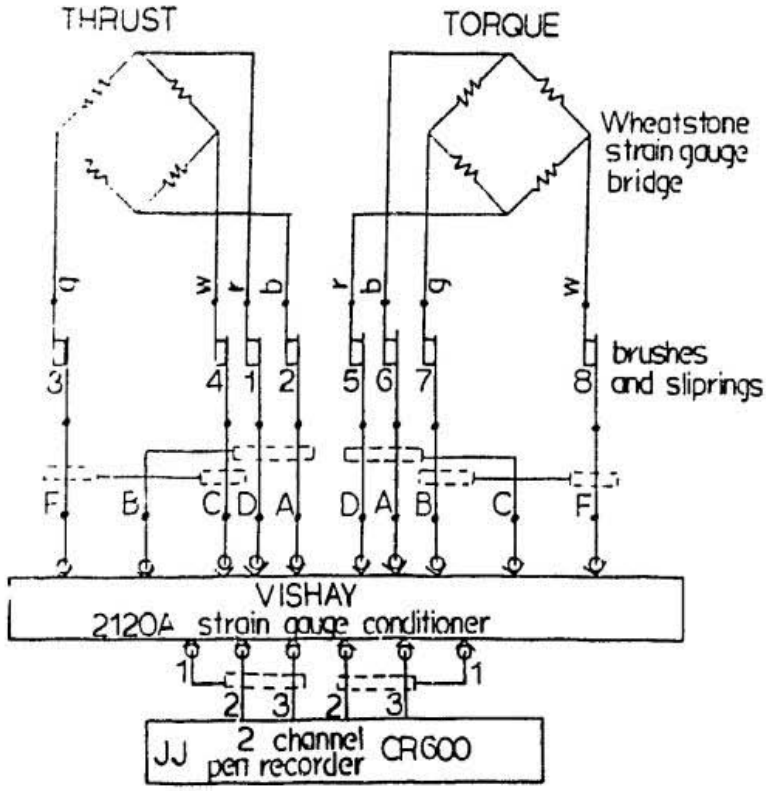

Figure 3.2: Strain gauge measuring and recording system.

where, σ_a is the axial stress; ϵ_a denotes the axial strain; P is the maximum thrust and A is the cross-sectional area of the hollow shaft section.

The strain was calculated and the output/input voltage ratio determined as before. It turned out that the thrust load was the limiting case because the sensitivity of the thrust strain gauges was very low compared with that for torque measurement. Calculations showed that the maximum stress could easily exceed the yield strength of the material and still give an output signal only about 10% of that of the torque strain gauge bridge. Therefore, fairly large amplification was required for the thrust (about 2500) while for the torque less amplification was required (about 250). This made the thrust recording more susceptible to electrical noise.

Table 3.2: Results of stress and strain calculations of the hollow stainless steel shaft. Strain gauge sensitivty for thrust and torque are given.

OD.	32 mm
ID.	19 mm
thrust	torque
design load	maximum torque
10000 N	700 Nm
compressive stress	shear stress
19.2 N/mm^2	125 N/mm^2
strain	
99.5 $\mu\epsilon$	839.4 $\mu\epsilon$
sensitivity	
0.199 $\frac{mV}{V}$	1.68 $\frac{mV}{V}$
maximum principal	stress 249 N/mm^2

Table 3.3: Material Properties: annealed 316 stainless steel shafting.

ultimate stress	620 N/mm^2
yield stress	275 N/mm^2
Young's modulus	190,000 N/mm^2
shear modulus	73,000 N/mm^2

Table 3.1 gives the results of calculations and table 3.2 gives a short summary of the shaft material properties.

3.3.3 Slip rings

When measuring propeller shaft strain, the electrical power supply and the output signals need to be transmitted from the rotating shaft to the stationary signal conditioning system and recording equipment. Two methods have been used suc-

cessfully for this purpose: 1) the White Fish Authority instrumented several fishing vessels in the United Kingdom by using slip rings (Bennet and Hatfield 1966); 2) the Japanese shipbuilders, Hitachi Shipbuilding and Engineering Company Ltd. of Osaka used radio telemetry methods (Kinoshita et al. 1962). Telemetry methods are useful for transmitting dynamic strain fluctuations, but they are quite expensive. They also have the advantage that the rings, brushes and cables can be eliminated from the circuit, thereby reducing electrical noise and making it possible to move the entire system from ship-to-ship without altering any shipboard equipment. Slip ring methods are less expensive, but they generate electrical noise which make dynamic measurements difficult. In the cases considered here, only steady thrust and torque were of interest; therefore, noise was not considered to be a serious limitation. This assumption was later proven wrong. Noise became a problem as the trials progressed. Dirt contamination of the slip rings produced so much noise at the end of the day so that the measurement signals for thrust were obscured.

Due to space restrictions on board, a new propeller shaft needed to be fabricated for the *MV SUGAR* to accomodate the removable instrumented section; however, the *MV BECKY A.* did not require another propeller shaft. The stub shaft was reduced in length to give adequate clearance by designing new shorter couplings and machining the shaft itself from eight inches in length to seven inches.

The slip rings were mounted over the hollow section and strain gauges to save

space. This also allowed the unit to be selfcontained and compact and facilitated installation and alignment of the brush holder.

Slip rings were manufactured from slices of copper tubing, these were mounted on a poly vinyl chloride (PVC) hub with insulators separating them. The arrangement is shown in drawing number 994290-23 in Appendix D and in figure 3.3. 14 gauge copper wires (insulated) were used to form terminals at the forward end of the slip ring hub and to connect the slip rings to the strain gauges. Figure 3.3 shows the stub shaft as installed on the *MV BECKY A.*. The brush holder has been released and turned down to expose the slip rings.

Brushes with holders were difficult to obtain locally. Finally, 1/4" X 1/4" carbon machine tool brushes were found which could be fitted with minor modification into Bakelite holders and then mounted on an aluminum box frame. See drawing number 994290-25 and 26 for details of mounting and arrangement. The box frame was mounted on l oard so that the brushes and slip rings were aligned both axially and transversely with retractable adjustment screws. Shielded cables of two 18 gauge wires each were then connected to the brushes and the strain gauge conditioner and amplifier and hence to the two channel pen recorder.

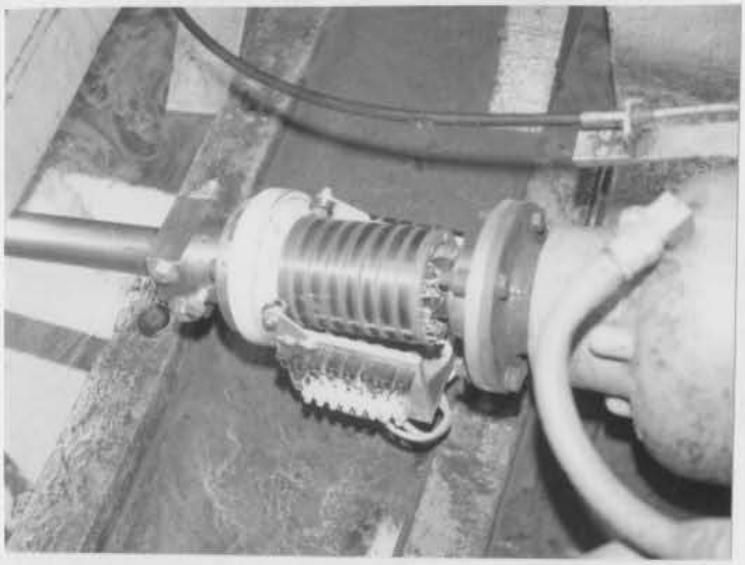

Figure 3.3: The stub shaft as installed on the *MV BECKY A.*.

3.3.4 Pen recorder

The pen recorder used to record the amplified strain gauge output signals was a two channel J.J. Lloyd Instruments Ltd., CR 600 recorder, with a maximum full scale deflection adjustable between 0 and 100 VDC and variable chart speed. This system was chosen, over computer data aquisition, because of concern about the reliability of power supply onboard the small vessel and as only steady state response data were of importance for the propeller performance analysis. In addition, small vessels rarely have a protected space where a computer could be installed and operated out of the weather; for example, on board the *MV BECKY A.*.

Figure 3.4: The *MV BECKY A.*.

3.3.5 Stub shaft calibration

The strain gauges were mounted on the hollow stub shaft by Intertechnology Limited. Final assembly and wiring of the measuring and recording system was done by the author. The shaft was calibrated by subjecting it to axial loads from an hydraulic press and then checked by using weights. Torsional loads were applied by using weights on a double lever arm. The calibration measurements were repeated several times to ensure reproducibilty of results. The torque measurements were very consistent with negligible variation between loading and unloading. The thrust calibration showed more scatter. It was difficult to establish what caused the scatter in the tests done using the hydraulic press with a loadcell. There seemed to be some inconsistency or hysteresis in the digital load readout. To verify this,

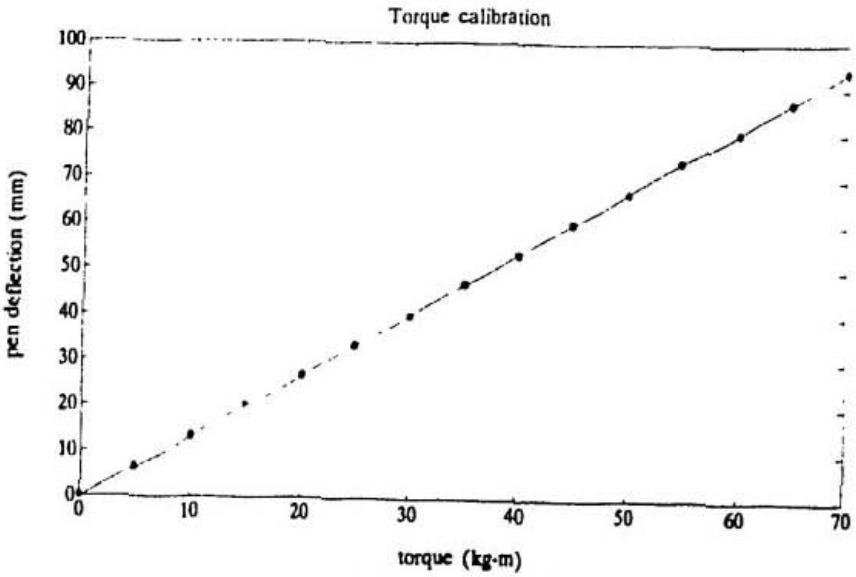

Figure 3.5: Calibration curve for torque measurement.

the shaft was end loaded using weights. However, due to the inherent instability of using free weights on the end of the shaft, it could not be loaded to full scale by using weights. The results of both calibration tests were plotted together. It could be concluded that the scatter was produced by the loadcell and not by the instrumentation of the shaft, because the loading done with weights was very consistent. The the torque strain gauge readings also produced a linear behaviour for the strain gauge bridge signals, as was expected.

The calibration results were fitted to a straight line (linear curve) using the regression and plotting routines available in the MATLAB software package. The curves are shown for both thrust and torque in figures 3.4 and 3.5.

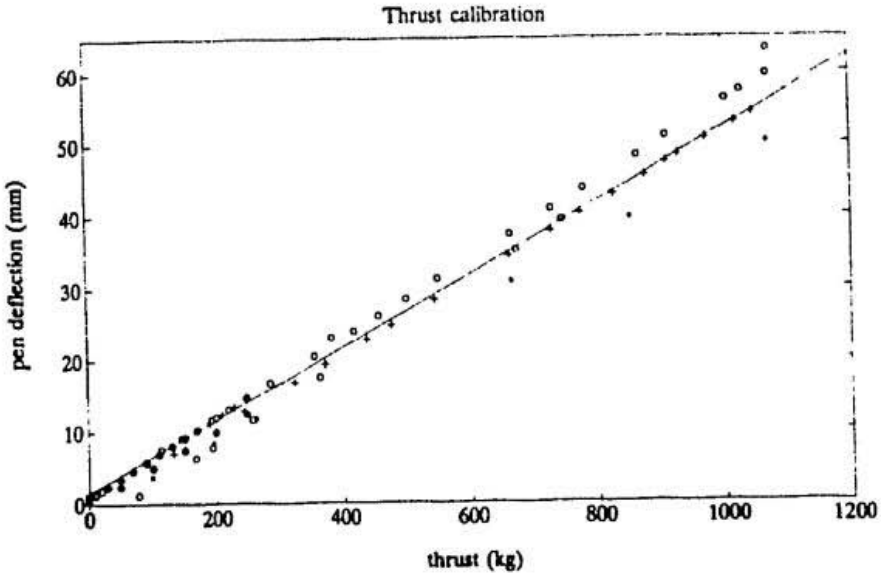

Figure 3.6: Calibration curve for thrust measurement.

3.4 Sea trials

Full scale tests were done on two typical 36' (10m) long fishing boat hulls. The *MV SUGAR* on Conception Bay and the *BECKY A.* in St.John's harbour.

The main objectives of the trials were to obtain data as about the performance of a propeller as it operates in the uneven wake behind the vessel. To do this, a series of tests were conducted whereby the propeller thrust, torque and revolutions were measured under different conditions of speed ranging from bollard to full speed. As the intention was to generate a set of points along the thrust and torque coefficient curves for the propeller, specific RPM's were chosen to give as wide a range of advance coefficients, J, as possible within the limits of the vessel capability. These were calculated by using the results of model tests conducted on the previously

described model of *MV SUGAR* (Wu 1991). By comparing the full scale speed and power predictions for the hull and the corresponding RPM with the engine manufacturer's power curves for the main engine, it was possible to estimate the RPM setting which would give the required value of advance coefficient J:

$$J = \frac{V_a}{nD}$$

where, V_a is the speed of advance of the propeller, and n and D are the revolutions per second and the propeller diameter, respectively. Table 3.3 gives these calculated J values. It was noted that as speed increased, the advance coefficients decreased; this was not the expected result. However, upon reconsideration it became apparent that as the boat speed (and resistance) increased, the RPM required by the engine to produce the higher power also increased which reduced the J values. Therefore, the J values actually do decrease when the RPM is increased. This is not the case when RPM is held constant as in propeller open water tests and numerical performance analysis.

Seatrials were conducted on board the *MV SUGAR* near Long Pond on Conception Bay on June 25, 1991. During the early part of the tests on the *MV SUGAR*, an insulating ring became dislodged from between the slip rings, that transmitted the thrust signals from the strain gauges. Therefore, thrust measurements made during the trials were unusable. Although this failure had occurred, inexperience with this type of measurement system prevented the problem from being diagnosed

Table 3.4: Calculated J values and corresponding shaft rpm from comparisons of propeller thrust power (and resistance) and engine power output.

Required thrust power (HP)	boat speed Vs (knots)	engine RPM	corresponding J
8.5	4.6	840	0.363
14.3	5.1	1100	0.307
21.8	5.6	1400	0.265
32.1	6.1	1800	0.224
48.0	6.6	2600	0.168

until after dissassembly of the measuring equipment. Time constraints at the time of the trials would not have allowed enough time to repair the slip rings and redo the tests at that time in any case. An assessment of the data collected revealed that although thrust measurement had been possible while maneouvring and sailing to the trials site, these measurements were transient because steady state conditions had not been reached. The speed trials were conducted near Little Bell Island on Conception bay. Engine RPM was varied in steps corresponding approximately to those given in table 3.3. When steady state conditions were reached, the timed run on the measured course was commenced and a continuous record of shaft torque and thrust was recorded by using the pen recorder; periodically, the shaft RPM was measured. These results could then be analysed to give vessel speed over the ground; and propeller thrust and torque and hence efficiency. Several runs were made at each speed in opposite directions so that wind and current effects could be

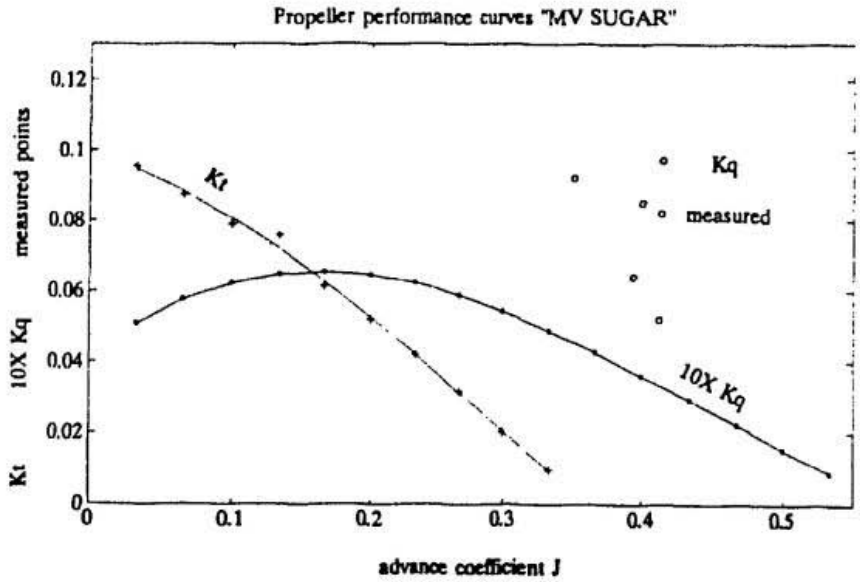

Figure 3.7: *MV. SUGAR* K_q results superimposed on PPT2 performance curves.

averaged out. Bollard tests were also conducted in both ahead and astern giving the variation of torque and thrust with RPM at zero advance.

Due to failure of the thrust measuring system, the *MV. SUGAR* trial results were limited to torque and vessel speed variations with RPM. In figure 3.7, calculated thrust and torque curves from PPT2 are given as solid lines while the measured torque coefficient points are plotted by the small circles. The predicted values are not lifting surface corrected and under-estimate the measured values. This is consistent with findings from performance analysis in section 2.2.4.

A set of tests under bollard conditions was also conducted in both ahead and astern. Again, thrust measurements were not available due to equipment failure. The measured torque curves for ahead and astern operation under bollard condi-

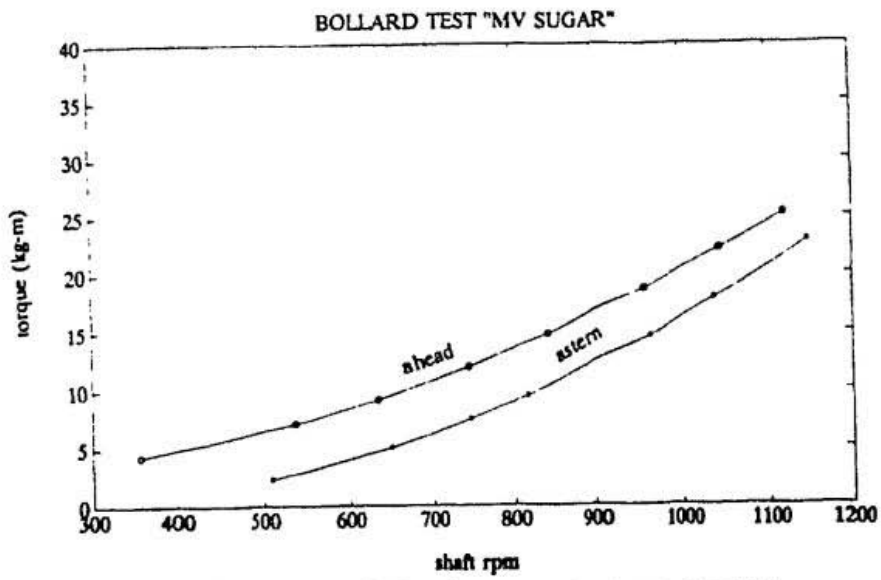

Figure 3.8: Bollard test results *MV. SUGAR.*

tions were plotted in figure 3.8.

The influence of waves and wind on the open water performance of a vessel was readily apparent when the graphs of ship speed with respect to shaft RPM were plotted for the two speed trials conducted on the *MV SUGAR.* The first speed runs were conducted over a measured course in open water between Bell Island and Little Bell Island, a distance of 0.44 nautical miles. The second set of runs was conducted in the inner harbour of Long Pond by using the cement wharf as the measured distance, distance of 250m (figure 3.9). In protected waters, speeds varied from about 4 knots at idle to just over eight knots at full RPM. At sea, the speed varied from about 3.25 knots to 7.25 knots.

The speeds attained in the harbour were substantially higher than those ob-

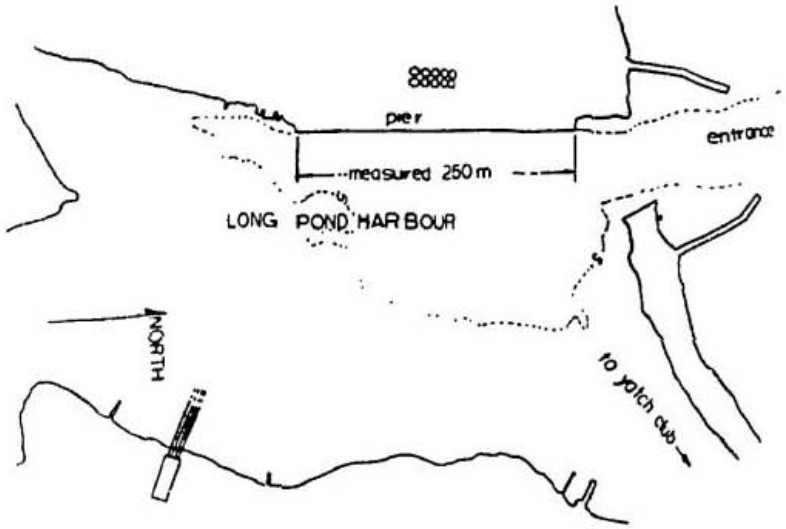

Figure 3.9: Speed trial site : *MV SUGAR.*

tained in open water. The maximum speed increased from about 7.25 knots to 8.1 knots, or about 10%. Figure 3.10 gives these curves.

The *MV BECKY A.* was a wooden, 10 year old, 36' (10m) long, open trap boat operating from Prosser's Rock small craft harbour, St.John's. This vessel was chosen as the second test case because: 1) it had the same basic dimensions and power as the *MV SUGAR*, but with a different yet similar and common hull form; and 2) the instrumented stub shaft could be inserted into the shaft line by pushing back the tail shaft and making new couplings. Drawing numbers 994290-31 and 32 in appendix D show the new couplings for this installation and appendix E gives details about this vessel.

The sea trials were conducted in St.John's harbour on Friday September 6,

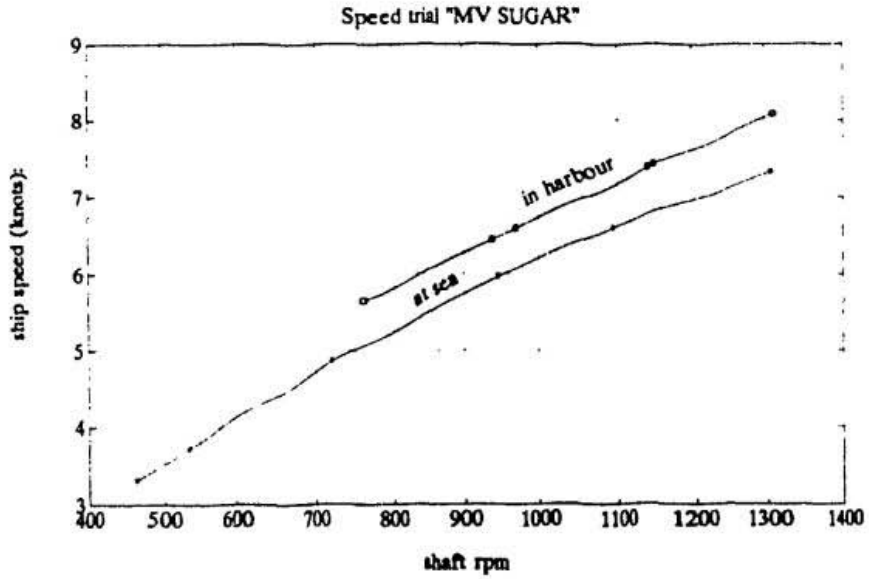

Figure 3.10: Speed trial results: *MV SUGAR.*

1991 after preparations were made the previous day. Speed trials were conducted by using similar values of RPM as before. The predictions made for J values in table 3.3 were considered valid because both vessels were assumed to have similar powering characteristics. The equipment was tested during the early morning. After some initial erratic recording, the signals stabilized, presumably when the brushes had been cleaned and seated (four new brushes had been fitted after their wires broke during the last trial).

Three sets of speed trials over the entire range of boat speed were conducted along the South Side Piers by using the east end of the National Sea Products plant and the west end of the ESSO warehouse as markers, a distance of 635m (figure 3.11). Figure 3.12 shows the ship speed with respect to engine RPM for the *BECKY*

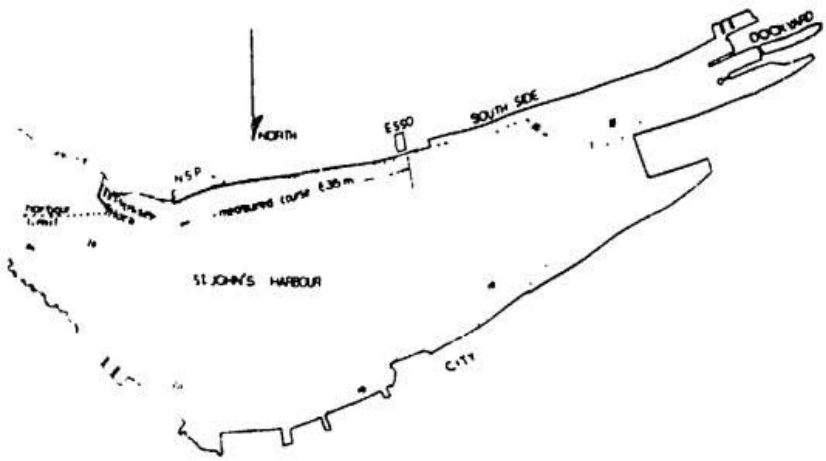

Figure 3.11: Speed trial site: *MV BECKY A.*.

A.. This vessel had a similar speed-resistance relationship in protected waters to the *MV SUGAR*. The speed varied between 4.75 knots at idle and 8 knots at full RPM. It was noticed during the speed trials that the engine was not attaining its maximum RPM at full load. This indicated that the propeller was slightly over pitched and did not match the engine as well as it should. A reduction in pitch could be recommended to allow the full RPM to be reached. The *MV. BECKY A.* seemed to be more responsive and cruises more smoothly, even with its higher displacement hull, than the *MV SUGAR*. A factor which could contribute to this is the finer, narrow transom afterbody design of this vessel. The trials were done in lightship condition.

The thrust and torque measurements were successful this time. All the results

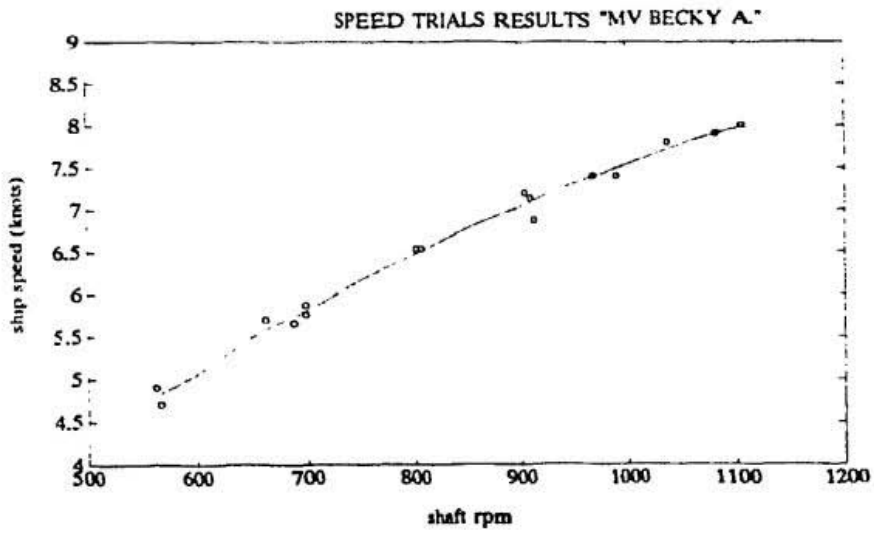

Figure 3.12: Speed trial results: *MV BECKY A.*.

were plotted in the form of thrust and torque coefficients, These are given in figure 3.13. The bollard test results are included at J=0 with a straight line fitted through all the data points in a least squares sense. The small range of J typical for a propeller operating behind a vessel is readily apparent from the grouping of the points on the graph. Without drastically altering the hull resistance of the vessel, a further increase in the range of J would not be possible. Figure 3.14 gives the corresponding propeller efficiencies for the plotted data points. The very low propeller efficiencies indicated here confirm the low values of efficiency common on these vessels. Propeller analysis by using PPT2 was not possible for this vessel because it could not be taken out of service to measure the propeller in detail.

The plotted values for torque and thrust coefficients show some scatter. The

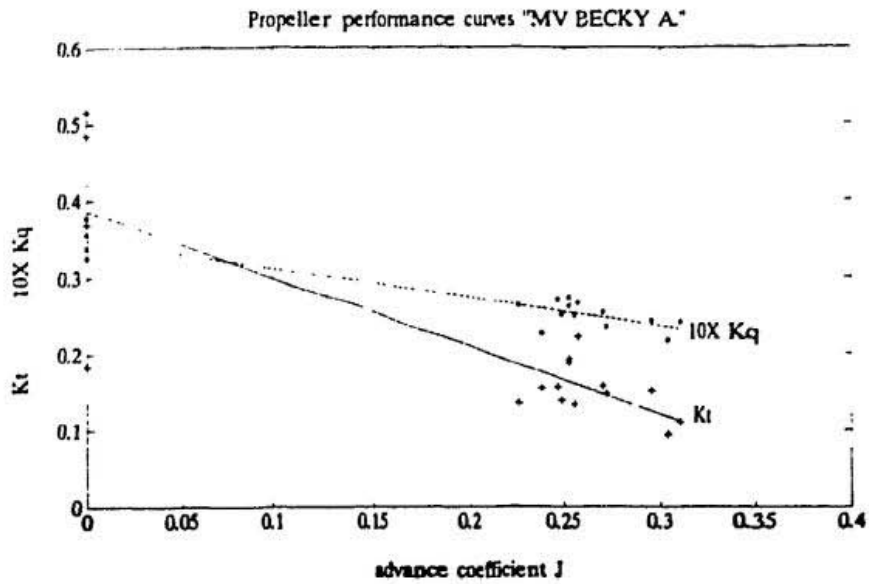

Figure 3.13: Thrust and torque coefficient curves: *MV BECKY A.*.

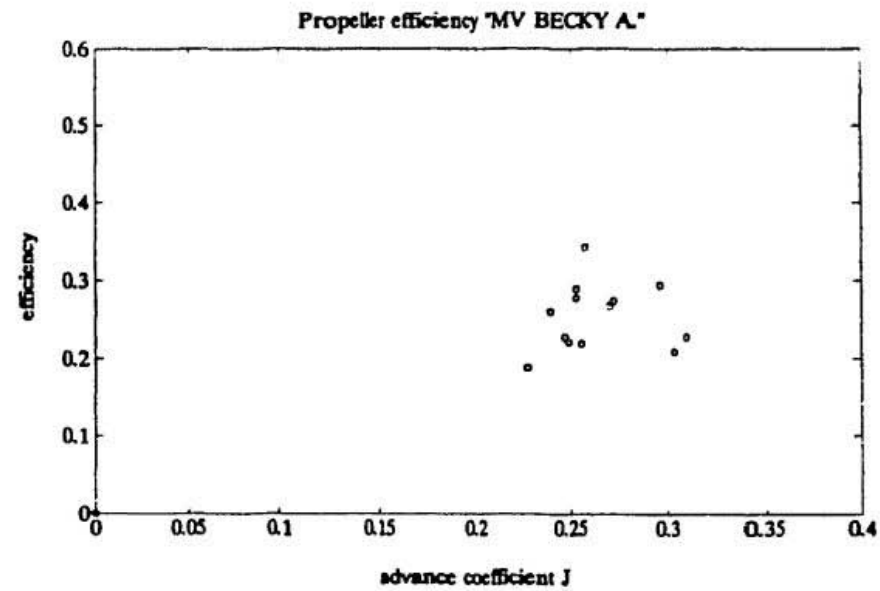

Figure 3.14: Corresponding propeller efficiencies: *MV BECKY A.*.

highest amount of scatter was found in the thrust readings. These varied by about 30% at speed, but by much more under bollard conditions (150%). Bollard tests were conducted three times during the day. The first two tests were conducted at midday after about three hours of operation. However, so much electrical noise was being generated by dirty slip rings that it was impossible to record the zero thrust pen position. The last set of bollard tests was done after thoroughly cleaning the slip rings and re-seating the brushes by using a brush stone. Thrust readings were now possible, but propeller induced vibration was still causing substantial variations in the recorded signals. The high propeller induced vibrations were caused by the close proximity of the propeller to the rudder after insertion of the stub shaft into the shaft line and the displacement of the propeller shaft aft. The average thrust value was difficult to establish from these recordings. Another problem was that we were reluctant to operate the vessel for extended periods under high bollard load because of a recurring engine over-heating problem and the high levels of vibration. Therefore, the length of recorded signal was limited. The torque readings were very stable throughout all the tests done on both vessels making analysis straight forward. Differences in torque measurements were consistently less than 10%. This can be seen by the close grouping of the measured points to the least squares curve in figure 3.13.

3.5 Discussion

By analysing the performance of the *MV SUGAR*'s propeller, an idea of the efficiency achievable was demonstrated. Unfortunately, only the torque coefficient values were obtained during full scale measurements. Full scale measurements were made on the *MV BECKY A.* as well. However, detailed measurements of the propeller have not been possible because the vessel is still in service and this precluded a theoretical performance analysis.

The shaft thrust and torque measurement system operated well except for its vulnerability to dirt contamination. As was noted in the photograph (figure 3.3), the slip rings are exposed and the brush holder is separately mounted. It was not anticipated that a small amount of dirt could have a large effect on the measurements nor that the slip rings would get contaminated so easily. The slip rings required periodic cleaning during both sea trials because of the erratic behaviour caused by dirty rings. After several hours of running, system performance suffered noticably through increased electrical noise on the thrust measurments. Even with these problems throughout the trials, some good results were obtained which gave new insight into the operation of propellers on Newfoundland trap boats.

Chapter 4

Propeller Manufacturing

4.1 Introduction

Propellers can be produced in several ways. Techniques have been developed whereby propellers can be machined from solid blocks of metal, fabricated by welding individually manufactured blades onto a machined hub or casting of the propeller in a foundry. Cast propellers can be made in one piece or the separately cast blades can be bolted to a hub (built-up propellers). The latter method was used extensively in the early days of large ship construction when existing foundry capacities were limited. All of these methods produce workable propellers, but their reliability and economy of production can be quite different. Fabricated propellers are not common. Although they are used for some commercial applications, they

have questionable structural reliability and are not usually approved by classification societies. Machined propellers can be produced to exceptional accuracy, but at tremendous cost. Therefore, this method is limited to very specialized applications such as research ships or naval vessels and model research propellers. Casting is by far the simplest and most economical method to produce a complicated shape such as a propeller.

Propellers are produced in several materials which combine properties such as high structural strength, ductility, corrosion resistance, repairability and ease of machining (AFS 1984, 1989). The materials consist of various steels, bronzes or aluminum alloys. Propellers operating in fresh water which could encounter foreign objects (sand bars, logs or ice) may be cast of steel for high strength and tolerable corrosion resistance given adequate cathodic protection. A similar propeller operating in salt water could be made from cast stainless steel for improved corrosion resistance. However, stainless steel is more expensive and more difficult to cast than bronze and tends to fail in brittle fracture. Bronzes have been developed specifically for marine use and in some cases for propellers. Manganese bronze is the most common propeller material. It has medium strength and acceptable corrosion resistance while being economical to produce and repair. Nickel aluminum bronzes are materials specially developed for marine propellers. They are high tensile bronzes with very good corrosion and erosion resistance. Their tensile strengths are com-

parable to stainless steel, but they are more ductile and will bend substantially before fracturing. Manganese aluminum bronze is a derivation of nickel aluminum bronze, but has better corrosion and load bearing characteristics which makes it suitable for machine parts exposed to sea water such as controllable pitch propeller blades and hubs. Both these types of alloys are more expensive than manganese bronze, but because they are easier to cast and machine than stainless steel, they are less costly than the latter. Propellers made of aluminum alloys are produced primarily for use with standard production propulsion units such as outboard motors and sterndrives. Most propellers are made of cast bronze; therefore, the focus of this study was on the production of bronze castings (Czyra and Niederberger 1975, Kress etal. 1984).

Propeller castings are produced by filling a mould with molten metal and allowing it to cool. Traditional casting techniques for propellers less than about 2.5-3.0 m in diameter, start with the crafting of a pattern of the propeller (or a single blade) from wood. Usually, this is done by using a technique known as cant construction (Goudie 1921; AFS 1986). The pattern is used to build a sand mould into which the molten metal is poured. For very large propellers, moulds are constructed by using sweep methods to form the helical blade surfaces; the sections are then built-up by using section templates and fillers. The manner in which the molten metal is supplied to the mould cavity is critical to casting quality both during filling and

during cooling. The filling ducts are called gates. Their primary purpose is to supply clean metal as quickly as possible to the mould cavity in an undisturbed manner. The gate is composed of three components: the pouring basin or cup; the down sprue which is sized to regulate the flow rate; and the runner which feeds the molten metal to the cavity itself.

The second feeding process is the supply of liquid metal to the casting while it cools. An extra volume of metal is needed to make up for contraction; this is accomplished through a riser system. The riser system consists of extra volumes of metal which are connected in such a way to the casting so that there is an uninterupted flow of molten metal to all the parts of the casting while it cools. The necessary volume and placement of these risers is dependent on the geometry of the casting, the material and cooling rate. The riser must be the last part of the casting to freeze if molten metal feeding is to take place. If a channel between the riser and another section freezes, then the supply of molten metal is cut off and the casting will be defective (Flinn 1963).

When cooled, the castings are removed from the sand mould; that is, they are "shaken-out". The solidified gating and riser systems are removed for recycling and the casting is cleaned, measured, machined and finished.

To facilitate the selection of gating and riser systems and to provide ready access to important information concerning the casting process, a knowledge based expert

system "PROCASTER" was developed. The user can seek specific information with regard to riser requirements, gating selections, or other considerations which may be important, such as the solidification mechanism, crystal growth or rules of thumb.

4.2 Propeller casting in non-ferrous metals

The casting of metals is a process that has changed little in principle since its beginning, but it has had many refinements along the way. The physics of molten metal flow and cooling are very complex, and to date, founders still rely heavily on experiment and experience to help them produce sound castings.

Casting can be described in crude terms as the process whereby molten metal is poured into a mould and left to solidify. The mould is then removed and the casting finished. The majority of products produced by industry are cast from one material or another and most of these cannot be manufactured in any other way. One of the most important parts of building a casting mould to produce a specific product is the design of the ducts which feed the molten metal into the cavity during filling and during cooling. These two items are related through the dimensions of the casting, its volume and the arrangement of the mould. How the metal is fed requires control of the filling rate and the cooling rate of the casting and mould combination while accounting for shrinkage, avoiding ingress of foreign materials and gas absorption by the melt. By proper design and good practice, most defects can be avoided or at least minimized (AFS 1984).

The criteria used to determine casting design, layout and dimensioning is based on many years of experience, trial and error and experimental work. Much of this knowledge has been documented, but every foundry still has its own techniques and

practices which work for them, but may be less satisfactory under other conditions. As new materials and products are developed, so must casting technology evolve. A common thread was perceived by the author, while working in the foundry at Osborne Propellers Ltd., to be crucial to casting production and methods refinement: consistency in production and practice can help to isolate problems and point to ways in which they can corrected.

4.2.1 The casting problem

Casting of metals consists of several major steps from inception to completion of a product. These are: demand for a casting of specific shape and size; production of drawings, patterns or prototypes which will guide the design and building of the production mould; and the application of simple experienced-based rules to ensure good molten metal behaviour. All of these require some engineering to produce a good casting and it will often take several attempts before a satisfactory result is obtained when a new product is developed. The procedures and techniques used to solve the various problem steps depend on the casting itself, the metal to be used, the material and moulding process and the standard practice of the foundry (Flinn 1963).

An expert system can be very useful for solving narrow scope well known problems which "an expert" can solve (see for example, Williams 1987). The knowledge-

based expert systems approach would be impractical and far too complex if general foundry technology were to be addressed. However, by applying it to a specific product such as marine propellers, the scope of the problem was reduced to a manageable size. The range of materials was limited to non-ferrous, seawater resistant materials; and by eliminating very expensive non-commercial alloys or specialty alloys the scope could be narrowed further. (Specific materials could be included at a later date without altering the exsisting system, for example, aluminum.) The problem was then focused further by realizing that monobloc (one-piece) propellers are all cast by using a similar mould layout, regardless of size, which allowed certain generalizations to be made with respect to gating and riser requirements. Figure 4.1 shows a typical propeller mould in cross-section. The main features are indicated: the mould cavity which becomes the casting; the gating system consisting of the down sprue and runner; and the riser system which feeds molten metal to the casting during solidification.

Special propellers such as built-up and controllable pitch propellers were outside the scope of the current problem because they consist of separately cast blades, hubs and other components. Although the basic principles apply to casting these parts, they are not included because these types of propellers are less common on small vessels and they lie outside the experience available to the author. The section on the source of knowledge gives details about sources used to develop the system.

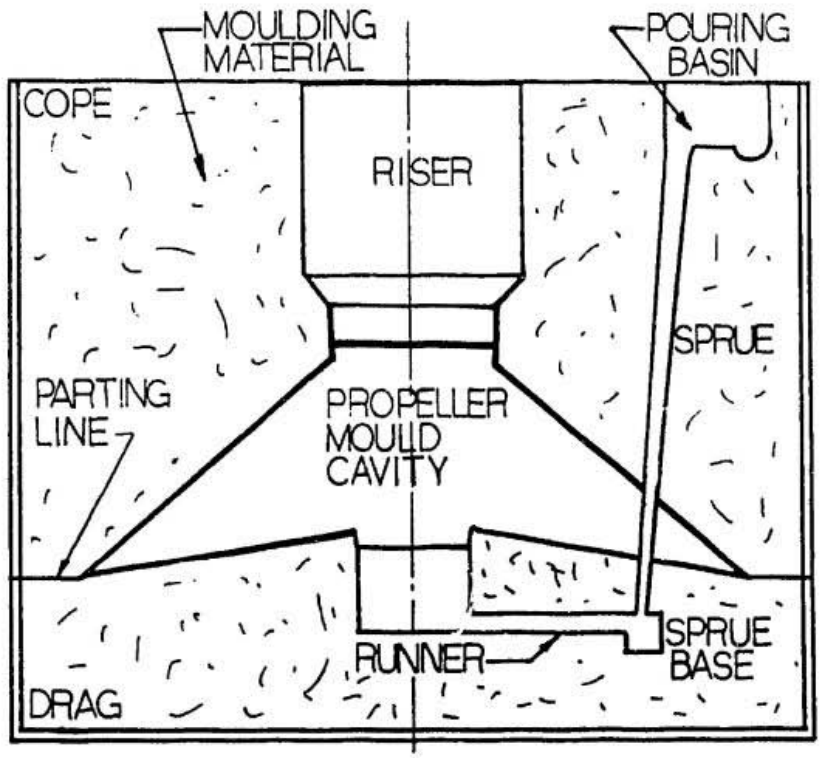

Figure 4.1: Typical propeller mould cross-section.

4.3 PROCASTER

A branch of artificial intelligence known as expert systems was identified as an ideal medium for the structuring and application of experience and knowledge to foundry practice by making it easy for foundry personnel to get information and substantiate customary procedures in the propeller foundry. In this way experimentation can be minimized during production and the rejection rate reduced.

PROCASTER is the result of the application of knowledge engineering techniques to foundry practice. It is the first attempt to make some of the empirical knowledge used in a propeller foundry available through the use of a computer to aid in maintaining uniformity and quality in a "prototype" production industry. That is, a propeller foundry rarely produces more than one or two of the same casting at any one time. There is no evidence in the literature of an application of expert systems to this subject.

Using the techniques of knowledge engineering and applying the EXSYS PROFESSIONAL expert system shell to riser and gating system design, an expert system was produced which helps to determine recommended dimensions for propeller casting gates and risers given metal weight and general dimensions. It also provided easy access to other non-numerical technical information which could be accessed by the user to answer specific questions about these topics. A real strength is the capability to update, expand and modify the system without changing the existng

knowledge base.

4.3.1 Source of knowledge

The knowledge base for this expert system was derived from two sources:

The primary source of "practical" knowledge was the author who had experience from some ten years involvement with ships' propellers in both manufacturing, service and repair. This involved engineering and technical duties as well as manual work at Lips B.V., the large Dutch based manufacturer; Osborne Propellers Ltd., the foremost wholly Canadian manufacturer; and Avalon Propulsion Systems Ltd. the only propeller repairer in the province of Newfoundland. Many conceptual and practical considerations are based directly on experience gained while employed by these companies.

Theoretical methods and technical data were obtained from Flinn (1963), AFS (1984) and AFS (1989). Further information and background came from Chakravarty (1967), Hofmann (1989), Langham (1964) and Stone Manganese Marine technical brief, No. 14 for example.

4.3.2 The problem

The problem to be solved by the expert system is two-fold. Firstly, the questions of gating and risering must be answered. Secondly, the user must have access to specific information which may be important to the overall planning of the mould and casting production. The solution of the problem can take from a few minutes for routine work up to several hours in the case of larger more complex shaped propellers.

A problem identified at Osborne Propellers was that of consistency in technique. There was a certain amount of experimentation done at times when the extensive experience and expertise available in the foundry should have been applied more consciously. It is very difficult to isolate problems in foundry practice if procedures are not repeated or repeatable. An expert system which uses a structured knowledge base applies the same methods and rules every time it is used; therefore, it is inherently consistent in its results. This can help to ensure consistent quality (or error) and reduce experimentation on production work.

Additionally, by incorporating a structured information capability, it is easier for foundry personnel to access important information without the need for searching reference material which is both frustrating and time consuming; therefore, the

system is more likely to be used.

Expected beneficiary

This system might be an attractive supplement to a large foundry because it generally has (or has access to) a metallurgical laboratory where detailed mould and casting designs is carried out and tested, procedures could be actively developed and incorporated into the expert system. A small foundry with limited personnel and resources could make use of such a system to help control its production. Personnel would have easy access to technical information they would not normally see and could use the system to check the standard practice for routine work (if they had access to a computer). The more likely situation might be whereby every job order has issued with it guidelines for moulding based on the output of the expert system.

It also gives the small foundry the capability to be flexible and adapt to new products by allowing modification and upgrading of the system and then applying standard procedures to new products.

4.3.3 Shell

PROCASTER was written using the EXSYS PROFESSIONAL expert system shell version 1.0.3 produced by Exsys Inc.

4.3.4 Structure

PROCASTER was structured in the form of a tree which has two main branches with several sub-branches. The first branch was the dimensioning section for the main components of the gating system. The second branch had two large sub-branches dealing with the sizing of risers and metal solidification respectively. Much of the system was dedicted to information retrieval covering much the same material as the technical aspects of this report. A detailed schematic of the tree is given in figure 4.1. The rules were written following the tree structure closely. During each run, Exsys evaluates all the rules to determine which ones apply, and then applies those to the problem addressed. For detailed information and rules, the reader is referred to the Ocean Engineering Report (Hofmann 1991d)

4.3.5 Running PROCASTER

PROCASTER can be used by first running the system shell runtime file EXSYSP.EXE. It will then require the input of the program name: the user types PROCASTER with the suitable location prefix. The program will then require the user to answer questions by typing the appropriate answer number.

To determine the dimension guidelines for gates and risers, the following information will be required as input: 1) the casting volume, 2) the metal type, 3) the thickness of the blade section at the fifth radius, 4) the diameter of the propeller to

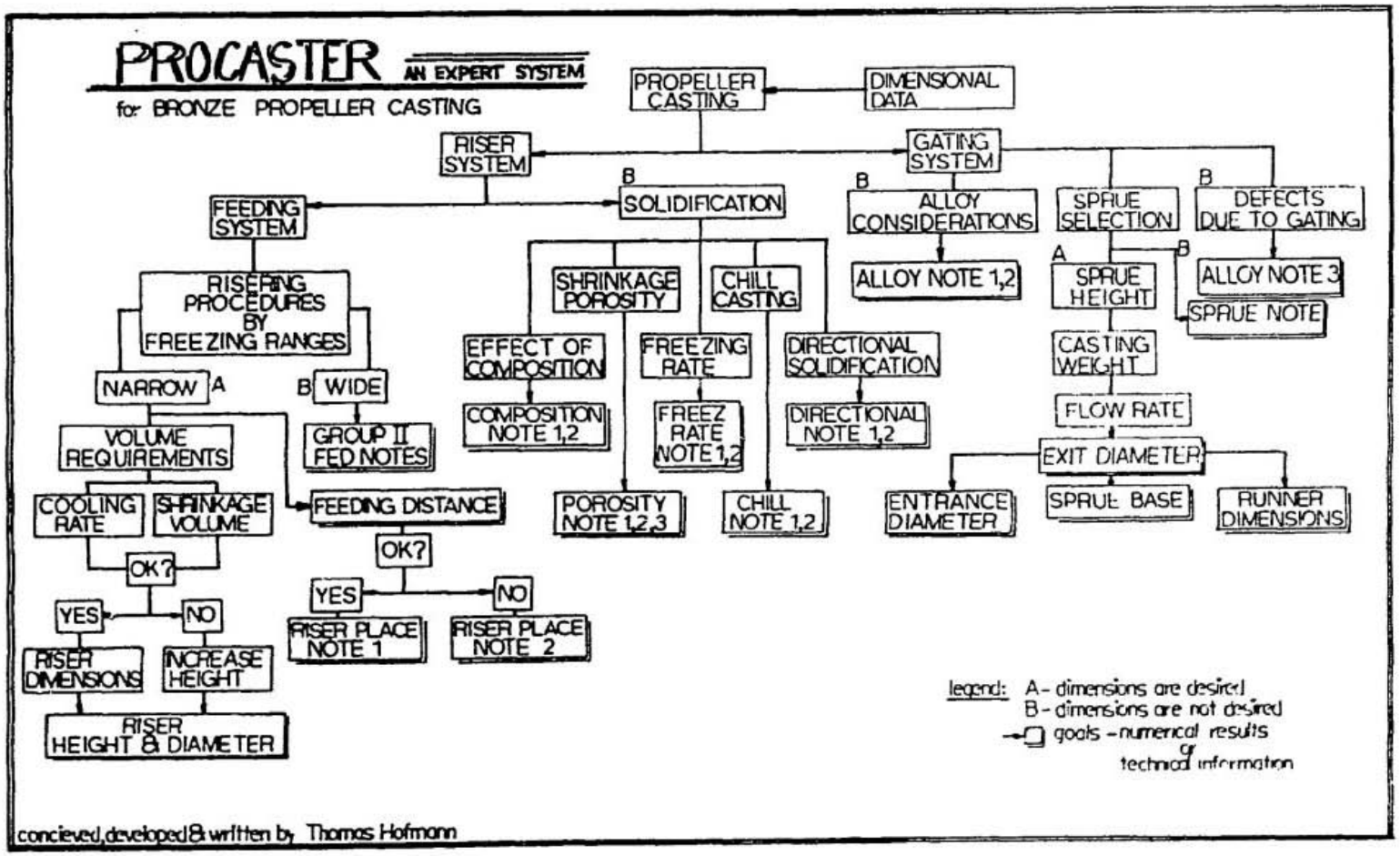

Figure 4.2: PROCASTER: expert system structure tree.

be cast, 5) the heights of the casting and sprue. If an item other than a propeller is to be cast, instead of entering the 5th radius thickness and the propeller diameter, the user should enter the smallest dimension of the cross-section and the longest dimension of the part to be cast. The assumption being, that the part can be approximated by a plate or bar shape. For accessing non-numerical information, the user follows the structure tree to answer the intermediate step questions as asked by the program. The results will then be printed on the screen. The menu at the bottom of the screen allows the user to determine how the results were achieved by printing the rules used. Other options include re-running the program with modified inputs and printing the results.

Detailed instructions on running the system shell are available at the beginning of the run by typing YES when the question is asked.

4.4 Main features of mould design

4.4.1 Gating system

The gating system consists of a pouring basin, a down sprue, a sprue base (or well), a runner and a swirl chamber at the bottom inlet of the casting (refer to figure 4.1). The horizontal runner is often replaced by a horn gate in small castings because it simplifies the moulding process somewhat. A horn gate consists of a curved and

slightly tapered pattern which can be easily extracted from the finished mould. A horizontal runner, on the other hand, requires a channel to be constructed in the mould which is more laborious, but it does not have the size limitation of the horn gate approach. A horn gate becomes impractical to use for large castings. Both these types are dimensioned in the same way. The three critical items: the down sprue, the sprue base and the runner, must be dimensioned such that the flow of metal is controlled as it fills the mould cavity. The metal should flow as quickly as possible to minimize the heat loss during delivery, yet avoiding turbulent flow. High flow velocity will cause turbulence and erosion of the mould walls. The material removed from these wash-outs will become inclusions in the casting. Excessive defects of this type will cause rejection of the casting. This is particularly true of propellers because inclusions tend to occur in the most highly stressed region of blade, at the blade root.

The main dimension to be determined is the sprue exit diameter (in this case the sprue is assumed to be an inverted cone) which is sized to regulate the flow of metal. All other dimensions in the gating system are based on this exit diameter. One way this dimension is determined is by using an empirical formula which determines the flow rate required for bronzes (AFS 1984, Flinn 1963):

$$flow\ rate = \frac{W_t^{1/2}}{0.086 + 1.09t}$$

where W_t is the total casting weight and t is the average thin section thickness. The

"thin" section is taken to be the smallest dimension of a cross-section to be fed with metal. In the case of a propeller the thickness is taken to be the blade thickness at the 5th blade section radius (midpoint of the blade length). Experience has shown that better results can be obtained if this flow rate is modified by a *delivery factor* to account for the variation in pressure head as the casting fills. Other dimensions are determined from linear empirical relationships and proportions that experience has found to be successful (AFS 1984).

Defects that could occur as a result of the gating system or pouring should also be kept in mind when designing a layout: cuts and washes due to too high velocities or abrupt changes in direction (erosion); dirt and slag; and other inclusions. Other defects such as expansion defects; misruns and cold shuts, open grain structure, rough surface, surface or subsurface shrinkage are also undesirable and should be avoided wherever possible. A list of casting defects is given in AFS (1989).

4.4.2 Riser system

The second and most critical part of producing a casting is the controlled solidification of the molten metal within the mould. Once the mould is full, additional molten metal must be fed into the cavity progressively to make up for volume deficiencies due to metal shrinkage during cooling. Although feeding and solidification are closely related, they can be discussed separately. Solidification is the heading

given to the many aspects which specifically concern the metallurgy of the freezing process of the metal. The feeding of molten metal to the casting from a riser or several risers is given the heading, feeding system.

Copper-base alloys fall roughly into one of two groups. These groups represent extremes in behaviour during cooling. Some alloys however, fall into an intermediate category because no sharply defined line exists between the groups. Group I alloys are those which freeze by skin formation at the mould wall followed by dendritic crystal growth at a specific temperature or a specific temperature range. These are said to have narrow freezing ranges. Group II alloys do not have a specific temperature (or temperature range) within which solidification takes place. These alloys tend to "gel" throughout the melt in an approximately uniform manner. Freezing begins with the formation of crystallites around the mould walls, the growth of these is almost immediately retarded (or even halted) because they are considerably poorer in alloying elements or impurities than the surrounding melt. Alloying element atoms are rejected from the crystallites when they form, thus enriching the liquid metal surrounding the crystallites and reducing the freezing temperature (AFS 1984). Further crystallites form and are subsequently halted. This cycle continues throughout the molten metal until it has numerous crystallites distributed through it. The temperature gradient across the melt is very slight as the entire melt cools at about the same rate. The solidification process is analo-

Table 4.1: Classification of copper-base alloys used in marine applications by solidification type (adapted from AFS 1984).

Group I alloys (short freezing range)	Group II alloys (long freezing range)
deoxidized copper	tin bronze*
manganese bronze*	leaded bronze*
yellow brass	red brass*
aluminum bronze	semi-red brass*
manganese-aluminum bronze	nickel-aluminum bronze
silicon bronze*	

* dependent on precise composition and conditions of freezing.

gous to setting concrete. The material is all liquid initially, then becomes mushy throughout and finally becomes rigid. This type of solidification produces a uniform, equiaxial microstructure commonly found in high strength metals.

These two processes represent extremes in freezing mechanisms. In reality most copper-base alloys fall between them in continuous intermediate modes of freezing. As the alloy content increases from pure copper, so does the tendency toward mushy solidification. The actual freezing rate, which is very difficult to predict, also has a great effect on the type of freezing. Intermediate freezing alloys exhibit a microstructure with dendritic crystal growth at the surface of the casting and more equiaxial grains toward the centre of the section. The proportion of one to the other will depend primarily on the cooling rate and hence on the section shape. Table 4.1 summarizes some of the marine bronzes and classifies them according to group.

As solidification and feeding are closely related and interdependent, the rest of the discussion here will be in terms of Group I or II alloys and not in terms of feeding versus solidification.

Other more practical concerns, upon which sound castings depend are discussed in detail in the report on the expert system PROCASTER (Hofmann 1991d).

Risering procedures

The purpose of a riser is to supply molten metal to the casting as it cools. The riser must be large enough to make up volume losses due to shrinkage. It must also be sized to ensure that it freezes after the casting has solidified so that it can supply molten metal. The size and location of risers is largely based on experience and requires a certain amount of experimentation when new products are developed. As shown in figure 4.1, most propellers are arranged with one large riser on top of the central hub which feeds all the blades and the hub itself. For propellers cast in stainless steel this would be inadequate because of the reduced feeding range of this material compared to bronze. Cases like this are not considered here specifically although the following analysis results from developments in the cast steel industry which have been applied to copper-base alloys (AFS 1984, Flinn 1963).

Group I alloys have similar feeding requirements to steel because they have similar solidification mechanisms. Gates and risers are located to ensure directional

Table 4.2: Approximate feeding ranges for some group I bronzes (AFS 1984).

Alloy	Section shape	Feeding distance in terms of thickness T
manganese bronze	square bars	$4T$ to $10T^{1/2}$ as thickness increases
	plates	5.5T to 8T
aluminum bronze	square bars	$8T^{1/2}$
ninckel-aluminum bronze	square bars	$< 8T^{1/2}$

Note: about 2/3 of feeding range is due to a free end.

solidification. This depends on the feeding distance (or range) of the alloy. In other words, how far along a section can a metal be fed before cut-offs occur (Flinn 1963). In general, use is made of the retarding effect of the riser mass on freezing and the accelerating effect of external corners and edges to form the V-shaped solidification front with the open end toward the riser. The riser will only feed a limited distance and must be placed to ensure that it can feed the entire section. This may require multiple risers if sections are very long and thin, for example. Table 4.2 gives the approximate feeding ranges for various propeller alloys.

Riser shape

Riser "efficiency", in terms of its capacity to supply molten metal and to store heat, depends on its volume and its surface area. To maximize volume and minimize surface area (and therefore heat loss) it can be shown that a cylindrical riser with a height to diameter ratio equal to one meets this criterion. If the riser were insulated,

even higher yields could be achieved. Yield is the percent weight of finished casting with respect to the poured weight of metal. The radiated heat loss from the top of the riser has been estimated to be as much as 50% for a non-insulated riser, but by insulating the top this value can be reduced by half. It is therefore essential that risers are covered with an exothermic compound or insulation to a minimum depth of 1/10 the riser diameter. Freeze-over of the riser must be prevented so that the feed metal is not isolated from atmospheric pressure (AFS 1984).

Riser dimensioning

Riser size and placement is critical to the production of sound castings. Various methods have been developed for sizing risers, but the most popular has been the one developed by the U.S. Naval Research Laboratory (NRL). This method uses empirically derived relationships between the casting to riser volume ratio and a shape factor based on the characteristic dimensions of the casting:

$$shape\ factor = \frac{L + W}{t}$$

where, L is the length, W is the width and t is the thickness of the section. Much of the published work in this topic is based on the NRL method (see for example, Flinn 1963). Another method, the "modulus" method, has received greater attention in recent years. Although used most extensively for steel castings, it is suitable for use with short freezing range (group I) copper-base alloys as it is reasonable to assume

a similarity between the feeding requirements of materials with similar freezing mechanisms.

Propellers are difficult to describe in terms of linear characteristic dimensions. Therefore, the modulus method, which does not depend on a shape factor as above, was considered more suitable to dimension risers for propellers and is therefore used in the expert system.

This method is derived from Chvorinovs rule for the freezing time T of a casting (Flinn 1963, AFS 1984, 1989).

$$T = k \times M^2$$

where, $M = V/A$ is the modulus of a casting with volume V and surface area A, and k is a constant. This relationship is valid for any cast shape including a propeller and its riser. The surface area considered includes only those portions which contribute to cooling. Applying this equation to both the casting and the riser (identified by subscripts c and r, respectively) the following derivation can be made. The actual freezing time is not of primary interest , but the relative time for solidification for riser and casting is. This means that $T_r > T_c$ or restated $T_r/T_c > F^2 > 1$ for the casting to be sound.

$$\frac{T_r}{T_c} = \frac{k \times M_r^2}{k \times M_c^2} = F^2$$

$$M_r^2 = F^2 \times M_c^2$$

$$M_r = F \times M_c$$

Practical experience has shown that for steel and ductile iron F=1.2 and for group I copper-base alloys a value of about 1.3 gives satisfactory results (AFS 1984). In this way a riser is proportioned so that it freezes more slowly than the casting to which it is connected; however, the riser must also have sufficient volume to provide the necessary amount of feed metal to the casting. To this end, the volume ratio of riser to casting is calculated to determine whether the minimum V_r/V_c criterion is met. This criterion is based on experience. For propellers cast in sand moulds, V_r/V_c ranges from about 30% to 60% by using risers of height /diameter ratio equal to one and as much as 75% for risers where the height is say, 50% greater than the diameter (Hofmann 1989, AFS 1984). If the minimum volume ratio is not met, then the riser height must be increased from the calculated dimension based on volumetric considerations.

Group II alloys comprise the greatest percentage of annual copper-base casting production. Soundness in these castings depend on section thickness and uniformity. Experience has shown that achieving soundness in these castings depends on avoiding slow cooling rates. Within the limitations of the moulding processes available and casting design, there are three ways in which cooling rate can be maximized: 1) minimize section thickness; 2) reduce and/or evenly distribute heat in the metal entering the mould cavity; 3) use chills and mould materials of high

chilling power (AFS 1984).

Soundness in these castings is generally judged by achieving pressure tightness of the casting. The extent of visible porosity and maintaining minimum mechanical properties for the metal are also important as indicators of quality.

4.5 Building a propeller

4.5.1 The strickle gear

The propeller founder is faced with the task of producing a casting of complicated shape as accurately and as cheaply as possible. Owing to the possible infinite variation of geometry of custom designed propellers, almost all those manufactured are "one-off" items. The aim is to reduce the finishing time to a minimum as this is generally the most expensive operation during manufacture. Therefore, the casting must be as close to finished dimensions as possible; ideally, it should require only polishing and machining of the bore to produce the finished propeller.

Manufacturing prototypes of light alloys using a sweeping method can be adapted to a wide variety of propeller configurations without complex numerical machining, and it eliminates the requirement for wooden patterns. A strickle gear is a fixture used to speep out blade surfaces in the moulding material. The mould is built and then cast directly on the strickle gear, which acts as a base and mould box. Light alloy cast patterns, manufactured by using a strickle gear, have the advantage that they can be reworked and altered for use with similar future designs, thus avoiding the need to produce a new one in some cases. Plaster patterns are vulnerable to mechanical damage when thin sections are required and therefore not recommended in these cases (Flinn 1963). In addition to this, by moulding the pattern directly

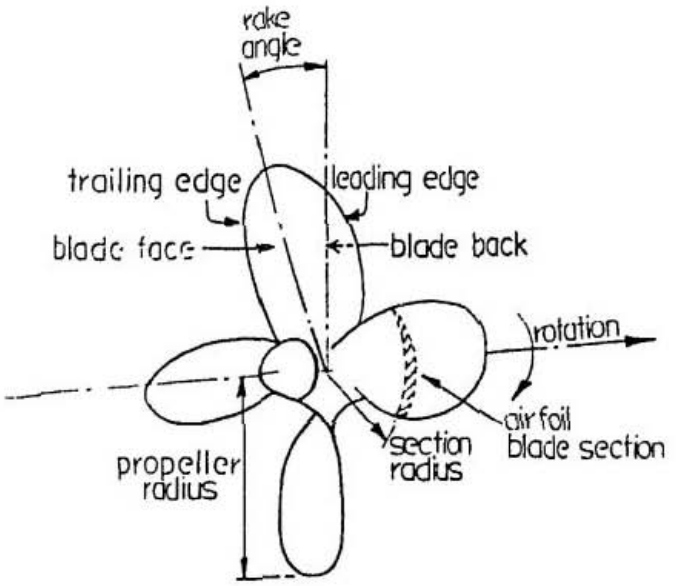

Figure 4.3: Propeller Geometry (adapted from O'Brien 1962)

in the medium into which it will be cast, the manufacturer avoids the intermediate step of using a single blade wooden pattern, for example, to produce a full solid pattern without the dimensional and positioning problems. This may not be of primary concern in some designs where dimensional accuracy is not critical, but it will definitely be required in high precision propellers or small diameter highly loaded propellers. Dimensional accuracy is even more critical in scale propellers designed for research purposes.

The strickle gear provided a method to produce a mould from which a pattern or prototype propeller can be cast in either a light alloy such as aluminum or a propeller bronze.

Strickle gear capacity requirements

The dimensions of the strickle gear were determined from the overall dimensions of propellers which were to be manufactured. These requirements for the manufacture of wake adapted propellers were as follows.

The diameter is the most important dimension of a marine screw propeller. Upon consultation with Avalon Propulsion Systems Ltd., it was decided that the maximum diameter would be restricted to approximately 24 inches for two reasons. Firstly, there is some difficulty in ordering custom propellers in the size range 10" to 24" in diameter; secondly, the gear should also be suitable for making model propellers. It was felt that a larger machine would make this very awkward. The normal model propeller diameter that can be tested in the cavitation tunnel at NRC - Institute for Marine Dynamics, St. John's, is 0.25m.

In most full scale applications of propellers in this size range the number of blades does not exceed four. Although propellers with five, six or even seven blades are common on larger ships, they are not usually applied to smaller vessels. The smoother operating characteristics of these propellers may be of no great benefit to smaller vessels less subject to vibration problems, and the associated losses in efficiency usually do not warrant the higher number of blades. These propellers are slightly more complicated in geometry, but they are constructed in the same way as the three and four blade cases.

There was a smaller strickle gear in use at Glasgow University, in Scotland, which had been used to make model propellers up to a diameter of 0.3m. The single blade moulds were made from plaster for casting whitemetal propellers. The individual blades had a 1/4 hub cast-on (for a three bladed propeller a 1/3 hub is cast-on etc.). These were machined and then mounted in another mould to fuse the blades together with more molten metal. The blades were then finished and the bore machined to produce the model propeller (private communication). A deficiency that was readily apparent in the Glasgow University strickle gear (which was not acceptable for our application) was the inability to easily incorporate positive rake into the propeller (2). Rake is defined as the angle of inclination of the propeller blade generater line (centre line) away from the radial position to give increased clearance between the hull and the blade tips. This reduces propeller induced pressure fluctuations on the hull surface. In the current design, to overcome this problem, an adjustable sweep arm was incorporated to allow a variation in rake from zero to fifteen degrees (a common maximum value; often a "standard" rake of 1" per foot of diameter is used). Figure 4.1 shows a typical propeller mould cross-section with rake. Note that the two blade sections shown have their tips angled downwards instead of straight out from the hub. Figure 4.3 describes general propeller nomenclature and geometry.

A wake adapted propeller has as its main characteristic a variation of pitch

along the length of the blade which is designed to suit the wake in which it is operating. The gear must therefore have the capability to produce a blade with radially varying pitch and a cambered surface. This can be done by using a custom set of helix plates which are used to guide the arm which sweeps the face of the blade. In the experimental casting discussed later in this chapter, a single plate was used to produce a uniform pitch helix in the mould material. The Glasgow University gear could only make uniform pitch blades accurately, radially varied pitch, though possible to make, required many adjustments and settings of the helix guide. This brought into question the uniformity of the set of blades that could be produced. The maximum pitch-diameter ratio was limited to approximately 1.5 for a 24" diameter propeller, to give a maximum pitch angle of approximately 38.5 degrees. This maximum ratio was decided upon based on the records of propeller repairs and sales over the past few years at Avalon Propulsion Systems Ltd.

Other non-propeller specific requirements of the strickle gear were: it had to be of rugged construction, able to withstand the rough handling of foundry and shop use; that is, it had to be movable even with a completed sand mould in place - lifting eyes were provided. The drag was equipped with a quick release clamping arrangement for the helix plates thus avoiding two problems seen with the Glasgow University model: firstly, the screws used for helix adjustment could quickly become damaged; and secondly, the repeatability of blade location and sweeping is critical

for moulding solid multi-blade patterns.

An additional feature incorporated into the new strickle gear was that it had a reversable cope which allowed for the complete mould to be built and the casting poured on the same unit. The copebox had built-in reinforcements for the cope sections to ensure ease of removal and replacement during successive blade moulding. The gating to be used will be a typical runner or horn type gating system with a particle trap at the bottom end of the down sprue (Hofmann 1989a).

Mould construction

The drag

A propeller is always moulded and cast face down to ensure that the metal flows upwards to fill the mould cavity in a continuous and undisturbed manner. This means that any small amounts of slag can be skimmed while pouring and will not be trapped inside the casting. The faces of the blades are constructed, with the spindle and hub cylinder pattern in place (see assembly drawing in Appendix G), by sweeping out their shape while using the helix plates to guide the arm. The hub cylinder pattern must be located above a plug of similar diameter which forms the swirl chamber of the horn gate (see figure 4.1). The runner itself is located so that the metal flows around the outside of the swirl chamber and fill the mould cavity from underneath; that is, the end is directed only slightly inward along the tangent

of the swirl chamber and not radially. In the latter case the metal would impinge on the opposite side causing turbulence which can lead to defects such as porosity in the casting.

The rake of the blades must be set on the sweep arm at the beginning of the operation by adjusting the angle of the arm. The varied pitch of the blades is swept successively starting at the inner radius and working outward as the inner radius will always have the steepest pitch angle. This is the same procedure as is used for very large propellers where solid patterns are not practical due to their size (Langham 1964; Chakravarty 1967). If this were attempted inwards from the outer radius the successive sweeps would destroy the previously swept surfaces. When the successive plates have been used and the surface is roughly swept it must be faired to avoid excessive finishing of the surface of the casting. It follows that the larger the number of helix plates the more accurate the swept surface will be and the less fairing will be required. Before the removal of the last helix plate the blade generator lines and the radii at which the blade sections will be mounted must be lightly marked to ensure correct positioning of the blades. When the moulding material has set (in the case of concrete, plaster or CO_2 sand) the drag portion of the mould is complete.

The mould material is a matter of choice and can be any one of green sand, concrete, plaster or chemically bonded sand. Depending on the propeller in question

one material may be more suitable then another. In the present study plaster of paris was used, following the example of Glasgow University. However, this turned out to be a poor choice for two reasons: firstly, it was found that the plaster set-up so quickly (about five minutes) that the face could not be swept out completely. Varied pitch could not have been constructed at all. The mould needed to be completed by using the wooden single blade pattern which was to be reproduced with the strickle gear technique. Secondly, the plaster mould did not cure properly under shop conditions. It was discovered later that plaster moulds require baking in an oven at about 400-500 ^{o}F for aluminum alloys and 1200 ^{o}F for copper alloys. No oven was avalible for this purpose. Although the mould performed its function and was successful, the high moisture content in the mould material itself caused extreme bubbling and spatter due to steam generation when the mould was about 3/4 full. This was readily apparent when the cooled casting was removed from the mould and inspected. The lower portion of the casting was sound, but the upper part and the riser were very porous. If green sand had been used, the casting would have been a complete success because the mould material does not require curing. Future moulds should be made from sand with suitable bonding agents.

The cope

The cope is the upper half of the mould. It creates the cavity of the actual shape of the propeller blades and their cross-sectional dimensions. The blade outline was

located and scribed on the swept surface of the drag by using a wooden blade pattern as a template. The swept surface was covered with plastic foil wrap (a parting agent such as starch or silica dust would be used when moulding with green sand) and the blade pattern was fixed on the swept surface properly located by using the blade outline and generator line for guidance. The spaces between the sections were filled with plaster. Templates, if needed for a pattern, would have had incorporated into them a double shrinkage and finishing allowance such that the pattern would have adequate material for finishing to the required dimensions and an allowance for shrinkage of the prototype.

With the blade now completely defined, the cope could be completed. After placing retaining boards in the cope around the defined blade, the cope was filled with moulding material (plaster). If sand is used, it should be suitably packed to ensure that no cavities are left near or on the surface of the blade and that the surfaces which are formed by the boards are also completely intact - particularly at the mating surfaces with the drag.

It was at this stage that the down sprue was installed. This was done by using a tapered pattern of sufficient length and proper cross-section. The end was fixed in the drag near the exposed end of the horn gate, it then protruded above the cope top. The cope was then completed around the down sprue plug, which when removed, left a clean hole right through the cope.

A riser was also provided at the hub which was of sufficient capacity to ensure adequate flow into the mould during cooling. In some cases, additional risers may need to be provided along the top edges of the blades if it is felt that due to the section dimensions and shape, flow will be inadequate from the hub riser alone. In general this is not necessary when casting in aluminum or bronze if the hub riser is of adequate size, but, it may be required if the casting is to be of steel or a steel alloy.

Completion of the mould

When the cope was completed and it was again separated from the drag, the mould was cleaned up along all joints and touching edges. The hub cylinder block is removed along with the swirl chamber pattern. Before removal of the runner it was necessary to cut a particle trap near the down sprue and connect it with a small runner to the gate by cutting it into the drag mould surface. These should be well away from the edge of the propeller cavity itself. The gate pattern was then removed and all exposed edges were rounded slightly so that there was no possibility of the edges crumbling when the mould was reassembled in preparation for pouring. At this stage it was also necessary to ensure that the blade root radii were formed correctly; in this case, the wooden blade pattern formed the hub also, it turned out that the pattern hub was slightly oblong making it very difficult to

remove. The mould was opened slightly at the blade roots so the pattern could be extracted. The mould was left open to dry over an electric heater over night.

All foreign materials were removed prior to closing up the mould. It is also good practice to keep all openings covered with pieces of weighted cardboard or the like to ensure nothing falls into the cavity until immediately prior to pouring. Any foreign matter will produce defects which could cause rejection of the casting.

The strickle gear is essentially a jig for building either a propeller mould for casting an aluminum pattern (which will then later be used for moulding a propeller), or for casting a propeller directly if no pattern is required. It allows a "low-tech" approach to creating high precision propeller castings and avoids the inherent difficulties and expense of numerical machining techniques or wooden patterns; although the casting could be finished using computer numerical controlled machining. The gear works on the same principles used for very large propellers. These are moulded directly in their mould pit using a loam board with a helical guide around its circumference (for example, Chakravarty 1967). The blade shapes are then built up and the mould completed for casting.

Alunimum was used to make the casting because the crude furnace which was built for this experiment could not melt bronze . As the casting was made from aluminum, PROCASTER could not be consulted for information. Rules of thumb were used to dimension the riser (about 1.5-2 times the hub length and 2-2.5 times

its diameter), horn gate (runner) and down sprue patterns were used from a bronze propeller of similar size.

4.5.2 Casting a prototype

To cast a propeller in a mould constructed by using the strickle gear and to show that the system developed here was useful for the purpose intended, a mould was constructed from plaster; firstly, by using a single bladed wooden pattern; and secondly, by using the strickle gear. Photos 1 and 2 show the drag and cope parts of the mould. As the plaster mould material set very quickly, insufficient time was available to complete the strickle gear blade, so it was completed by using the pattern such that the casting could be completed. Photo 3 shows the mould closed and weighted, ready for pouring.

A small reverberating furnace was constructed to melt aluminum to cast the propellers. Photo number 4 shows the author inserting the torch into the lower section of the furnace. A naturally asperated 400,000 Btu/hr propane torch was the heat source. The torch was positioned so that the flame entered the furnace tangentially to ensure a good swirl around the ladle and to ensure maximum heat transfer. It had a capacity of about 225 cubic inches of metal in a fabricated steel ladle. The metal was melted and heated until it was completely melted and glowing slightly red. No means of temperature measurement was available, but from

experience it was about right for pouring. It was then poured into the mould. When the mould was about 3/4 full, excessive moisture in the mould due to incomplete curing caused the metal to bubble and spatter violently. Pouring was continued to subdue the spattering and fill the mould as much as possible. The excess metal in the ladle was pigged (poured into an ingot).

Once cooled, the castings were shaken-out. Photos 5 and 6 show the rough castings as removed from the mould. Photo 5 shows the face (underside) of the casting. The gate has been removed, but the swirl chamber can be seen clearly. The intricate detail possible with plaster casting is demonstrated by the reproduction on a measuring scratch on the pattern which has been reproduced in the casting (this line is also visible in photo 1). Photo 5 shows the backs of the blades and lower half of the riser. A small amount of leakage occurred from the upper edge of the blade. This is visible in the form of drips of solidified metal. Inspection of the castings revealed that the mould construction itself was successful. It had leaked a small amount at the parting line near the hub where the steam pressure had separated the halves slightly. This in itself would be a minor defect, but would not have any bearing on the quality of the casting itself as it could simply be cut off. The upper part of the propeller blades were incompletely filled and porous due to the bubbling out of the steam. The porosity could also be readily seen at the break between the upper and lower part of the riser.

The casting experiment was, in general, a success except for those items mentioned which depend directly on the type of moulding material used: the mould was constructed correctly, the scrap aluminum was successfully smelted and then remelted for casting, and the strickle gear is expected to work quite well given a moulding material which allows sufficient time to complete the mould properly.

4.5.3 Finishing the propeller

After cooling, the propeller casting would be shaken out of the mould. The gating system and riser would be cut off for recycling. The rough casting hub must be faced off and the bore machined for the required shaft taper.

The blade faces would be ground smooth using hand grinders in preparation for measuring. The blades are then laid off with the correct outline and the local pitch measured at each of the radii. If the pitch were not within specifications due to distortion (for example), then a pitch adjustment would be made by preheating and twisting the blade. Once the pitch is determined to be within tolerance, usually according to International Standards Organization standards (ISO 1981) the blades must be trimmed and ground to shape both on the face and the back. The better the casting, the less finishing would be required. After grinding smooth all the outer surfaces of the propeller, it is balanced according to ISO standards and sanded to a smooth shiny finish.

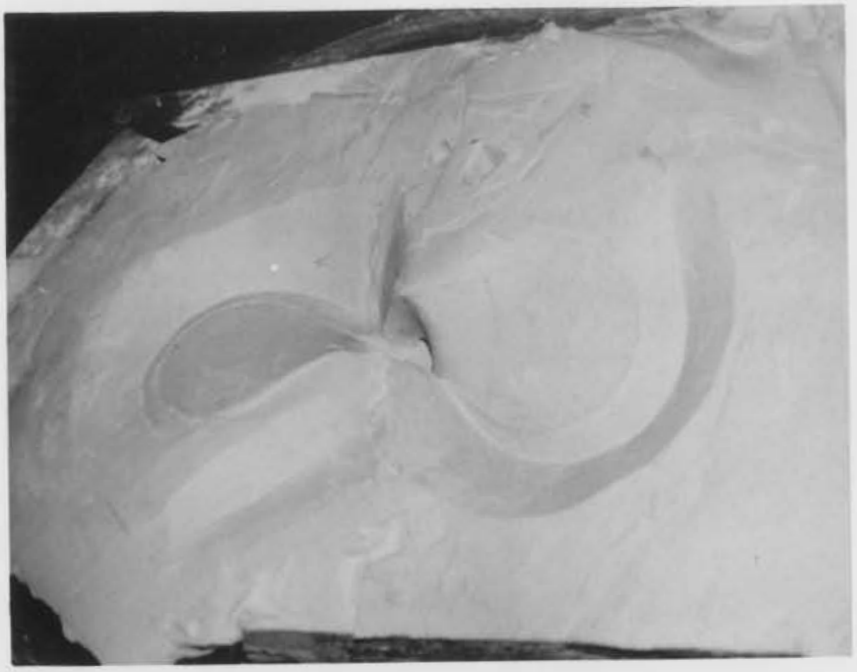

photo 1

photo 2

photo 3

photo 4

photo 5

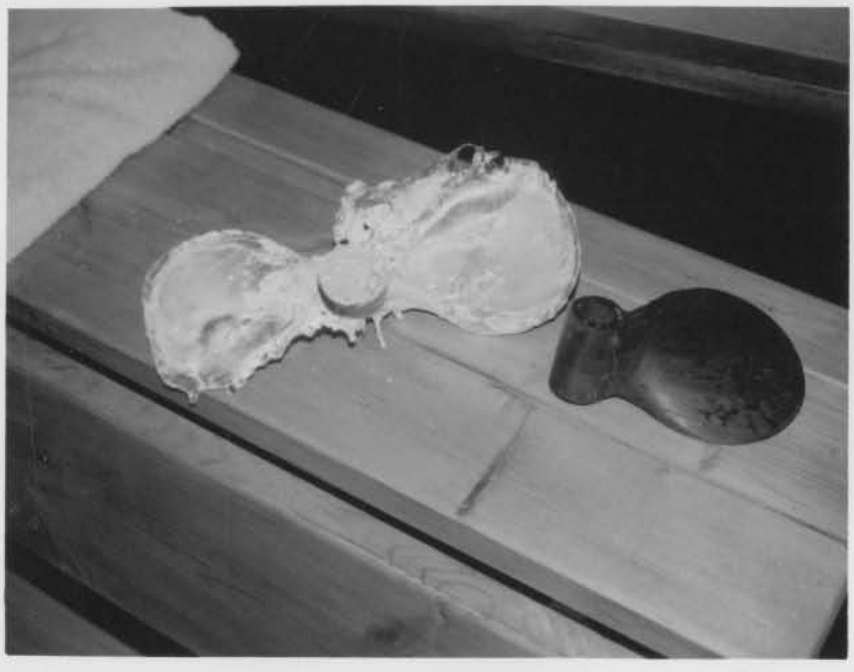

photo 6

4.6 Discussion

Small standard propellers are readily obtainable in Atlantic Canada from established firms which produce a variety of foundry products for the marine industry. However, custom designed propellers are very difficult to obtain and expensive to buy because traditional pattern costs cannot be written off on several jobs. A vessel owner will pay substantially more for a custom propeller (as demonstrated by the owner of the *MV. BEAR COVE POINT*), yet, the ability to acquire a custom design is hampered by the lack of technical capability of existing manufacturers. They cannot produce designs beyond their pattern inventory. Therefore, the need to develop a capability to custom cast small propellers was seen to be the next step in providing a complete professional and industrial propeller service. Interest in the work has been expressed by several individuals and firms, including the Canadaian Department of National Defence, and Canada's biggest manufacturer of large propellers, Canadian Stone Marine.

The geometry of a propeller is complex in the sense that almost all external surfaces are compound curves. The question is how can these specific shapes be reproduced in the mould so that the propeller can be cast.

To help reproduce the complex and variable propeller blade geometry in a mould, a strickle gear was designed and constructed. The strickle gear used the sweeping technique for producing the helical blade faces in much the same way

that very large propellers are swept-out with a loam board in the foundry pit. This strickle gear can incorporate rake and variable pitch into the blade face. These are inprovements over previous devices. The mould is then completed by building up the section profiles in some way. For example by using templates at radial locations along the span. In this way the need for a solid pattern is avoided, or if repeat orders are to be expected, this method can be used to make a solid pattern for quicker moulding in the future without the need for a highly skilled pattern maker.

To help with quality control and mould design, an expert system was developed to make proper mould design easier. When a new casting order is recieved, PRO-CASTER can be consulted, as a matter of routine, to ensure that experimentation is minimized. Feeding system dimensions may vary, but their configurations should be standardized to avoid recurrence of avoidable defects. This was percieved to be a major problem at another foundry. Other material specific information would also be availble to remind the foundryman of possible problem sources. The expert system will also be useful for training new foundry personnel and others.

Chapter 5

Conclusion

5.1 Propeller design

The design program WAOPTPROP, based on Lerbs' (1952) lifting line method, was written and tested. It reproduces the published results of calculation examples in Lerbs' paper. The program calculates the induced velocities at the blade sections from a non-optimum circulation distribution and then the required pitch distribution and the thrust and torque coefficients for the design condition. Propeller design using this program amounts to determining the hydrodynamic pitch distribution by comparing the design point coefficient with the pitch distribution/propeller coefficient relationship calculated.

The design program was used to design a new propeller for a 75ft steel stern

trawler. The result was compared with two other design methods and found to agree within the limits of known propulsive data for the vessel. To verify the new design, the existing propeller for the vessel was extensively altered by Avalon Propulsion Systems Limited: by adjusting the pitch to the new value, P/D=0.84; by increasing the expanded blade area by 20% to reduce the mean blade loading and to avoid premature cavitation; and by increasing the diameter from 68 to 70 inches. The altered propeller was put back into service. The vessels's owner reported that a 2-2.5 knot increase in speed at full load had been achieved. A new propeller was subsequently ordered based on the new design.

This case demonstrated that by applying sound engineering principles to difficult problems, good solutions can be found. The wake adapted design capability of the program has not yet been used on a real vessel, but it is expected to produce efficient designs in cases where wake data is available.

5.2 Performance analysis

The propeller preformance program PPT2 was written by combining thin airfoil theory and the Eckhardt and Morgan (1955) lifting line design method. PPT2 results for six B-series propeller analyses were compared with those measured experimentally and with the results of the lifting surface analysis program MIT-PSF-2. It was shown that the differences between the performance curves generated by PPT2

and those from the experimental results were attributable to differences between lifting surface theory and lifting line theory.

Thin airfoil theory was used to represent the blade sections of the propeller blades. Two NACA meanlines, a=0.8 and 1.0, and circular arc sections were built-in as possible options for analysis. The circular arc section lift and drag experimental data published by Riegels (1961) was re-analysed and then formulated in standard thin airfoil format. An idealized section lift model was used in conjunction with numerically calculated lift to determine the angle of attack at which a section was operating. The actual lift and drag could then be estimated; hence, the section thrust and torque contributions could be found. This was done at each section along the blade span; these values were then integrated to give the total thrust and torque for the whole propeller.

To assess the accuracy of the program, results for B-series propellers were generated. The approach gave consistent, smooth coefficient curves, which underestimated the experimental results by amounts ranging from 5 to 50% for thrust and up to as much as 100% for torque. MIT-PSF-2 gave results on the B-series experimental data curves, this implied that the differences were due to lifting surface effects. Lifting surface corrections for these differences were derived which depended on the pitch/diameter ratio and the blade loading (or advance coefficient) of the propeller. These corrections were applied to the same six propellers within PPT2.

The new performance results were plotted and shown to approximate the experimental curves more closely: the errors in thrust coefficients had been reduced to less than 10% in all cases. The errors in torque coefficients were also reduced, but they still varied between 10 and 40%. However, now the torque coefficients tended to over-estimate the B-series results, leading to conservative results.

Together, these two programs allowed the design and analysis of conventional marine propellers for small propellers. They could be used for design optimization of wake adapted propellers operating under sub-cavitating conditions. Lifting surface corrections were derived for two pitch/diameter ratios which approximately correct for the differences between lifting line and lifting surface theory. These corrections should be extended over a much wider range of geometric variations to make them more widely applicable. They were tested and found to give consistent engineering estimates of the thrust, torque and propeller efficiency under design and off-design conditions.

5.3 Full scale tests

A transducer to measure propeller thrust and torque by measuring the shaft material strains using strain gauges was designed and built. The excitation of the Wheatstone bridge circuits and the measurement signals were transmitted to the strain gauge conditioner via copper slip rings, carbon machine tool brushes and

shielded cables.

Sea trials were conducted on two 36'0" fishing vessel hulls: the *MV. SUGAR* and the *MV. BECKY A.*. The propeller thrust, torque and shaft RPM were measured at different boat speeds over a measured distance and timed. The results were analysed and plotted. Due to equipment failure, thrust measurements were not successful on the *MV. SUGAR*, but torque measurements were made throughout the sea trial. The torque coefficients calculated from the measured torque values were plotted as points on the performance curves from PPT2 (figure 3.1). The preformance curves are not corrected for lifting surface effects; therefore, a shift upward of the torque coefficient curve could be expected if corrections were applied which would have brought the measured points nearer the predicted curve. The trials of the *MV. BECKY A.* were successful. The analysed thrust and torque measurements indicated propulsion efficiencies which did not exceed about 35% (scatter of the results was about 30% of the measured values). These values confirmed by direct measurements the poor efficiencies common on these vessels. Bollard tests were also conducted on both vessels, but these measurements produced a large amount of scatter (about 100-150% of the measured value). A major source of scatter was electrical noise due in part to dirt contamination of the slip rings and in part to high levels of propeller induced vibration in the bollard condition. The ease with which the slip rings were contaminated was unexpected and not accounted for in

the design of the slip rings and pick-ups resulting in high noise levels in the thrust readings. The torque readings were relatively unaffected by noise, but determining zero thrust and torque was a problem. At low shaft speeds, brush induced noise was also noticed. This noise could be due to poor seating and chatter of the brushes in their holders.

The trial results re-affirmed the poor propulsive efficiency of fishing vessels. The highest value measured was only about 35%. Theoretically, higher values of about 50-55% should be attainable, but diameter restrictions due to inadequate aperture size may limit this to about 40%. Substantial increases in efficiency should be possible using good design practice in place of rules of thumb.

Speeds measured during the trial of the *MV. SUGAR* in protected and open water were compared and found to be substantially different. The speeds were about 10% higher over the entire range in protected waters and varied from about 4 knots to over 8 knots. The speeds attained by the *MV. BECKY A.* in St.John's harbour were similar to those attained by the other boat in protected waters. It could be expected that a similar reduction in speed with RPM would occur when the vessel leaves the confines of the harbour. These observations indicate a substantial increase in power requirement for a vessel operating on the open sea. Adequate service allowances must be made when determining the available power for propulsion.

The measured thrust and torque coefficient values for the *MV BECKY A.*

demonstrate the restricted range of advance coefficient, J, within which a vessel operates while free sailing. A propeller design must be optimized within this range. If a propeller has its highest efficiency outside this range, its performance will be very poor and the boat may not use all of the available power and may not attain its design speed; alternately, the engine will become overloaded before full speed is achieved.

If the case of a trawling propeller is considered, a sea trial would be useful to determine the wider range of advance coefficient, J, over which the trawler must operate due to increased load of the net. In effect, the net increases the resistance of the vessel, and the possible range of J. The lower end of the range will be extended. A towing propeller would then need to be optimized at some point between the free sailing and towing speed. The weighting toward one or the other would depend on the operational profile of the vessel. For this reason, when owners have several licences, they may also have different propellers optimized for the specific fishery which is pursued at the time, for example trawling or alternately fixed gear where no towing is done.

Optimization of this type can readily be done by using the performance analysis program PPT2. Competing propeller designs are indivdually evaluated and the best one chosen.

5.4 Manufacture of propellers

To produce custom propellers, the capability to make castings must exist. This initiated the work to develop aids to moulding propellers and to develop techniques to cast these economically. Two aids to moulding were developed to help in the design and dimensioning of a mould without requiring a solid propeller blade pattern. An expert system, PROCASTER, was developed to help define design criteria and dimensioning of mould components, and a strickle gear was designed and constructed that was used to construct the propeller blade shape. A crude reverberatory furnace was built to melt aluminum to test the constructed mould by casting a small propeller.

The moulding material chosen for the experiment was plaster. It has several attractive properties which include excellent dimensional stability, very low shrinkage during curing and very good detail reproduction. However, it was found that the plaster did not cure sufficiently under shop conditions to cast aluminum. It was determined that plaster moulds required baking for use when casting above a few hundred degrees. For aluminum the mould must be baked at 400-500^{0}F and for copper alloys at temperatures exceeding 1200^{0}F are required (P.M.C.A. 1983). The high moisture content of the un-baked plaster mould generated steam inside the cavity which caused porosity in the upper portion of the casting. The steam also separated the cope and drag slightly allowing some minor leakage of molten

metal to occur at the trailing edge parting line. Another unexpected problem arose while attempting to use the strickle gear to sweep out the helical blade surface. The plaster of paris set so quickly that the sweeping could not be completed. The mould had to be completed by using the solid wooden pattern. The problems encountered were a result of the choice of moulding material. The mould construction and layout functioned as desired; the metal was filled from the pouring cup and flowed through sprue and gate filling the cavity in a continuous undisturbed manner. When the cavity was about 3/4 full, the steam generated caused spattering and porosity. A sand mould would not require curing and would allow ample time to sweep the blade face and construct the mould.

Chapter 6

Recommendations

6.1 ...for improvments of software

- A more comprehensive set of lifting surface corrections should be developed and applied to both the design program and the performance analysis program.

- The programs should be made more user friendly by some flexibility in input data and more error traps to avoid crashes.

- Detailed documentation should be produced for both programs including sample runs and results.

- Propeller strength for detailed blade section design should be addressed in the design program as the next step in development.

- Section data should be modularized in data files to avoid the need for extensive

data input unless it is so desired.

- More section data for common section types should be incorporated. For example the NACA 66 modified profiles have been used extensively for large marine propellers.

- Detailed design output should be available for input into lifting surface programs.

6.2 ...for future full scale testing

- Improvements in the design of the stub shaft should include a sealed brush holder which is mounted integral and supported by the stub shaft. This would avoid dirt contamination of the slip rings and brushes and make installation onboard simpler and less prone to damage. A smaller and more compact brush set would enable a shortening of the stub shaft which would make it possible to install it in a wider selection of boats given that the thrust and torque limitations are not exceeded.

- Radio telemetry methods should be investigated for signal transmission.

- Further full scale testing should be undertaken to gather data concerning propulsive characteristics, resistance and wake.

- A wider range of advance coefficients could be tested by towwing another boat with the test boat to alter the resistance. This however will introduce other problems such as towing instability due to stretching of the towing line. This approach was discussed, but since propellers do not operate under these conditions under normal

circumstances (ie. not towing), it was not pursued further.

6.3 ...for manufacturing

- The strickle gear should be tested further for versatility. Several improvements can suggested even at this stage. A smaller and lighter sweep arm should be designed for close-in work (model propellers). The centre shaft is too long and should be shorter unless high pitch ratios require it to be full length. Excessive length makes it awkward to use. In addition, it must be smooth and slightly tapered at the bottom so that it can be easily removed from the mould. The current shaft was difficult to extract. The outer edge of the strickle gear should be calibrated for easier blade positioning (angular). Repeatability of blade shapes and profiles and blade tracking (surface height relative to other blades) should also be verified. A varied pitch propeller mould should be constructed using a set of pitch plates.

- The crude furnace operated beyond expectation. With improvement of the upper cylindrical cover by insulating and better sealing around the base, this furnace should be capable of melting small quantities of bronze.

- Bonded sand should be used for casting. This will require some basic handling equipment including a storage hopper to keep it clean when not in use and a muller for breaking up lumps and mixing the sand, clays and water for moulding.

- A sand muller should be designed and built.

- *More accurate casting and finishing requires* a more accurate and simpler measuring facility. A digital measuring machine with scale zeroing should be designed and built.

- Computer software should be written to convert design specifications from design *programs to manufacturing blade off-sets for shop use.*

- Develop a low cost floor mounted melting furnace. It should have a sufficient capacity for a two meter diameter propeller (400 kg of bronze). The melting time should reasonable, but higher heat capacities will require more expensive equipment. Naturally aspirated burners should be investigated.

References

Abbott, I.H., von Doenhoff, A.E., Stivers, L.S., 1945, *Summary of Airfoil Data: Report No. 824, Part I,II.* Langley Memorial Aeronautical Laboratory, Langley Field, Va., pp. 63.

Abbott, I.H., von Doenhoff, A.E., 1959, *Theory of Wing Sections*, Dover Publications Inc., New York, pp. 693.

AFS, 1984, *Casting Copper-base Alloys*, American Foundrymen's Society Inc. , pp.250.

AFS, 1986, *Patternmaker's Manual*, American Foundrymen's Society Inc., pp.200.

AFS, 1989, *Metal Caster's Reference Guide*, American Foundrymen's Society Inc., pp.647.

Bennet, R., Hatfield,M., 1966, " Development of Strain Guage Techniques for the Measurement of Propeller Shaft Torque in Distant water trawlers", White Fish Authority, *Journal of Strain Analysis*, Vol. 1, No.2., pp.102-109.

Betz, A., 1910, " Schrauben Propeller mit Geringstem Energie Verlust", translated from German by T.Hofmann and N.Bose, " Screw Propellers with Minimum Energy Loss", 1990, *Ocean Engineering Research Centre*, Memorial University of Newfoundland, Rep.No. OERC90-HYD-LR-02., pp.20.

Bose,N., 1983, " The Design of a Wind Turbine Propulsion System", *ISSHES-83*, El Pardo, Paper No. IX.1, Sept., pp.8.

Burrill, L.C., 1943-44, " Calculation of Marine Propeller Performance Characteristics", *Trans. North East Coast Institute of Engineers and Shipbuilders*, Vol.60, p. 269-298.

Burrill, L.C., 1965, " Aerodynamics and Marine Propeller Design", *Trans. North East Coast Institute of Engineers and Shipbuilders*, Vol.81., pp.149-174.

Burtner, E., 1953, " A Relationship for Preliminary Propeller Diameter", *Journal of the American Society of Naval Engineers Inc.*, Vol. 65, No. 3.

Chakravarty, T., 1967, *Manufacture of Large Marine Propellers*, Short term course in modern foundry practice (Feb. 20 - May 13, 1967), Foundry Training Center, Dept. of Mechanical Engineering, I.I.T. Kharagpur, India, pp.52.

Cox, G.G., 1961, " Corrections to the Camber of Constant Pitch Propellers". *R.I.N.A.*, Vol.103, pp.227-243

Czyrca, E.J., Niederberger, R.B., 1975, " Mechanical, Fatigue and Corrosion Properties of Propeller Bronzes", *Society of Naval Architects and Marine Engineers. Propellers 75*, No.8, July 22-23, pp.8.1-8.17.

Dally,J.W., Riley,W.F., 1965, *Experimental Stress Analysis*, Second Ed. McGraw Hill Kogahusha Ltd., 1965, 1978, pp.571.

Dickman, H., 1938, "Thrust Deduction, Wave Making Resistance of a Propeller and Interference in Ship Waves", original German, *Ingenieur-Archiv*, Vol. 9, pp.452-480.

Eckhardt, M.K., Morgan W.B., 1955, " A Propeller Design Method", *Trans. Society of Naval Architects and Marine Engineers*, Vol. 63, pp.325-374.

Flinn, R.A., 1963, *Fundementals of Metal Casting*, Addison Wesley Pub. Co. Inc., Reading Mass.

Gerr, D., 1989, *Propeller Handbook*, International Marine Publishing Company, Cambden, Me., pp.152.

Glauert,H., 1947 *The Elements of Airfoil and Airscrew Theory*, Second Ed., Cambridge University press, Cambridge 1983, c.1947 Cambridge Science Classics Series.

Glover, E.J., 1987, "Developments in Propeller Theory and Their Relevance To Propeller Design", *I.M.A.E.M.* Bulgaria,Varna, May, pp.6.1-6.7.

Goldstein, S., 1929, " On The Vortex theory of Propellers", *Proceedings of the Royal Society*, Series A, Vol. 63, pp.440-465.

Goudie, W.J., 1920, *The Geometry of the Screw Propeller*, Blackie and Son Ltd., London, pp.42.

Greely, D.S., Kerwin, J.E., 1982, " Numerical Methods for Propeller Design and Analysis in Steady Flow", *Trans. Society of Naval Architects and Marine Engineers*, Vol. 90, pp.415-453.

Guilloton, R., 1949, "The Calculation of Ship Screws", *Institution of Naval Architects*, London, Vol. 91.

Hoerner, S.F., Borst, H.V., 1985, *Fluid Dynamic Lift sec.ed.*, Pub. Mrs. Liselotte A. Hoerner, pp.362.

Hofmann, T., 1989a, *Notes: Foundry Practice at Osborne Propellers Ltd.*, Winter (unpublished), pp.4.

Hofmann, T., 1989b, *A Method of Marine Screw Propeller Design Through the Use of Computerized Iterations*, Work Term Report 5, submitted to Dept. of Co-ordination, Faculty of Engineering and Applied Science, Memorial University of Newfoundland, St. John's, Newfoundland, April, (unpublished), pp.55.

Hofmann, T., Dec. 1989c, *WAP.EXE Version 1.0 - A Lifting Line Propeller Design Program*, Workterm Report 6, submitted to Dept. of Co-ordination, Faculty of Engineering, Memorial University of Newfoundland, (unpublished), pp.50.

Hofmann,T., April 1990a, *Propeller Performance Simulation*, Senior Design Project Report for Engineering 8000 - Ship design, submitted to Prof. W.J.Milne, Chairman, Naval Architectural Engineering Dept., Memorial University of Newfoundland, April, (unpublished), pp.55.

Hofmann, T., 1990b, "Strickle Gear for Propellers", *Ocean Engineering Research Centre*, Memorial University of Newfoundland, Rep.No. OERC90-HYD-LR-01, pp.15.

Hofmann, T., 1990c, "PROCASTER: An expert System for Bronze Propeller Casting", *Ocean Engineering Research Centre*, Memorial University of Newfoundland, Rep.No. OERC91-HYD-TR001, pp.58.

ISO, 1981, *International Organization of Standardization 484/2 Shipbuilding - Ship Screw Propellers - Manufacturing Tolerances, Part 2: Propellers of 0.80 m and 2.50 m Inclusive*, pp.6.

Kerwin, J.E., 1959, " Machine Computation of Marine Propeller Characteristics", *International Shipbuilding Progress*, vol. 6, no. 60, August, pp.343-354.

Kerwin, J.E. 1986, "Marine Propellers", *Annual Review Fluid Mechanics*, 18, pp.367-403.

Kinoshita, M., Okada S., Sudo S., 1962, " Experimental and Analytical Results of Thrust Measurements on Actual Merchant Ships", *Fourth Symposium of Naval Hydrodynamics*, Washington D.C., August 27-31, pp.407-427.

Kramer, K.N., 1939, " The Induced Efficiency of Optimum Propellers Having a Finite Number of Blades", *NACA Technical Memorandum*, No. 884, Washington, pp.18-38.

Kress, R.F., van Oekel, J., Prager, M., 1984, "Economics and Suitability of Typical Marine Propeller Materials", *Society of Naval Architects and Marine Engineers, Propellers 84 Symposium*, May 15-16, paper No. 18, pp.18.1-18.17.

Kruppa, C.F.L., 1967, *High Speed Propellers, Hydrodynamics and Design*, A 3-Day Intensive Course for Engineers, Oct. 9-11, University of Michigan. Continuing Engineering Education. pp.99.

Lammeran, W.P.A.van, Manen, van J.D., Oosterveld, M.W.C., 1969, "The Wageningen B-Screw Series", *Trans. Society of Naval Architects and Marine Engineers*, Vol. 77, pp.269-317.

Langham, J.M., 1964, "The Manufacture of Marine Propellers with Particular Reference to the Foundry", *Stone Manganese Marine*, Technical Papers issue no. 1, pp.4.

Lerbs, H.W., 1952, "Moderately Loaded Propellers with a Finite Number of Blades and an Arbitrary Distribution of Circulation", *Trans. Society of Naval Architects and Marine Engineers*, Vol.60, pp.73-123.

Manen, J.D. van, Troost, L., 1952, "The Design of Ship Screws of Optimum Diameter for an Unequal Velocity Field", *Trans. Society of Naval Architects and Marine Engineers*, Vol.60, pp.442-468.

Morgan, W.B., 1954, "An Approximate Method of Obtaining Stresses in a Propeller Blade", *David Taylor Model Basin*, Report no. 919, Washington D.C., pp.18.

Morgan, W.B., Silovic, V., Denny, S.B., 1968, "Propeller Lifting Surface Corrections", *Trans. Society of Naval Architects and Marine Engineers*, Vol.76, pp.309-347.

Moriya, T., 1933, "On the Induced velocity and Characteristics of a Propeller", *The Journal of the Faculty of Engineering Tokyo Imperial University*, Tokyo, Japan, Vol. XX, No. 7, pp.146-162.

Muckle, W., 1941, "Stresses in Propeller Blades", *The Shipbuilder and Marine Engine Builder*, Vol. 47, No. 388, pp.336-341.

Nordco Ltd., 1990. "An Investigation of the Resistance, Self-Propulsion and Seakeeping Characteristics of a 65ft Fishing Vessel", Report Project No. 212-89 I.

O'Brien, T.P., 1962, *The Design of Marine Screw Propellers*, Hutchinson and Company, Scientific and Technical, London, pp.397.

Paulson, J.F., Doorn,v. J.P., Franson, H.P., 1982, " Subcavitating Propeller Design for High Powered Small Craft",*International Conference on Propulsion for Small Craft, Propellers, Sterngear, Engines and Installations*, Royal Institution of Naval Architects, RINA Small Craft Group, November 9,10.

P.M.C.A. 1983, *The Plaster Mold casting Handbook*, The Plaster Mold Casting Association, pp.83.

Prandtl, L., 1918-19, *Wing Theory I and II*, Gottinger Nachricten.

Private Communication, 1964, " Strickle Gear", *University of Glasgow*, Dept. of Naval Architecture and Ocean Engineering.

Riegels, F.W., 1961, *Aerofoil Sections*, London Butterworths, pp.165-167.

Romson, J.A., 1952, "Propeller Strength calculation", *The marine Engineer and Naval Architect*, February, p.52-54,117-122.

Schubert, H., 1940, "The determination of the Dynamic Characteristics of Lightly Loaded Propellers of Arbitrary Shape", *Deutsche Luftfahrtforschung*, Jahrbuch 1940.

Stone Manganese Marine, "Comparitive Properties of Propeller Alloys", SMM Technical Brief No. 14, pp.4.

Williams, M., 1987, "At DuPont, Expert Systems are Key to AI Implementation", *PC Week*, January13, 1987, p.35.

Wu, S., Bose, N., 1991," An Experimental Investigation into the Propulsive Efficiency of Two Newfoundland Fishing Vessel Forms", Ocean Engineering Research Centre Report No. OERC91-WTT-TR001, Faculty of Engineering, Memorial University of Newfoundland, Canada, pp.45.

Wu, Yao-tsu, 1965, "Some Recent Developments in Propeller Theory", *Schiffstechnik, Forschungsheft für Schiffbau and Schiffsmaschinenbau*, heft 60 (12 band).

Appendix A

Empirical propeller selection

The first method of selecting a stock propeller is most often used when very little information about a boat is available. It is based on the comparison of the propeller "horsepower curve", which is roughly the thrust power developed by a stock propeller, and the power curve of the engine. These two curves should intersect at the maximum operating rpm of the engine. Usually, the 70-85 % maximum rpm is used because most engines have the lowest specific fuel consumption in this speed range. This also makes allowances for some of the other unknowns involved. This method often gives a propeller that will not overload the engine but its performance remains questionable. In most cases where this method is used, the installed power is relatively low and performance is not a primary consideration, but engine loading is. The propeller thrust changes with boat speed and the propeller may not necessarily absorb all the power available at a given rpm, but, usually a free running propeller is designed to absorb all the available power at maximum rpm. Hence, the achieved boat speed remains a function of the engine power installed.

The second method which has been in use in North America for many years is the slip method or Crouch's method. It is an empirical method whereby the propeller pitch is matched to the boat speed at about 90 % of maximum rpm. The pitch is calculated without taking into account the slip [1]. The pitch without slip is then increased by the amount of slip which is calculated empirically or guessed at based on experience. That is, if the slip is approximately 40 %, then the pitch is increased approximately 40 % to give the required pitch of the propeller. The installed engine power must then be capable of producing the amount of power demanded by the propeller to avoid overload. This method gives a quick and approximate first estimate for stock propellers used in applications where efficiency is of less importance; these include, powerboats, speedboats and workboats. For workboats, more experience is required to make this method work and some knowledge of the type of operation (that is, is it used for towing, maneuvring, or simply self-propulsion as in a barge, say). The method is used widely by small craft designers and some propeller representatives for first estimates and replacement of old propellers (Gerr 1989). Often a pitch adjustment may be necessary to ensure the maximum engine rpm is reached in cases where overload or underload becomes a problem.

A third level of sophistication can be introduced into propeller matching by using the results from tests on model propellers to determine their performance. Although many systematic series of propellers have been tested over the years, the most comprehensive and widest range of testing was carried out by the Netherlands Ship

[1] Slip is a term used to account for the induced velocities of a propeller. The slip is the difference between the distance a propeller would travel in a solid medium and the distance it travels in water. Apparent slip = theoretical advance (pitch X rpm) - actual advance. True slip can be determined from a measured mile run at a known rpm and propeller pitch.

Model Basin at Wageningen, the Netherlands (NSMB now MARIN). The NSMB B-series (also known as the Troost B-Series) model propellers have been extensively tested in open water (without the influence of a hull) and the results plotted in the form of charts (van Manen and Troost 1952, van Lammeran and Oosterveld 1969). The power factor, B_p, is plotted as a function of advance coefficient, δ, for variations of pitch/diameter ratios. Hence, the method is called the B_p-δ chart method. So, based on a power factor, B_p, calculated for the case under consideration and the design speed (advance coefficient) the pitch ratio and propeller open water efficiency can be read off. This method has been used since the first series of tests were completed. It is very useful for designing propellers which are geometrically similar to the B-series propellers but certain corrections must be made to account for operation behind a hull. For example, it has been shown that a 3-4 % reduction from the optimum open water diameter performs better on a single screw ship (Gerr 1989, van Manen and Troost 1952). The experimental data is also used in other ways. The K-J and $\mu - \sigma$ charts are very useful in performance analysis at off design conditions. These are plots of the same experimental data in forms which lend themselves to extracting preformance information such as thrust and torque coefficients and open water efficiency at speeds other than the design speed or to determine the extra thrust available for towing. Another very useful presentation of the data is in the form of polynomials based on regression analysis and curve fitting. These give thrust and torque coefficients by direct calculation and are written in terms of the pitch-diameter ratio, advance coefficient (speed) and rpm. These are especially attractive for computer applications. A program, BKTKQ was written by using these polynomials to calculate the performance of the B-series propellers

over their entire operating range. This program was used to verify the output form the program PPT2.

In some cases, designers use these results for preliminary work with special propellers, such as supercavitating propellers, by introducing some empirical corrections. The B_p-δ charts are however less useful near their limits because the coefficients as plotted go off the charts. As in all engineering work, results should be checked by other means. However, since very high speed applications, 50-60 knots, fall outside the useful range of subcavitating propellers (conventional propellers), it is not recommended that the charts be used under these conditions.

To summarize, B_p-δ charts are very useful in preliminary design calculations, for determining propeller diameter. They can also be used to evaluate alternative propulsion configurations (at least qualitatively). Other methods such as the slip method can be very useful for checking design results or sizing propellers when very little is known about the vessel. Many repairers and manufacturers also have rules of thumb which they can use to determine pitch changes or size propellers knowing the operating conditions of similar vessels.

Appendix B

Fortran listing of WAOPTPROP

```
C WAKE ADAPTED LIFTING LINE PROGRAM BASED ON LERB'S METHOD TO FIND
C THE INDUCED VELOCITY DISTRIBUTIONS ON THE VORTEX
C SHEETS THROUGH A CIRCULATION DISTRIBUTION.
C ---------------------------------------------
C SYMBOL DEFINITION:
C
C G=NUMBER OF BLADES
C LS=ADVANCE COEFFICIENT OF SHIP
C WO=TAYLOR WAKE FRACTION
C W(X)=LOCAL RADIAL WAKE FRACTION
C X=RADIUS FRACTION
C XH=RADIUS FRACTION AT HUE CYLINDER
C PHI=REFERNCE ANGLE PARAMETER OF X
C XO=VORTEX LOCATION RADIUS FRACTION
C PHIO=REFERNCE ANGLE PARAMETER OF XO
C Q=MAXIMUM NUMBER OF FOURIER COEFFICIENTS
C N,M=MAXIMUM NUMBER OF STATIONS ON BLADE (MUST BE EQUAL)
C BIO=PITCH ANGLE OF VORTEX
C WAV, WTV= AXIAL AND TANGENTIAL INDUCED VELOCITY VS. SHIP SPEED
C           RATIO
C CPI=INPUT POWER COEFFICIENT
C CP=POWER COEFFICIENT (CALCULATED)
C CT= THRUST COEFFICIENT (CALCULATED)
C CIRC=LOCAL SECTION CIRCULATION
C GCIRC=FOURIER COEFFICIENT OF CIRCULATION EXPANSION
C
C ---------------------------------------------
C
C VARIABLE DECLARATION
C
REAL LS,X(7),XO(7),XH,PISIN,LISX,WTV(7),WAV(7),circ(7)
REAL CIRC2(14),FI(14),RADX(14),EFF,FWAV(7),FWTV(7)
double precision IT(7,7),IA(7,7),INT(7,7),INA(7,7),YO,Y
DOUBLE PRECISION XOX(7,7),BIO(7),A(7,7,8),phio(7),phi(7),phio1
DOUBLE PRECISION A2(7,8),XT(7),COSINA(7,7),SININA(7,7)
DOUBLE PRECISION COSINT(7,7),SININT(7,7),SUMCOS(7,7),A3(7,8)
DOUBLE PRECISION XA(7),SUMCOT(7,7),HA(7,5),HT(7,5),GA(5,6)
DOUBLE PRECISION GCIRC(5),sumsin(7,8),SUMINTO(7),SUMINAO(7)
DOUBLE PRECISION SUMSIT(7,8),MSUMINTO(7),MSUMINAO(7)
DOUBLE PRECISION NINTO(7),NINAO(7),SUMNINTO(7),SUMNINAO(7)
DOUBLE PRECISION COSINTN(7),COSINAN(7),SCOSINTN(7)
DOUBLE PRECISION SCOSINAN(7),MSCOSINT(7),MSCOSINA(7)
DOUBLE PRECISION NCOSINT(7),NCOSINA(7),SNCOSINT(7),SNCOSINA(7)
DOUBLE PRECISION JPI,JPI1,pd(7),tanbi(7),pd1,p,d,W(7),ETANOT
DOUBLE PRECISION WO,WAKEFCN(7),DIFFCP,CPI
INTEGER N,M,NP,G,COUNT,K,MP,I,J,Q,N2,iteration
C
OPEN(UNIT=9,NAME='WAOPTPROP.OUT',TYPE='NEW')
C
C INITIAL VALUE OF IDEAL PROPELLER EFFICIENCY
C
ETANOT=0.3
iteration=0.0
C
C PROPELLER DIAMETER
C
D=1.0
C
C NUMBER OF BLADES
C
G=4
C
```

```
C ADVANCE COEFFICIENT
C
Ls=0.25
C
C HUB RADIUS FRACTION
C
XH=0.2
C
C REQUIRED INPUT POWER COEFFICIENT
C
CPI=0.784
C
C OVERALL AND LOCAL WAKE FRACTIONS
C
W0=0.272
W(1)=0.686
W(2)=0.624
W(3)=0.432
W(4)=0.266
W(5)=0.192
W(6)=0.164
W(7)=0.155
C
C ARRAY DIMENSIONING
C
N=7
M=7
Q=5
NP=N+1
MP=M+1
C
PI=3.141592654
PHI01=PI/(N-1)
C
C INITIALIZE ALL ARRAYS
C
 1111 DO 1 I=1,M
X(I)=0.0
PHI(I)=0.0
DO 2 J=1,N
BIO(J)=0.0
XO(J)=0.0
PHIO(J)=0.0
IT(I,J)=0.0
IA(I,J)=0.0
INT(I,J)=0.0
INA(I,J)=0.0
XOX(I,J)=0.0
a2(i,j)=0.0
A3(I,J)=0.0
COSINA(I,J)=0.0
COSINT(I,J)=0.0
SININA(I,J)=0.0
SININT(I,J)=0.0
SUMSIN(I,J)=0.0
SUMSIT(I,J)=0.0
SUMCOT(I,J)=0.0
SUMCOS(I,J)=0.0
 2 CONTINUE
 1 CONTINUE
```

```
C
C DEFINE VORTEX REFERNCE ANGLES
C
DO 10 I=1,N
PHIO(I)=PHIO1*(I-1)
 10 CONTINUE
C
C DEFINE RADIUS FRACTION REFERENCE ANGLE
C
DO 20 I=1,N
PHI(I)=PHIO1*(I-1)
 20 CONTINUE
C
C DEFINE RADIUS FRACTIONS
C
DO 29 I=1,N
XO(I)=0.5*(1+XH)-0.5*(1-XH)*COS(PHIO(I))
 29 CONTINUE
C
C X(1)=0.00001
DO 30 I=1,N
X(I)=0.5*(1+XH)-0.5*(1-XH)*COS(PHI(I))
 30 CONTINUE
C
C WAKE ADAPTATION
C
DO 35 I=1,N
WAKEFCN(I)=ETANOT*((1-W(I))/(1-WO))**0.5
write(9,*) 'wakefcn(',i,')=',wakefcn(i)
 35 CONTINUE
C
C DEFINE VORTEX PITCH ANGLES
C
DO 40 I=1,N
IF (XO(I).EQ.0.0) THEN
BIO(I)=1.570796327
GOTO 40
END IF
BIO(I)=ATAN(LS/X(I)*(1-W(i))/WAKEFCN(I))
 40 CONTINUE
DO 41 I=1,N
DO 42 J=1,N
XOX(I,J)=XO(J)/X(I)
 42 CONTINUE
 41 CONTINUE
WRITE(9,*) '   PHI             PHIO                BIO'
DO 43 I=1,N
WRITE(9,*) PHI(I),PHIO(I),BIO(I)
 43 CONTINUE
c WRITE(9,*) '   XO              X'
c DO 46 I=1,N
c WRITE(9,*) XO(I),X(I)
c 46 CONTINUE
c DO 44 I=1,N
c         DO 45 J=1,N
c WRITE(9,*) ' XOX(',I,J,' )=',XOX(I,J)
c 45    CONTINUE
c 44 CONTINUE
C
C CALL SUBROUTINE INDUCT TO CALCULATE THE LERBS INDUCTION FACTORS
C
CALL INDUCT(IT,IA,BIO,XOX,G,N,M)
```

```
C
C
C FOR EACH VALUE OF PHI SET UP FOURIER COEFFICIENT MATRIX
C USING SUBROUTINE FCINDUCT AND THEN SOLVE THE MATRIX USING
C THE SUBROUTINE GAUSS. FIRST FOR TANGENTIAL COMPONENT 'IT'
C THEN FOR THE AXIAL COMPONENT 'IA'.
C
DO 70 I=1,M
       CALL FCINDUCT(A,IT,N,M,PHIO,I)
c WRITE(9,*) ' PHI=',I,' OUTSIDE FCINDUCT'
C DO 69 J=1,N
C DO 68 K=1,N+1
C WRITE(9,*) ' A(',I,J,K,' )=',A(I,J,K)
C 68 CONTINUE
C 69 CONTINUE
   DO 60 J=1,N
DO 65 K=1,N+1
A2(J,K)=A(I,J,K)
c WRITE(9,*) ' A2(',J,K,' )=',A2(J,K)
 65 CONTINUE
 60    CONTINUE
   CALL GAUSS(XT,A2,N,NP)
C    WRITE(9,*) ' OUTSIDE GAUSS'
C    WRITE(9,*) ' INDUCTION FACTOR FOURIER COEFFICIENTS'
   DO 66 K=1,N
INT(I,K)=XT(K)
C         WRITE(9,*) ' INT(I,K)',XT(K),INT(I,K)
 66    CONTINUE
 70 CONTINUE
DO 51 I=1,M
   CALL FCINDUCT(A,IA,N,M,PHIO,I)
   DO 52 J=1,N
DO 53 K=1,N+1
A3(j,k)=A(I,J,K)
C WRITE(9,*) ' A3(',J,K,' )=',A3(J,K)
 53 CONTINUE
 52    CONTINUE
   CALL GAUSS(XA,A3,N,NP)
   DO 54 K=1,N
INA(I,K)=XA(K)
 54    CONTINUE
 51 CONTINUE
C
c WRITE(9,*) ' PHI                PHIO'
c DO 71 I=1,N
c    WRITE(9,*) PHI(I),PHIO(I)
c 71  CONTINUE
c WRITE(9,*) ' '
c WRITE(9,*) ' XOX                          INT
c     *        INA'
c DO 72 I=1,M
c write(9,*) ' '
c WRITE(9,*) ' PHI=',i,PHI(I)
c WRITE(9,*) ' '
c DO 73 J=1,N
c WRITE(9,*) XOX(I,J),INT(I,J),INA(I,J)
c 73 CONTINUE
c 72 CONTINUE
C
```

```
C BEGIN CALCULATION OF hm TERMS
C
DO 80 I=1,M
     DO 90 J=1,N
COSINA(I,J)=INA(I,J)*DCOS((J-1)*PHI(I))
SININA(I,J)=INA(I,J)*DSIN((J-1)*PHI(I))
COSINT(I,J)=INT(I,J)*DCOS((J-1)*PHI(I))
SININT(I,J)=INT(I,J)*DSIN((J-1)*PHI(I))
 90      CONTINUE
 80 CONTINUE
C WRITE(9,*) '                    COSINA                    SININA'
C DO 81 I=1.3
C      DO 91 J=1,N
C WRITE(9,*) I,J,COSINA(I,J),SININA(I,J)
C 91      CONTINUE
C 81 CONTINUE
C WRITE(9,*) '                    COSINT                    SININT'
C DO 82 I=1,3
C     DO 92 J=1,N
C WRITE(9,*) I,J,COSINT(I,J),SININT(I,J)
C 92      CONTINUE
C 82 CONTINUE
DO 100 I=1,M
SUMCOT(I,1)=COSINT(I,1)
SUMCOS(I,1)=COSINA(I,1)
DO 110 J=2,N
SUMCOS(I,J)=SUMCOS(I,(J-1))+COSINA(I,J)
SUMCOT(I,J)=SUMCOT(I,(J-1))+COSINT(I,J)
 110 CONTINUE
 100 CONTINUE
C write(9,*) '                    SUMCOS                    SUMCOT'
C DO 115 I=1,3
C WRITE(9,*) ' '
C DO 116 J=1,N
C WRITE(9,*) I,J,SUMCOS(I,J),SUMCOT(I,J)
C 116 CONTINUE
C 115 CONTINUE
do 120 I=1,M
SUMSIN(I,1)=0.0
SUMSIN(I,2)=0.0
SUMSIN(I,N+1)=0.0
SUMSIT(I,1)=0.0
SUMSIT(I,2)=0.0
SUMSIT(I,N+1)=0.0
DO 130 J=N,3,-1
SUMSIN(I,J)=SUMSIN(I,J+1)+SININA(I,J)
SUMSIT(I,J)=SUMSIT(I,J+1)+SININT(I,J)
 130 CONTINUE
 120 CONTINUE
C WRITE(9,*) '                    SUMSIN                    SUMSIT'
C DO 105 I=1,3
C WRITE(9,*) ' '
C DO 106 J=1,N
C WRITE(9,*) I,J,SUMSIN(I,J),SUMSIT(I,J)
C 106 CONTINUE
C 105 CONTINUE
C
C FOR CONDITIONS WHERE PHI=0 DEGREES
```

```
C
SUMINTO(1)=INT(1,1)
SUMINAO(1)=INA(1,1)
DO 107 J=2,N
SUMINTO(J)=SUMINTO(J-1)+INT(1,J)
SUMINAO(J)=SUMINAO(J-1)+INA(1,J)
 107 CONTINUE
DO 108 J=1,N
MSUMINTO(J)=(J-1)*SUMINTO(J)
MSUMINAO(J)=(J-1)*SUMINAO(J)
 108 CONTINUE
DO 109 J=1,N
NINTO(J)=(J-1)*INT(1,J)
NINAO(J)=(J-1)*INA(1,J)
 109 CONTINUE
SUMNINTO(N)=NINTO(N)
SUMNINAO(N)=NINAO(N)
DO 250 J=N-1,3,-1
SUMNINTO(J)=SUMNINTO(J+1)+NINTO(J)
SUMNINAO(J)=SUMNINAO(J+1)+NINAO(J)
 250 CONTINUE
DO 260 J=1,Q
HT(1,J)=PI*(MSUMINTO(J+1)+SUMNINTO(J+2))
HA(1,J)=PI*(MSUMINAO(J+1)+SUMNINAO(J+2))
 260 CONTINUE
C
C
C FOR PHI BETWEEN 0 AND 180 DEGREES...
C
DO 140 I=2,M-1
C write(9,*)i,' phi=',phi(i)
PISIN=PI/SIN(PHI(I))
C WRITE(9,*) ' PISIN=',PISIN
   DO 150 J=1,Q
SINPHI=SIN((J)*PHI(I))
COSPHI=COS((J)*PHI(I))
C WRITE(9,*) ' SINPHI=',SINPHI,' COSPHI=',COSPHI
C WRITE(9,*) ' SUMCOS=',SUMCOS(I,J+1),'
C     *SUMSIN=',SUMSIN(I,J+2)
C WRITE(9,*) ' SUMCOT=',SUMCOT(I,J+1),'
C     *SUMCOT=',SUMCOT(I,J+2)
C WRITE(9,*) ' '
C
HA(I,J)=PISIN*(SINPHI*SUMCOS(I,J+1)+COSPHI*SUMSIN(I,(J+2)))
C
HT(I,J)=PISIN*(SINPHI*SUMCOT(I,J+1)+COSPHI*SUMSIT(I,(J+2)))
C
 150     CONTINUE
 140 CONTINUE
C
C CONDITION FOR PHI=180 DEGREES
C
DO 280 J=1,M
JPI=(J-1)*PI
COSINTN(J)=DCOS(JPI)*INT(N,J)
COSINAN(J)=DCOS(JPI)*INA(N,J)
 280 CONTINUE
SCOSINTN(1)=COSINTN(1)
```

```
SCOSINAN(1)=COSINAN(1)
DO 281 J=2,N
SCOSINTN(J)=SCOSINTN(J-1)+COSINTN(J)
SCOSINAN(J)=SCOSINAN(J-1)+COSINAN(J)
 281 CONTINUE
DO 282 J=1,N
MSCOSINT(J)=(J-1)*SCOSINTN(J)
MSCOSINA(J)=(J-1)*SCOSINAN(J)
 282 CONTINUE
DO 283 J=1,N
JPI=(J-1)*PI
NCOSINT(J)=DCOS(JPI)*(J-1)*INT(N,J)
NCOSINA(J)=DCOS(JPI)*(J-1)*INA(N,J)
 283 CONTINUE
SNCOSINT(N)=NCOSINT(N)
SNCOSINA(N)=NCOSINA(N)
DO 284 J=N-1,3,-1
SNCOSINT(J)=SNCOSINT(J+1)+NCOSINT(J)
SNCOSINA(J)=SNCOSINA(J+1)+NCOSINA(J)
 284 CONTINUE
DO 290 J=1,Q
JPI1=J*PI
HT(N,J)=-PI*DCOS(JPI1)*(MSCOSINT(J+1)+SNCOSINT(J+2))
HA(N,J)=-PI*DCOS(JPI1)*(MSCOSINA(J+1)+SNCOSINA(J+2))
 290 CONTINUE
C
C
C
WRITE(9,*) '                    HA                              HT'
DO 141 I=1,M
   WRITE(9,*) ' '
   DO 151 J=1,Q
WRITE(9,*) I,J,HA(I,J),HT(I,J)
 151    CONTINUE
 141 CONTINUE
C
C CALCULATE AUGMENTED FOURIER COEFFICIENT MATRIX FOR CIRCULATION
C
DO 160 I=2,N-1
C WRITE(9,*) I,' Ls=',Ls,' X=',X(I)
LISX=LS*(1.-W(I))/X(i)
C WRITE(9,*) ' LIX=',LIX
DO 170 J=1,Q
C WRITE(9,*) J,'HA=',HA(I,J),'HT=',HT(I,J)
GA(I-1,J)=J*(WAKEFCN(I)*HA(I,J)+LISX*HT(I,J))
 170 CONTINUE
 160 CONTINUE
DO 180 I=2,N-1
GA(I-1,Q+1)=(1.-XH)*(1.-W(I))*(1.-WAKEFCN(I))
 180 CONTINUE
DO 161 I=1,Q
DO 171 J=1,Q+1
C WRITE(9,*) ' GA(',I,J,' )=',GA(I,J)
 171 CONTINUE
 161 CONTINUE
C
C CALL GAUSS TO SOLVE FOR THE FOURIER COEFFICIENTS OF
C CIRCULATION DISTRIBUTION.
C
QP=Q+1
```

```
CALL GAUSS(GCIRC,GA,Q,QP)
C
WRITE(9,*) ' '
DO 181 I=1,Q
WRITE(9,*) ' GCIRC(',I,' )=',GCIRC(I)
 181 CONTINUE
C
C CALCULATE CIRCULATION DISTRIBUTION
C
DO 210 I=1,N
   DO 220 J=1,Q
CIRC(I)=CIRC(I)+GCIRC(J)*SIN(J*PHI(I))
 220    CONTINUE
 210 CONTINUE
WRITE(9,*) ' '
DO 211 I=1,N
WRITE(9,*) ' CIRC(',I,' )=',CIRC(I)
 211 CONTINUE
C
C CALCULATE DOUBLE NUMBER OF POINTS OF CIRCULATION
C
N2=N*2
DO 212 I=1,N2
FI(I)=PHI01*(I-1)/2
RADX(I)=0.5*(1.+XH)-0.5*(1.-XH)*COS(FI(I))
 212 CONTINUE
DO 213 I=1,N2
  DO 214 J=1,Q
CIRC2(I)=CIRC2(I)+GCIRC(J)*SIN(J*FI(I))
 214 CONTINUE
 213 CONTINUE
WRITE(9,*) ' CIRCULATION WITH INTERMEDIATE POINTS'
WRITE(9,*) ' '
DO 215 I=1,N2
WRITE(9,*) I,'RADX=',RADX(I),' CIRC2=',CIRC2(I)
 215 CONTINUE
C
C CALCULATE  TANGENTIAL AND AXIAL COMPONENTS OF INDUCED VELOCITY
C
DO 182 I=1,N
WTV(I)=0.0
WAV(I)=0.0
 182 CONTINUE
DO 190 I=1,N
   DO 200 J=1,Q
WTV(I)=WTV(I)+(1./(1.-XH))*J*GCIRC(J)*HT(I,J)
WAV(I)=WAV(I)+(1./(1.-XH))*J*GCIRC(J)*HA(I,J)
 200    CONTINUE
 190 CONTINUE
WRITE(9,*) ' INDUCED VELOCITIES'
DO 191 I=1,N
WRITE(9,*) ' WTV(',I,' )=',WTV(I),' WAV(',I,' )=',WAV(I)
 191 CONTINUE
c
c hydrodynamic pitch angle
c
do 195 i=1,n
tanbi(i)=((1.-W(I))+wav(i))/(x(i)/LS-wtv(i))
write(9,*) ' tanbi(',i,')=',tanbi(i)
 195 continue
c
```

```
c CALCULATE POWER AND THRUST COEFFICIENTS
C
CP=0.0
CT=0.0
DO 330 I=1,N
FWAV(I)=4*G*X(I)*CIRC(I)*(1.+WAV(I))/Ls
FWTV(I)=4*G*CIRC(I)*((X(I)/Ls)-WTV(I))
 330 CONTINUE
DO 340 I=2,N
CP=CP+(FWAV(I)+FWAV(I-1))/2*(X(I)-X(I-1))
CT=CT+(FWTV(I)+FWTV(I-1))/2*(X(I)-X(I-1))
 340 CONTINUE
C
C CHECK REQUIRED THRUST COEFFICIENT, IF ERROR TOO LARGE
C INCREMENT ASSUMED IDEAL PROPELLER EFFICIENCY.
C
DIFFCP=(CP-CPI)/CPI
write(9,*) 'diffcp=',diffcp
IF (abs(DIFFCP).GE.0.1) THEN
etanot=etanot+0.05
iteration=iteration+1
GOTO 1111
END IF
c
c pitch/diameter ratio
c
do 350 i=1,n
 pd(i)=pi*x(i)*tanbi(i)
 350 continue
c
c AVERAGE face pitch
c
do 360 i=1,n
pd1=pd1+pd(i)
 360 continue
p=pd1/n*d
write(9,*) ' 88888888888888888888888888888888888888888'
write(9,*) ' iterations required',iteration
write(9,*) ' CPI=',CPI
Write(9,*) ' diameter=',d,'pitch=',p
EFF=CT/CP
WRITE(9,*) 'CT=',CT,'CP=',CP
WRITE(9,*) 'EFF=',EFF
WRITE(9,*) ' PITCH/DIAMETER RATIO  DISTRIBUTION'
DO 361 I=1,N
WRITE(9,*) 'PD(',I,')=',PD(I)
 361 CONTINUE
write(9,*) ' 888888888888888888888888888888888888888888'
STOP
END
C
SUBROUTINE INDUCT(IT,IA,BI,XOX,G,N,M)
C
c SUBROUTINE INDUCT  TO CALCULATE LERBS INDUCTION FACTORS
C
DOUBLE PRECISION BI(N),IA(N,N),IT(N,N),XOX(N,N),YO,Y,A2,B2
REAL YY,YOYO
INTEGER G
C
c WRITE(9,*) ' NOW INSIDE INDUCT  DATA TRANSFER'
```

```
c WRITE(9,*) '        G=',G,'      N=',N,'      M=',M
c DO 3 I=1,N
c WRITE(9,*) ' BI(',I,' )=', BI(I)
c 3 CONTINUE
c DO 1 I=1,N
c    DO 2 J=1,N
c WRITE(9,*)  ' XOX(',I,J,' )=',XOX(I,J)
c 2    CONTINUE
c 1 CONTINUE
COUNT=0.0
DO 10 I=1,N
   DO 20 J=1,N
COUNT=COUNT+1.0
C WRITE(9,*) ' iteration #', count
C WRITE(9,*) ' XOX=',XOX(I,J),' BI=',BI(J)
C
   IF (XOX(I,J).LT.1.000) THEN
C
IF ((BI(I).GT.1.570).AND.(BI(I).LT.1.571)) THEN
IA(I,J)=0.0
IT(I,J)=0.0
c WRITE(9,*)' 1ST BI=90 CONDITION COMPLETED'
GOTO 20
END IF
C
IF (XOX(I,J).LT.0.0001) THEN
IT(I,J)=G
IA(I,J)=0.00000
c WRITE(9,*) ' COMPLETE LOOP 1 - NULL CONDITION'
GOTO 20
End if
C
         Y=1/(XOX(I,J)*TAN(BI(J)))
YO=1/TAN(BI(J))
YY=SQRT(1.+Y**2)
YOYO=SQRT(1.+YO**2)
C
A1=(YY-YOYO)-0.5*ALOG((YOYO-1.)*(YY+1.)/((YOYO+1.)*(YY-1.)))
E=1/(EXP(G*A1)-1)
C
B1=SQRT(YOYO/YY)*(E-YO**2/(2*G*YOYO**3)*ALOG(1.+E))
C
IA(I,J)=-G*Y*(XOX(I,J)-1.)*B1
IT(I,J)=-G*(XOX(I,J)-1.)*(1.+B1)
GOTO 20
END IF
C
   IF ((XOX(I,J).GT.0.9999).AND.(XOX(I,J).LT.1.0001)) THEN
IT(I,J)=SIN(BI(J))
IA(I,J)=COS(BI(J))
c WRITE(9,*) ' COMPLETE LOOP 2 - UNITY CONDITION'
GOTO 20
   END IF
C
   IF (XOX(I,J).GT.1.0000) THEN
C
IF ((BI(I).GT.1.570).AND.(BI(I).LT.1.571)) THEN
IA(I,J)=0.0
IT(I,J)=0.0
```

```
c WRITE(9,*)' 2ND BI=90 CONDITION COMPLETED'
GOTO 20
END IF
C
IF (XOX(I,J).GT.1000.0) THEN
IT(I,J)=0.0
IA(I,J)=G*(XOX(I,J)-1.0)/(XOX(I,J)*TAN(BI(J)))
c WRITE(9,*) ' COMPLETE LOOP 3 - INFINTY COND.'
GOTO 20
end if
   Y=1/(XOX(I,J)*TAN(BI(J)))
   YO=1/TAN(BI(J))
        YY=SQRT(1+Y**2)
        YOYO=SQRT(1+YO**2)
c
c WRITE(9,*) '  Y                              YO'
c WRITE(9,*) Y,YO
c WRITE(9,*) '  YY                    YOYO'
c WRITE(9,*) YY,YOYO
c
  A2=-(YY-YOYO)+0.5*ALOG((YOYO-1)*(YY+1)/((YOYO+1)*(YY-1)))
E=1/(EXP(G*A2)-1)
C
  B2=SQRT(YOYO/YY)*(E+YO**2/(2*G*YOYO**3)*(ALOG(1+E)))
C
                IT(I,J)=G*(XOX(I,J)-1.)*B2
IA(I,J)=G*Y*(XOX(I,J)-1.)*(1.+B2)
END IF
 20     CONTINUE
 10 CONTINUE
C
c WRITE(9,*) ' RESULTS INSIDE INDUCT'
c WRITE(9,*) (BI(J),J=1,N)
c WRITE(9,*) '      I               J         IT
c     *           IA'
c DO 30 I=1,N
c DO 31 J=1,N
c WRITE(9,*) I,J,IT(I,J),IA(I,J)
c 31 CONTINUE
c 30 CONTINUE
RETURN
END
C
SUBROUTINE GAUSS(X,A,N,NP)
C
C GAUSSIAN ELIMINATION ROUTINE
C N=NUMBER OF EQUATIONS
C NP=N+1 NUMBER OF COLUMNS IN AUGMENTED MATRIX
C A=MATRIX OF COEFFICIENTS AND RHS (N X NP)
C X=SOLUTION VECTOR
C
DOUBLE PRECISION A(N,NP),X(N),LARG
NM1=N-1
NP1=N+1
C WRITE(9,*) ' INSIDE GAUSS'
C write(9,*) ' N=',N,' NP=',NP
C WRITE(9,*) ' A(I,I)'
C WRITE(9,*) A(1,1),A(2,2),A(3,3)
C WRITE(9,*) A(4,4),A(5,5),A(6,6)
```

```
C WRITE(9,*) A(7,7),A(7,8)
C
C FOR EACH COLUMN I DO THE FOLLOWING
C
DO 10 I=1,NM1
IP1=I+1
C
C FIND THE LARGEST COEFFICIENT BENEATH A(I,I) IN COLUMN I
C
LARG = ABS( A(I,I) )
L=I
DO 5 J=IP1,N
IF (LARG.LT.ABS( A(J,I) )) THEN
L=J
LARG=ABS( A(J,I))
END IF
 5 CONTINUE
C IS A ROW INTERCHANGE NECESSARY
IF (L.NE.I) THEN
C INTERCHANGE I AND L
DO 6 J=I,NP1
TEMP=A(I,J)
A(I,J)=A(L,J)
A(L,J)=TEMP
 6 CONTINUE
END IF
C
C BEGIN ELIMNATION PROCESS, ALL X(I) BENEATH A(I,I) ELIMINATED
C
DO 7 K=IP1,N
DO 8 M=IP1,NP1
C (K,M) REPRESENTS AN ELEMENT IN THE KTH ROW AND MTH COLUMN
C TO THE RIGHT OF THE ITH COLUMN
C
A(K,M)=A(K,M)-A(K,I)*A(I,M)/A(I,I)
 8 CONTINUE
 7 CONTINUE
C EQUATE TO ZERO ALL OTHER ENTRIES IN LOWER DIAGONAL MATRIX
DO 9 K=IP1,N
A(K,I)=0.0
 9 CONTINUE
 10 CONTINUE
C
C FIND SOLUTION BY BACK SUBSTITUTION
C
X(N)=A(N,N+1)/A(N,N)
DO 11 I=NM1,1,-1
IP1=I+1
SUM=0.0
DO 12 J=IP1,N
SUM=SUM+A(I,J)*X(J)
 12 CONTINUE
X(I)=( A(I,N+1) - SUM )/A(I,I)
 11 CONTINUE
RETURN
END
C
SUBROUTINE FCINDUCT(A,II,N,M,PHIO,K)
C
C SUBROUTINE FCINDUCT TO SET UP FOURIER COEFFICIENT MATRIX
C TO SOLVE FOR FOURIER COEFFICIENTS OF INDUCTION FACTORS
C
```

```
      DOUBLE PRECISION A(M,N,N+1),II(M,N),PHIO(N)
      INTEGER N,NP1,M,K
C
C     WRITE(9,*) ' INSIDE FCINDUCT'
C     WRITE(9,*) ' N=',N,' M=',M,' K=',K
C     DO 1 I=1,M
C     DO 2 J=1,N
C     WRITE(9,*)  ' II(',I,J,' )=',II(I,J)
C   2 CONTINUE
C   1 CONTINUE
C
                DO 10 i=1,N
      DO 11 j=1,N
      A(K,I,J)=DCOS((j-1)*PHIO(i))
   11 CONTINUE
   10      CONTINUE
C
      np1=n+1
        DO 12 i=1,N
      A(K,i,NP1)=II(K,i)
   12      CONTINUE
C     WRITE(9,*) ' MATRIX A INSIDE FCINDUCT'
C     WRITE(9,*) ' PHI=',K
C          DO 20 I=1,N
C     DO 30 J=1,NP1
C     WRITE(9,*) 'A(',K,I,J,' )=',A(K,I,J)
C  30 CONTINUE
C  20      CONTINUE
      RETURN
      END
```

Appendix C

Fortran listing of FPT2

```
C-------------------------------------------------------------
CCC         PROPELLER PERFORMANCE
CCC         PROGRAM VERSION 2.0
CCC
C     WRITTEN BY: THOMAS HOFMANN ((C)) 1991
C-------------------------------------------------------------
CCC
C     DEFINITIONS:
C
C     VS - SHIP SPEED M/SEC
C     VA - SPEED OF ADVANCE M/SEC
C     JAY - ADVANCE COEFFICIENT
C     W - OVERALL WAKE FRACTION
C     N - SHAFT SPEED  RPS
C     RO - WATER DENSITY
C     D - MAXIMUM PROPELLER DIAMETER
C     P - PITCH
C     Q - TORQUE
C     T - THRUST
C     KQ - TORQUE COEFFICIENT
C     KT - THRUST COEFFICIENT
C     KTI - IDEAL THRUST COEFFICIENT
C     KQI - IDEAL TORQUE COEFFICIENT
C     KAP - GOLDSTEIN NON-UNIFORM FLOW CORRECTION FOR FINITE
C           NUMBER OF BLADES
C     E - DRAG LIFT RATIO OF AERO-FOIL SECTION
C     L - ADVANCE RATIO
C     LI - INDUCED ADVANCE RATIO
C     X - BLADE SPAN FRACTION
C     B - ADVANCE ANGLE
C     BI - INDUCED ADVANCE ANGLE
C     APRIME - ROTATIONAL INTERFERNCE FACTOR
C     NB - NUMBER OF BLADES
C     I - BLADE SECTION INDEX (1 - 0.2R)
C     J - ANGLE OF INCIDENCE INDEX (1= -10.0 DEGREES)
C-------------------------------------------------------------
C
        real  x(8),td(8),cd(8),mc(8),tc(8),pd(8),d,ear,nn,n,w,wx(8)
real sec(8),pa,ee,pi,ro,jay,jayc(20),va,vs,tanb(8)
real phi(8),alpha1,alpha,cl(8,100),clt(8,100),deltcl
real cla,clb,cltta,clttb,alphaa,alphab,clta(8),alfaa(8)
real betta(8),landa(8),etta(8),t3,aprim(8),cdt(8),epsiln(8)
real ktipri(8),kqipri(8),kt,ktsm,kq,kqsm,ktc(20),wakefn(8)
real kqc(20),thrust,torque,eff,effc(20),vsc(20)
real ktpri(8),kqpri(8),kap1(8),kappa(8),corkt,corkq,fkt,fkq
double precision xa(8),tda(8),cda(8),mca(8),tca(8),pda(8)
        integer  k,l,z,nnn,nb,ans
C
CC  K  DEFINES THE RADIUS FRACTION NUMBERS
CC  L  DEFINES THE NUMBER OF ANGLES OF ATTACK STARTING FROM -10 DEGREES
C
        K=8
        L=100
C
CC      CALL LOPEN (3,'PRN')
C       CALL SCLEAR
        open(unit=2,file='ppt2.out',type='new')
        WRITE (5,*) ' '
        WRITE (5,*) ' '
        WRITE (5,*) ' '
```

```
      write(5,*) ' '
      write(5,*) ' '
      write(5,*) ' '
      WRITE (5,*) ' '
      WRITE (5,*) '                                  PPT2 (VERSION 2.0)'
      WRITE (5,*) ' '
      WRITE (5,*) '                               PROPELLER PERFORMANCE PROGRAM'
      WRITE (5,*) '                                     THOMAS HOFMANN'
      WRITE (5,*) '                                      (( C )) 1991'
      WRITE (5,*) ' '
      WRITE (5,*) '                              USE OF THIS PROGRAM IS RESTRICTED'
      WRITE (5,*) ' '
      WRITE(5,*) ' '
      WRITE(5,*) ' '
      WRITE(5,*) ' '
      WRITE(5,*) ' '
      WRITE(5,*) ' '
      WRITE(5,*) ' '
      WRITE (5,*) ' '
      WRITE (5,*) ' '
 20   WRITE (5,*) ' PRESS "1" TO CONTINUE'
      read (5,*) Z
      IF (Z.EQ.1) THEN
          GO TO 21
          ELSE
          GO TO 20
       END IF
 21   WRITE (5,*) ' '
C      CALL SCLEAR
      WRITE (5,*) ' '
       write(5,*) ' '
write(5,*) ' '
      WRITE (5,*) ' '
      WRITE (5,*) '          A C K N O W L E D G E M E N T'
      WRITE (5,*) ' '
      WRITE (5,*) ' '
      WRITE (5,*) ' '
      WRITE (5,*) ' '
      WRITE (5,*) ' '
      WRITE (5,*) ' THE  AUTHOR  WOULD  LIKE  TO THANK DR.NEIL BOSE'
       WRITE (5,*) ' OF  THE  NAVAL  ARCHITECTURAL ENGINEERING  DEPT.'
      WRITE (5,*) ' MEMORIAL UNIVERSITY  OF NEWFOUNDLAND, ST.JOHN S '
      WRITE (5,*) ' NEWFOUNDLAND FOR HIS  TECHNICAL GUIDANCE  DURING'
      WRITE (5,*) ' THE WRITING OF THIS PROGRAM.'
      WRITE (5,*) ' '
      WRITE (5,*) ' '
      WRITE (5,*) ' '
      WRITE (5,*) ' '
      WRITE (5,*) ' '
      WRITE (5,*) ' '
      WRITE (5,*) ' '
 30    WRITE (5,*) ' PRESS "1" TO CONTINUE'
      READ (5,*) Z
```

```
      IF (Z.EQ.1) THEN
           GO TO 31
           ELSE
           GO TO 30
      END IF
 31 WRITE (5,*) ' '
C       CALL SCLEAR
      WRITE (5,*) ' '
C     WRITE (5,*) ' PLEASE ENSURE PRINTER IS SWITCHED "ON-LINE"'
C 40    WRITE (5,*) ' PRESS "1" TO CONTINUE'
C      READ (5,*) Z
C      IF (Z.EQ.1) THEN
C           GO TO 41
C           ELSE
C           GO TO 40
C      END IF
C 41    WRITE(5,*) ' '
C       CALL SCLEAR
C       CALL CURSOR(2,0,OLDROW,OLDCOL)
      WRITE (5,*) ' '
     WRITE (5,*) ' '
      WRITE (5,*) ' '
C
C    DEFINING RADIUS FRACTIONS X(I)=r/R
C
       Xa(1)=0.2
     Xa(2)=0.3
      Xa(3)=0.4
      Xa(4)=0.5
      Xa(5)=0.6
      Xa(6)=0.7
      Xa(7)=0.8
      Xa(8)=0.9
C
nnn=k
C NNN IS THE NUMBER OF STATIONS OF INPUT DATA
C GEO IS GEOMETRIC BLADE SECTION DATA INTERPOLATION ROUTINE
C
CALL GEO(TDa,CDa,MCa,TCa,PDa,Xa,nnn)
C
do 7 i=1,k
td(i)=sngl(tda(i))
cd(i)=sngl(cda(i))
mc(i)=sngl(mca(i))
tc(i)=sngl(tca(i))
pd(i)=sngl(pda(i))
x(i)=sngl(xa(i))
 7 continue
c       CALL SCLEAR
        WRITE (5,*) '           GENERAL PROPELLER DATA'
        WRITE (5,*) ' '
        WRITE (5,*) ' '
        WRITE (5,*) '        PROPELLER DIAMETER (meters)?'
        READ (5,*) D
c       WRITE(2,*) 'DIA=',D
        WRITE (5,*) ' ENTER THE NUMBER OF PROPELLER BLADES.'
 11     WRITE (5,*) ' (POSSIBLE CHOICES: 3,4,5 or 6 BLADES)'
```

```
        READ (5,*) NB
c        WRITE(2,*) ' NB=',NB
C
C BLADE NUMBER VERIFICATION LOOP
C
        IF ((NB.Eq.3).OR.(NB.Eq.4).OR.(NB.Eq.5).OR.(NB.Eq.6)) THEN
            goto 12
            else
            WRITE (5,*) ' PLEASE RE-ENTER NUMBER OF BLADES'
            GOTO 11
        END IF
 12     WRITE (5,*) ' '
 23     WRITE (5,*) '  '
write(5,*) ' ENTER EXPANDED BLADE AREA RATIO'
READ(5,*) EAR
c WRITE(2,*) ' EAR=',EAR
        WRITE (5,*) ' ENTER SHAFT RPM'
        READ (5,*) NN
c        WRITE (2,*) ' SHAFT RPM NN=',NN
N=NN/60.0
        WRITE (5,*) ' ENTER OVERALL WAKE FRACTION'
WRITE (5,*) ' (FOR UNIFORM FLOW ENTER ZERO)'
        READ (5,*) W
C        WRITE (2,*) ' W=',W
C
WRITE (5,*) '    Do you require wake adapted analysis?'
WRITE (5,*) '      If yes type "1", if not type "0".'
WRITE (5,*) ' (default sections are NACA a=1.0 mean lines)'
read(5,*) ans
if (ans.eq.1) then
goto 44
else
goto 45
end if
 44 WRITE (5,*) ' Enter the local wake fractions at each radius.'
WRITE (5,*) '      (for uniform flow enter "0".)'
do 50 i=1,k
WRITE (5,*) ' x(',i,')=',x(i)
read(5,*) wx(i)
wakefn(i)=(1.-wx(i))/(1-w)
 50 continue
WRITE (5,*) ' All correct? If yes type 1, else type 0.'
read(5,*) ans
if (ans.eq.0) then
goto 44
end if
 45 do 51 i=1,k
wakefn(i)=1.0
 51 continue
C
        WRITE (5,*) ' ENTER PITCH RATIO AT EACH SECTION'
        DO 97 I=1,k
            write(5,*) ' X(',I,' )'
            READ (5,*) PD(I)
 97     CONTINUE
c        WRITE(2,*) ' P/D UNIFORM =',PD(6)
```

```
C
        WRITE (5,*) ' IS DATA ENTERED CORRECT ?'
        WRITE (5,*) ' (IF YES TYPE "1" ELSE TYPE "0")'
        READ (5,*) Z
        IF (Z.EQ.0) THEN
           GO TO 23
           ELSE
           GO TO 24
        END IF
 24     WRITE (5,*) ' '
        WRITE (5,*) ' '
c
 26 write(5,*) ' Do you wish to specify the type of airfoil'
write(5,*) ' sections to be used? If yes type 1, if not'
write(5,*) ' type 0. (Default is NACA a=1.0 mean line.)'
read(5,*) ans
if (ans.eq.0) then
do 81 i=1,k
sec(i)=1.
 81 continue
end if
if (ans.eq.1) then
write(5,*) ' Section types currently available for'
write(5,*) ' propeller analysis are:'
write(5,*) ' NACA a=1.0 mean line - 1'
write(5,*) ' NACA a=0.8 mean line - 2'
write(5,*) ' Circular back/flat face sections - 3'
write(5,*) ' '
write(5,*) ' Type the appropriate number to specify the kind'
write(5,*) ' of section required for each radius.'
do 82 i=1,k
write(5,*) ' x(',i,')=',x(i)
read(5,*) sec(i)
 82 continue
end if
C
        WRITE (5,*) ' IS DATA ENTERED CORRECT ?'
        WRITE (5,*) ' (IF YES TYPE "1" ELSE TYPE "0")'
        READ (5,*) Z
        IF (Z.EQ.0) THEN
           GO TO 26
           ELSE
           GO TO 27
        END IF
 27     WRITE (5,*) ' '
        WRITE (5,*) ' '
c
C       CALL SCLEAR
        WRITE (5,*) ' CALCULATING - PLEASE WAIT FOR PRINT-OUT'
        WRITE (5,*) '               OF RESULTS.'
C
C    INITIALIZATION OF CONSTANTS
C
        PA=101325
        EE=1720
        PI=3.141592654
        RO=1025
C
```

```
C     BEGIN ADVANCE COEFFICIENT STEP UP TO MAXIMUM =12
C
smax=16
DO 70 S=1,smax
C
C     DESIGN POINT ADVANCE RATIO, ADVANCE COEFFICIENT AND REQUIRED
C     THRUST COEFFICIENT.
C
JAY=S/30.
c WRITE(2,*) ' JAY=',JAY
jayc(s)=JAY
VA=JAY*N*D
VS=VA/(0.5144*(1-W))
C
        DO 98 I=1,K
           TANB(I)=JAY/(PI*X(I))*wakefn(i)
           PHI(I)=ATAN(PD(I)/PI/X(I))
c         WRITE (2,*) ' TANB(',I,' =',TANB(I),' PHI(',I,' =',PHI(I)
 98     CONTINUE
C
C  FOR ANGLES OF INCIDENCE -10 TO 60 DEGREES CALCULATE THE
C     FOLLOWING COMPONENTS OF THEORETICAL LIFT COEFFICIENT.
C
do 99 i=1,k
c write(2,*) ' i=',i
          ALPHA1=-10.
c WRITE(2,*) ' ALPHA1 INITIALIZED TO ', ALPHA1
           DO 100 J=1,L
           ALPHA1=ALPHA1+1
           ALPHA=ALPHA1*PI/180.0
C
CCC
C  CALL NUMLFT SUBROUTINE TO CALCULATE THE LIFT COEFFICIENTS
C  NUMERICALLY USING A MODIFIED ECKARDT AND MORGAN METHOD.
C
c WRITE(2,*) 'NB=',NB,' BEFORE NUMLFT'
c write(2,*) 'wakefn=',wakefn(i)
c write(2,*) ' phi=',phi(i),' tanb=',tanb(i)
c write(2,*) ' alpha1=',alpha1,' deg. and alpha=', alpha,' rad.'
c write(2,*) ' '
C
CALL NUMLFT(CL,PHI,TANB,NB,CD,X,PI,K,L,alpha,wakefn,i,j)
C
CCC
C     CALL SUBROUTINE FOR ACTUAL LIFT COEFFICIENT, ANGLE OF
C     INCIDENCE AND DRAG COEFFICIENT OF THE SECTION.
C
c WRITE(2,*) 'NB=',NB,' before TRULFT'
c write(2,*) ' wakefn(i)=',wakefn(i)
c write(2,*) ' phi=',phi(i),' tanb=',tanb(i)
c write(2,*) ' alpha1=',alpha1,' deg. and alpha=', alpha,' rad.'
c write(2,*) ' '
c
        CALL TRULFT(CLT,MC,PI,K,L,ALPHA,SEC,I,j)
C
CC    FOR THE ANGLE OF INCIDENCE alfaa AT WHICH EACH SECTION IS
C     OPERATING  CALCULATE THE ELEMENTAL COEFFICIENTS.
C
c write(2,*) ' ************************************************'
c write(2,*) ' numlft results outside numlft'
c write(2,*) '          i        j         cl'
```

```
c write(2,*) i,j,cl(i,j)
c write(2,*) ' '
C
c write(2,*) ' truelift results outside trulft'
c write(2,*) '          i         j          clt'
c write(2,*) i,j,clt(i,j)
c write(2,*) ' ##################################################'
C
c determine intersection of theoretical and model lift curves.
c
deltcl=cl(i,j)-clt(i,j)
if (deltcl.lt.0.) then
c write(2,*) ' Have intersection between points:'
alphaa=(alpha1-1.)*pi/180
c write(2,*) ' alphaa=',alphaa,' alpha=',alpha
c
c   Data transfer check
c
c write(2,*) ' '
c write(2,*) ' inputs to ATTACK outside ATTACK'
c write(2,*) ' '
c WRITE(2,*) 'NB=',NB,' k=',k,' l=',l
c write(2,*) ' wakefn(i)',wakefn(i)
c write(2,*) ' phi=',phi(i),' tanb=',tanb(i)
c write(2,*) ' cd=',cd(i),'x=',x(i),' pi=',pi
c write(2,*) 'mc=',mc(i),' sec=',sec(i)
c write(2,*) ' alphaa',alphaa
c write(2,*) ' '
c
C CALL SUBROUTINE ATTACK TO FIND ANGLE OF ATTACK AND
C CORRESPONDING LIFT COEFFICIENT.
C
CALL ATTACK(CLTA,ALFAA,alphaa,K,L,
     *phi,tanb,nb,cd,x,pi,wakefn,mc,sec,i,j)
C
c write(2,*) 'TRULIFT',i,' clta=',clta(i),' alfaa=',alfaa(i)
goto 99
end if
 100 continue
 99 continue
c
        DO 107 I=1,K
           BETTA(I)=PHI(I)-alfaa(i)
           LANDA(I)=X(I)*TAN(BETTA(I))
           ETTA(I)=tanb(i)/TAN(BETTA(i))/wakefn(i)
           T3=1.0+TAN(BETTA(I))**2
           APRIM(I)=TAN(BETTA(I))**2*(1.0-ETTA(I)*sqrt(wakefn(i)
     *))/ T3
 107 CONTINUE
c write(2,*) ' Inputs to DRAG'
c write(2,*) ' i       betta        landa             etta
c    *aprim'
c do 1081 i=1,k
c write(2,*) betta(i),landa(i),etta(i),aprim(i)
c 1081 continue
C
C CALL SUBROUTINE DRAG TO CALCULATE DRAG COEEFICIENTS CDT(I) AT
```

```
C EACH BLADE SECTION.
C
do 101 i=1,k
CALL DRAG(CDT,ALFAA,MC,TC,D,PI,N,APRIM,CD,BETTA,X,EAR,NB,K,SEC
     *,i,clta,wakefn)
c
c write(2,*) 'DRAG',i,' cdt=',cdt(i),' clta=',clta(i)
 101 continue
C
DO 1069 I=1,K
          EPSILN(I)=cdt(i)/clta(i)
 1069 CONTINUE
C
c       WRITE (2,*) '         I      CDT       CLTA         EPSILN'
c       DO 1071 I=1,K
c       WRITE (2,*) I,CDT(I),CLTA(I),EPSILN(I)
c 1071   CONTINUE
c WRITE(2,*) '   LANDA      BETTA'
c         DO 1072 I=1,K
c WRITE(2,*) LANDA(I),BETTA(I)
c 1072   CONTINUE
C
        DO 108 I=1,K
C
c   Call subroutine for single subscripted Goldstein coefficients.
c
        CALL GOLST1(KAP1,LANDA,NB,i)
        KTIPRI(I)=PI**3*X(I)**3*KAP1(I)*APRIM(I)*(1.0-APRIM(I))
c        WRITE (2,*) '  KTIPRI=',KTIPRI(I)
 108    CONTINUE
        DO 109 I=1,K
           KQIPRI(I)=X(I)*KTIPRI(I)*TAN(BETTA(I))/2.0
c           WRITE (2,*) ' KQIPRI(',I,' =',KQIPRI(I)
 109    CONTINUE
        DO 110 I=1,K
           KTPRI(I)=KTIPRI(I)*(1.0-EPSILN(I)*TAN(BETTA(I)))
           KQPRI(I)=KQIPRI(I)*(1.0+(EPSILN(I)/TAN(BETTA(I))))
c           WRITE (2,*) ' KTPRI',I,' =', KTPRI(I),' KQPRI=',KQPRI(I)
 110    CONTINUE
C
C    CALL SUBROUTINE SIMSON TO INTEGRATE THRUST AND TORQUE
C    COEFFICIENTS.
C
c write(2,*) ' integrate thrust coefficient'
        CALL SIMSON(KTSM,KTPRI,K)
c write(2,*) 'ktsm=',ktsm
        KT=KTSM*0.1/3.0
c       WRITE (2,*) ' KT=',KT
c
c lifting surface corrections applied for p/d(6)=0.7
c thrust coefficient
c
if (pd(6).eq.0.8) then
fkt=21.6241*jay**3-16.2785*jay**2+4.4236*jay-0.1558
end if
if (pd(6).eq.1.0) then
fkt=12.1919*jay**3-12.0786*jay**2+4.0395*jay-0.2838
end if
corkt=fkt*kt+kt
```

```
ktc(s)=corkt
C
c write(2,*) ' integrate torque coefficient'
        CALL SIMSON(KQSM,KQPRi,K)
        KQ=KQSM*0.1/3.0
c        WRITE (2,*) ' KQ=',KQ
c
c lifting surface correction for torque coeff.
c
fkq=17.0107*jay**3-18.3133*jay**2+6.1630*jay-0.3628
corkq=fkq*kq+kq
kqc(s)=corkq
C
CCCCCC
C     CALCULATION OF TOTAL THRUST AND TORQUE DEVELOPED.
CCC
C       THRUST = corKT * RO * N**2 * D**4
C       TORQUE = corKQ * RO * N**2 * D**5
        EFF=JAY*corkt*100/(2.0*PI*corkq)
EFFC(S)=EFF
VSC(S)=VS
c write(2,*) ktc(s),kqc(s),effc(s),jayc(s),vsc(s)
C
 70 CONTINUE
        WRITE (2,*) ' '
        WRITE (2,*) ' PROPELLER PERFROMANCE DATA:'
        WRITE (2,*) ' ---------------------------'
C       WRITE (2,*) ' '
C
C     PROPELLER  OUTPUT
C
WRITE(2,*) ' OPERATING CONDITIONS:'
        WRITE (2,806) D
WRITE(2,807) PD(7)
        WRITE (2,808) NB
WRITE(2,809) NN
WRITE(2,810) VS
WRITE(2,817) W
WRITE(2,*) ' '
WRITE(2,*) ' PERFORMANCE CHARACTERISTICS:'
C        WRITE (2,814) THRUST
C        WRITE (2,815) TORQUE
C        WRITE (2,816) EFF
C WRITE(2,*) ' '
C WRITE(2,812) KT
C WRITE(2,813) KQ
C WRITE(2,811) JAY
C
WRITE(2,818)
DO 75 T=1,smax
WRITE(2,*) VSC(T),JAYC(T),KTC(T),KQC(T),EFFC(T)
 75 CONTINUE
C
 806    FORMAT(' ',10X,' DIAMETER :',14X,F15.2,2X,' m')
 807 FORMAT(' ',10X,' PITCH RATIO:'12X,F15.2,2X)
```

```
 808    FORMAT(' ',10X,' NUMBER OF BLADES : ',15X,I2)
 809 FORMAT(' ',10X,' SHAFT RPM:',16X,F15.2)
 810 FORMAT(' ',10X,' MAXIMUM SHIP SPEED:',8X,F15.2,2X,' KNOTS')
C 811 FORMAT(' ',10X,' ADVANCE COEFFICIENT:',12X,F15.5)
C 812 FORMAT(' ',10X,' THRUST COEFFICIIENT:',12XF15.5)
C 813 FORMAT(' ',10X,' TORQUE COEFFICIENT:',13X,F15.5)
C 814    FORMAT(' ',10X,' THRUST DEVELOPED : ',F15.2,2X,' N')
C 815    FORMAT(' ',10X,' TORQUE PRODUCED  : ',F15.2,2X,' N-m')
C 816    FORMAT(' ',10X,' PROPELLER EFFICIENCY : ',F10.2,2X,'  %')
 817 FORMAT(' ',10X,' OVERALL WAKE FRACTION:',4X,F15.3)
 818 format(' ',10x,' Vs',10x,' J',10x,' Kt',10x,' Kq',10x,' eff')
C
       stop
       END
C

ccccccccccccccccccccccccccccccccccccccccccccccccccccccccccccccccccccccc
C
c subroutine to calculate the lift coefficient at each section
c according to a modified Eckardt and Morgan design  method.
c
SUBROUTINE NUMLFT(CL,PHI,TANB,NB,CD,X,PI,K,L,alpha,wakefn,i,j)
C
REAL cl(8,60),phi(8),tanb(8),cd(8),x(8),pi,alpha,wakefn(8)
real beta(8),tanbi(8),etai(8),t1,aprime(8),kappa(8)
real lamdai(8),t2
INTEGER NB,K,L,i,j
C
c WRITE(2,*) ' NOW INSIDE NUMLFT',' NB=',NB,' tanbi=',tanb(i)
c WRITE(2,*) ' CD(',i,')=',CD(i),' PI=',PI,' X(i)=',X(i),i,j
c       WRITE(2,*) ' ALPHA=',ALPHA,'wakefn=',wakefn(i),' phi=',phi(i)
c write(2,*) ' tanb=',tanb(i)
c
c begin calculation
c
         BETA(I)=PHI(I)-ALPHA
c       WRITE(2,*) ' BETA(',I,' )=',BETA(I)
           TANBI(I)=TAN(BETA(I))
c        WRITE(2,*) ' TANBI',I,')=',TANBI(I)
           ETAI(I)=TANB(I)/TANBI(I)/wakefn(i)
c       WRITE(2,*) ' ETAI',I,')=',ETAI(I)
           T1=1+(TANBI(I))**2
           APRIME(I)=(TANBI(I)**2)*(1.0-ETAI(I)*sqrt(wakefn(i)
     *))/T1
c       WRITE(2,*) ' APRIME',I,')=',APRIME(I)
           LAMDAI(I)=X(I)*TANBI(I)
c       WRITE(2,*) ' LAMDAI(',I,')=',LAMDAI(I)
CCC
CCC    CALL SUBROUTINE FOR GOLDSTEIN COEFFICIENTS
C
          CALL GOLST1(KAPPA,Lamdai,NB,i)
C
CC
c               WRITE(2,*) ' KAPPA',I, kappa(i)
CC
CC    THEORETICAL LIFT COEFFICIENT
```

```
C
C
          T2=NB*CD(I)*(1.0-APRIME(I))*SQRT(1.0+TANBI(I)**2)
          CL(I,J)=4.0*KAPPA(I)*APRIME(I)*PI*X(I)/T2
C
c write(2,*) ' '
c write(2,*) ' theoretical lift coefficient'
c write(2,*) ' '
c       WRITE(2,*) ' CL(',i,j,')=',cl(i,j)
RETURN
END
C
CCCCCCCCCCCCCCCCCCCCCCCCCCCCCCCCCCCCCCCCCCCCCCCCCCCCCCCCCCCCCCCCCCCCCCC
C
C     SUBROUTINE TO CALCULATE ACTUAL SECTION LIFT COEFFICIENT CLT.
C
Coptions x,a=100,s=600,q
C
          SUBROUTINE TRULFT(CLT,MC,PI,K,L,ALfA,SEC,I,j)
C
          real clt(8,60),mc(8),pi,alfa,sec(8),clstall,alfaov
real dclda,alfstal,alfa06,slope
integer K,L,I,j
C
c          WRITE (2,*) 'NOW INSIDE TRUELFT'
c       WRITE(2,*) ' i,j= ',i,j  ,' sec=',sec(i)
c          WRITE(2,*) ' MCi=',MC(i),' alfa=',alfa
c         WRITE(2,*) ' PI=',PI ,'K=',K,'L=',L
C
clstall=1.2
c
c call subroutine STNTYP for lift slope dclda and zero lift
c angle alfaov.
c
call stntyp(alfaov,dclda,cli,sec,mc,i,pi,k)
c
alfstal=clstall/2/pi+alfaov
alfa06=18.435*pi/180
c WRITE(2,*) ' '
c write(2,*) ' INSIDE TRULIFT,  ALFA=',alfa
c write(2,*) ' alfstal=', alfstal,' alfa06=',alfa06
c
C ...for angles upto stall at max. cl=1.2
c
if (alfa.lt.alfstal) then
c write(2,*) ' CLT=1.2 calc. loop'
c
          CLT(I,J)=dclda*(alfa+alfaov)
c
end if
c
c ...in stall region upto max angle 18.435 degrees
c
          if (alfa.ge.alfstal) then
c write(2,*) ' CLT between 10.94 and 18.435 deg.'
          slope=-(alfstal-alfa)/(alf06-alfstal)
c write(2,*) ' slope=',slope
clt(i,j)=clstall+(clstall-0.6)*slope
end if
c
```

```
C
C
if (alfa.ge.alfa06) then
c write(2,*) ' clt  FOR ANGLE BEYOND 18 DEG. calc. loop'
C
clt(i,j)=2.0*sin(alfa)*cos(alfa)
C
end if
C
c  write(2,*) ' '
c  write(2,*) ' true lift coefficient'
c  write(2,*) ' '
c       WRITE(2,*) ' CLT',i,j,' =',CLT(i,j)
RETURN
END
C
CCCCCCCCCCCCCCCCCCCCCCCCCCCCCCCCCCCCCCCCCCCCCCCCCCCCCCCCCCCCCCCCCCCCCCCCCCCCCCC
C
c subroutine for determining the lift curve characteristics for
c  different section types.
C
subroutine STNTYP(alfaov,dclda,cli,sec,mc,i,pi,k)
C
real alfaov,dclda,sec(8),mc(8),pi,cli,mu(8),mcmax,alfai,lm
integer i,k
C
c write(2,*) ' inside STNTYP.'
c write(2,*) ' sec(',i,')=',sec(i),' mc=',mc(i)
c write(2,*) ' pi=',pi,' k=',k
C
c for sections with NACA a=1.0 mean lines:
C
if (sec(i).eq.1.) then
cli=1.0
mu(i)=0.74
mcmax=0.05515
alfai=0.0
lm=cli/mcmax
alfa0v=mu(i)*(alfai*lm*mc(i)-lm*mc(i)/(2*pi))*pi/180
dclda=2*pi
end if
C
c for sections with NACA a=0.8 mean lines:
C
if (sec(i).eq.2.) then
cli=1.0
mu(i)=1.0
mcmax=0.0679
alfai=1.54*pi/180
lm=cli/mcmax
alfa0v=mu(i)*(alfai*lm*mc(i)-lm*mc(i)/(2*pi))*pi/180
dclda=2*pi
end if
C
c for sections with circular profiles, rounded at leading edge
c and sharp trailing edge similar to the Gottingen Go xx K series.
C
if (sec(i).eq.3.) then
c for thin sections
if (mc(i).lt.0.055) then
cli=9.7942*mc(i)+0.0077
```

```
c for thick sections
else
cli=5.6046*mc(i)+0.2292
end if
alfaov=(-115.6622*mc(i)+0.0635)*pi/180
dclda=1.58*pi
end if
return
end
c
ccccccccccccccccccccccccccccccccccccccccccccccccccccccccccccccccccccccc
c
C SUBROUTINE ATTACK CALCULATES THE ANGLE OF ATTACK AND THE
C CORRESPONDING LIFT COEFFICIENT.
C
SUBROUTINE ATTACK(CLTA,C,alpha1,K,L,
     *phi,tanb,nb,cd,x,pi,wakefn,mc,sec,i,jj)
C
real clta(8),c(8),alpha1,wakefn(8)
real cl(8,60),clt(8,60),phi(8),tanb(8),cd(8),x(8),pi,mc(8)
real sec(8),cll1,cll2,cltt1,cltt2,alf1,alf2,step
integer k,l,nb,i,j,jj
c
c write(2,*) ' inside ATTACK.',' alpha1=', alpha1,i,jj
c write(2,*) ' cd=',cd(i),' pi=',pi,' mc=',mc(i),' sec=',sec(i)
c write(2,*) ' phi=',phi(i),' tanb=',tanb(i),' nb=',nb
c write(2,*) ' wakefn=',wakefn(i),' x=',x(i)
c
c   Starting with alpha1, step up angle of attack in steps of 0.05,
c calculate cl and clt, again find the intersection angle, then
c  the lift coefficient for
c that section at angle of attack c.
c
step=0.05
do 10 j=1,20
alpha1=alpha1+(step*pi/180)
c write(2,*) ' alpha1=',alpha1,' i=',i
c WRITE(2,*) 'NB=',NB,' BEFORE NUMLFT',' x=',x(i)
c write(2,*) ' wakefn(i)=',wakefn(i)
c write(2,*) ' phi=',phi(i),' tanb=',tanb(i)
c write(2,*) ' k,l,',k,l,' pi=',pi,' cd=',cd(i)
c write(2,*) ' '
c
call numlft(cl,phi,tanb,nb,cd,x,pi,k,l,alpha1,wakefn,i,j)
c
c WRITE(2,*) 'NB=',NB,' before TRULFT'
c write(2,*) ' phi=',phi(i),' tanb=',tanb(i)
c write(2,*) ' alpha1=',alpha1,' deg. and alpha=', alpha,' rad.'
c write(2,*) ' '
c
call trulft(clt,mc,pi,k,l,alpha1,sec,i,j)
c
c write(2,*) ' &&&&&&&&&&&&&&&&&&&&&&&&&&&&&&&&&&&&&&&&&&&&&&&&&&&&&&&&'
c write(2,*) ' truelift results outside truelfit'
c write(2,*) '         i        j         cl'
c write(2,*) i,j,cl(i,j)
c write(2,*) ' '
C
```

```
c write(2,*) ' truelift results outside truelfit'
c write(2,*) '          i         j          clt'
c write(2,*) i,j,clt(i,j)
c write(2,*) ' &&&&&&&&&&&&&&&&&&&&&&&&&&&&&&&&&&&&&&&&&&&&&&&&&&&&&&&&&&&&&&&&&'
c
c    re-evaluate crossing point, calculate corresponding lift coeff.
c
delcl=cl(i,j)-clt(i,j)
if (delcl.lt.0) then
alf1=alpha1-(step*pi/180)
alfave=(alf1+alpha1)/2.
call Trulft(clt,mc,pi,k,l,alfave,sec,i,j)
clta(i)=clt(i,j)
c(i)=alfave
goto 99
end if
 10   continue
c
 99 write(5,*) ' '
c         write(2,*) 'XXXXXXXXXXXXXXXXXXXXXXXXXXXXXXXXXXXXXXXXXXXXXXXX'
c         WRITE(2,*) '       RESULTS INSIDE ATTACK!!'
c write(2,*) '          i      clta             c(i)'
c        WRITE(2,*) i,clta(i),c(i)
c WRITE(2,*) '       FINISH SUBROUTINE attack'
c write(2,*) 'XXXXXXXXXXXXXXXXXXXXXXXXXXXXXXXXXXXXXXXXXXXXXXXX'
         RETURN
         END
c
ccccccccccccccccccccccccccccccccccccccccccccccccccccccccccccccccccccccc
c
c subroutine to calculate the drag coefficient at each
c section.
c
subroutine DRAG(cdt,alfa,mc,tc,d,pi,n,aprim,cd,betta,x,EAR,NB,
     *K,sec,i,clta,wakefn)
c
real cdt(8),alfa(8),mc(8),tc(8),d,pi,n,aprim(8),cd(8)
real betta(8),x(8),ear,alfstal,t2,vr(8),re(8),sec(8)
real cf(8),t1,alfaov,alf06,cli,dang,clta(8),wakefn(8)
integar nb,i,k
c
c WRITE(2,*) ' NOW INSIDE SUBROUTINE CD'
c WRITE(2,*) I,'ALFA=',ALFA(I),'MC=',MC(I),'TC=',TC(I)
c WRITE(2,*) 'APRIM=',APRIM(I),'CD=',CD(I),'BETTA=',BETTA(I),X(I)
c
call STNTYP(alfaov,dclda,cli,sec,mc,i,pi,k)
c
clstall=1.2
alfstal=clstall/2/pi-alfaov
alf06=18.435*pi/180
c relative velocity at section
c
t2=sqrt(1.0+tan(betta(i))**2)
vr(i)=(1.0+aprim(i))*PI*N*X(i)*d*t2/wakefn(i)/60.
c
c WRITE(2,*) ' VR',I,' =',VR(I)
c
c Reynold's number
```

```
c
Re(i)=vr(i)*cd(i)*D/0.000001141
c RE(I)=0.572*EAR*1000000/NB
c
c flat plate friction coefficient
c
C CF(I)=0.075/(LOG10(RE(I))-2.0)**2
cf(i)=0.455/(log10(Re(I)))**2.58
c WRITE(2,*) I,' Re=',RE(I),' Cf=',CF(I)
c
c pre-stall drag coefficient up to angle of attack alfstal
c
c for round - back sections
if (sec(i).eq.3) then
cdt(i)=0.0028*(1.0+28.57*tc(i))+0.0786*
     *(clta(i)-cli)**2+0.0162*(clta(i)-cli)
else
cdt(i)=2.0*cf(i)*(1.0+1.2*tc(i)+70.0*tc(i)**4)+0.011*(
     *cli-clta(i))**2
end if
c
c stall region drag between angles of attack alf12 and 18.435
c degrees.
c
if (alfa(I).gt.alfstal) then
cdstall=2.0*cf(i)*(1.0+1.2*tc(i)+70.0*tc(i)**4)+0.011*(
     *clstall-cli)**2
dang=((alfa(i)-alfstal)/(alf06-alfstal))
cdt(i)=cdstall+(0.2-cdstall)*dang
c
IF (ALFA(I).Gt.alf06) THEN
CDT(I)=2.0*(SIN(ALFA(I)))**2
END IF
END IF
c
c write(2,*)' ***************************'
c WRITE(2,*) ' Drag RESULTS INSIDE drag'
c WRITE(2,*) ' CDT',I,' =',CDT(I)
c WRITE(2,*) ' FINISH SUBRT. Drag'
c write(2,*)' ***************************'
RETURN
END
c
ccccccccccccccccccccccccccccccccccccccccccccccccccccccccccccccccc
c
c  single variable goldstein coefficient subroutine.
c
        SUBROUTINE GOLST1(KAP,LI,NB,i)
C
CC
C    GOLDSTEIN FACTOR CURVES, EXPONENTIAL CURVE FIT FROM
C    T.M.B. PAPER CHARTS.
CC
C
        REAL KAP(8),LI(8)
        INTEGER NB,i
c        WRITE (2,*) ' NOW INSIDE GOLSTN1'
c        WRITE(2,*) ' '
c        WRITE(2,*) ' NB=',NB,' i=',i
c WRITE(2,*) ' LI',I,' =',LI(I)
C
```

```
C     FOR 3-BLADE PROPELLER
          IF (NB.eq.3) THEN
C
if (i.eq.1) then
          KAP(i)=1.729272-0.25471/LI(i)+0.022196/LI(i)**2
c           write (2,*) ' kap1', kap(i)
end if
if (i.eq.2) then
          KAP(i)=1.181454-0.08787/LI(i)+0.00900/LI(i)**2
c           write (2,*) ' kap2' ,kap(i)
end if
if (i.eq.3) then
          KAP(i)=0.854727+0.029462/LI(i)-0.00143/li(i)**2
c           write (2,*) ' kap3' ,kap(i)
end if
if (i.eq.4) then
          KAP(i)=0.630606+0.112772/LI(i)-0.00924/LI(i)**2
c           write (2,*) ' kap4' ,kap(i)
end if
if (i.eq.5) then
          KAP(i)=0.451454+0.173416/LI(i)-0.01462/LI(i)**2
c           write (2,*) ' kap5' ,kap(i)
end if
if (i.eq.6) then
          KAP(i)=0.328090+0.199939/LI(i)-0.01636/LI(i)**2
c           write (2,*) ' kap6' ,kap(i)
end if
if (i.eq.7) then
          KAP(i)=0.322181+0.125204/LI(i)-0.00280/LI(i)**2
c           write (2,*) ' kap7' ,kap(i)
end if
if (i.eq.8) then
          KAP(i)=0.120909+0.170560/LI(i)-0.01196/LI(i)**2
c           write (2,*) ' kap8' ,kap(i)
end if
          END IF
C
C     FOR 4-BLADE PROPELLER
          IF (NB.EQ.4) THEN
C
if (i.eq.1) then
          KAP(i)=1.636636-0.22760/LI(i)+0.020303/LI(i)**2
C           WRITE (2,*) ' KAP41' ,KAP(i)
end if
if (i.eq.2) then
          KAP(i)=1.23500-0.09904/LI(i)+0.009545/LI(i)**2
C           WRITE (2,*) ' KAP42' ,KAP(i)
end if
if (i.eq.3) then
          KAP(i)=0.989018-0.01158/LI(i)+0.001621/LI(i)**2
C           WRITE (2,*) ' KAP43' ,KAP(i)
end if
if (i.eq.4) then
          KAP(i)=0.783254+0.072421/LI(i)-0.00657/LI(i)**2
C           WRITE (2,*) ' KAP44' ,KAP(i)
```

```
end if
if (i.eq.5) then
        KAP(i)=0.596545+0.158530/LI(i)-0.01590/LI(i)**2
C         WRITE (2,*) ' KAP45' ,KAP(i)
end if
if (i.eq.6) then
        KAP(i)=0.464145+0.180266/LI(i)-0.01507/LI(i)**2
C         WRITE (2,*) ' KAP46' ,KAP(i)
end if
if (i.eq.7) then
        KAP(i)=0.34000+0.19159/LI(i)-0.01507/LI(i)**2
C         WRITE (2,*) ' KAP47' ,KAP(i)
end if
if (i.eq.8) then
        KAP(i)=0.193363+0.176348/LI(i)-0.01287/LI(i)**2
C         WRITE (2,*) ' KAP48' ,KAP(i)
end if
        END IF
C
C    FOR 5-BLADE PROPELLER
        IF (NB.EQ.5) THEN
C
if (i.eq.1) then
        KAP(i)=1.516454-0.19037/LI(i)+0.017424/LI(i)**2
C         WRITE (2,*) ' KAP51' ,KAP(i)
end if
if (i.eq.2) then
        KAP(i)=1.226909-0.09890/LI(i)+0.010075/LI(i)**2
C         WRITE (2,*) ' KAP52' ,kAP(i)
end if
if (i.eq.3) then
        KAP(i)=1.052709-0.032000/LI(i)+0.003727/LI(i)**2
C         WRITE (2,*) ' KAP53' ,KAP(i)
end if
if (i.eq.4) then
        KAP(i)=0.874454+0.045765/LI(i)-0.00446/LI(i)**2
C         WRITE (2,*) ' KAP54' ,KAP(i)
end if
if (i.eq.5) then
        KAP(i)=0.724090+0.107507/LI(i)-0.01068/LI(i)**2
C         WRITE (2,*) ' KAP55' ,KAP(i)
end if
if (i.eq.6) then
        KAP(i)=0.560636+0.177227/LI(i)-0.01803/LI(i)**2
C         WRITE (2,*) ' KAP56' ,KAP(i)
end if
if (i.eq.7) then
        KAP(i)=0.425818+0.183272/LI(i)-0.01575/LI(i)**2
C         WRITE (2,*) ' KAP57' ,KAP(i)
end if
if (i.eq.8) then
        KAP(i)=0.261454+0.175242/LI(i)-0.013030/LI(i)**2
C         WRITE (2,*) ' KAP58' ,KAP(i)
end if
        END IF
C
```

```
C     FOR 6-BLADE PROPELLER
        IF (NB.EQ.6) THEN
C
if (i.eq.1) then
        KAP(i)=1.408727-0.15297/LI(i)+0.014166/LI(i)**2
C         WRITE (2,*) ' KAP61' ,KAP(i)
end if
if (i.eq.2) then
        KAP(i)=1.223818-0.09912/LI(i)+0.010227/LI(i)**2
C         WRITE (2,*) ' KAP62' ,KAP(i)
end if
if (i.eq.3) then
        KAP(i)=1.070363-0.03761/LI(i)+0.004166/LI(i)**2
C         WRITE (2,*) ' KAP63' ,KAP(i)
end if
if (i.eq.4) then
        KAP(i)=0.952527+0.008606/LI(i)-0.00032/LI(i)**2
C         WRITE (2,*) ' KAP64' ,KAP(i)
end if
if (i.eq.5) then
        KAP(i)=0.82800+0.064037/LI(i)-0.00628/LI(i)**2
C         WRITE (2,*) ' KAP65' ,KAP(i)
end if
if (i.eq.6) then
        KAP(i)=0.685545+0.119946/LI(i)-0.01174/LI(i)**2
C         WRITE (2,*) ' KAP66' ,KAP(i)
end if
if (i.eq.7) then
        KAP(i)=0.499818+0.175553/LI(i)-0.016280/LI(i)**2
C         WRITE (2,*) ' KAP67' ,KAP(i)
end if
if (i.eq.8) then
        KAP(i)=0.300454+0.182454/LI(i)-0.01030/LI(i)**2
C         WRITE (2,*) ' KAP68' ,KAP(i)
end if
        END IF
C
c DO 27 I=6,7
c         WRITE(2,*) ' KAP',I,' =',KAP(I)
c 27 CONTINUE
C         WRITE(2,*) ' FINISH SUBROUTINE GOLSTN1'
C         WRITe(2,*) ' '
        RETURN
        END
```

Appendix D

Stub shaft drawings

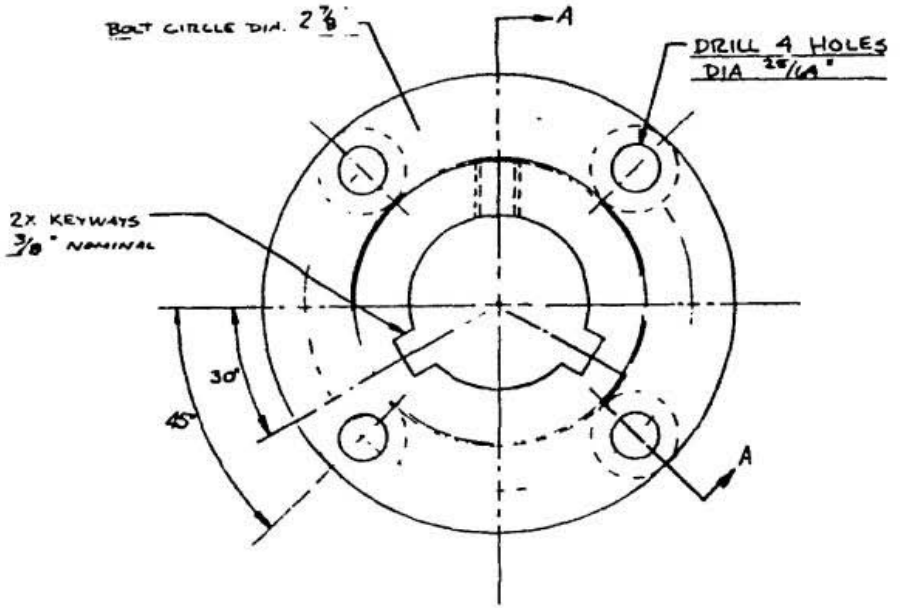

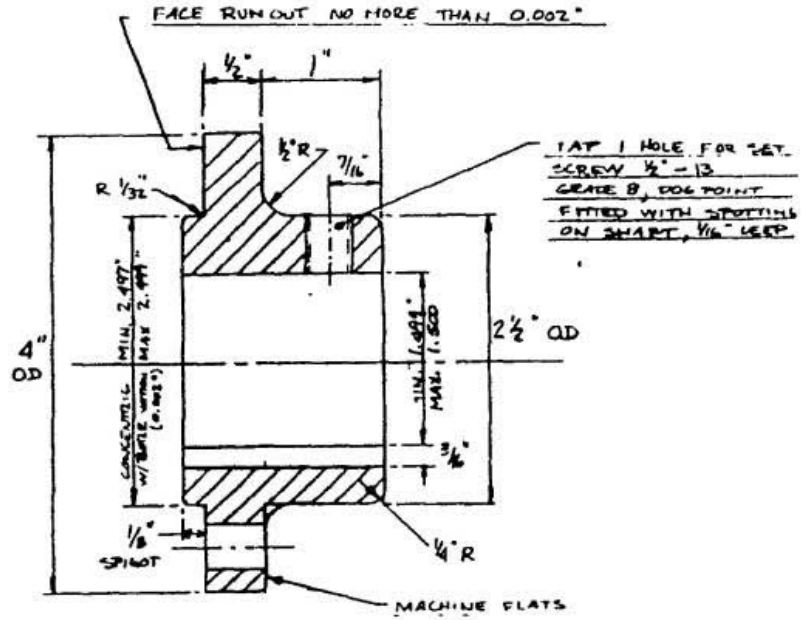

SECTION A-A

PART NUMBER : 2

1 ONLY : MATERIAL STEEL TO "ISO ER" SW-1

NOTE: PROPELLER SHAFT END TO BE FLUSH WITH SPIGOT FACE, END TO BE MACHINED TO SUIT COUPLING.

"MV SUGAR" PROPELLER SHAFT 1/2 COUPLING	FACULTY OF ENGINEERING MEMORIAL UNIVERSITY OF NEWFOUNDLAND	DATE MARCH 23, 74	SCALE

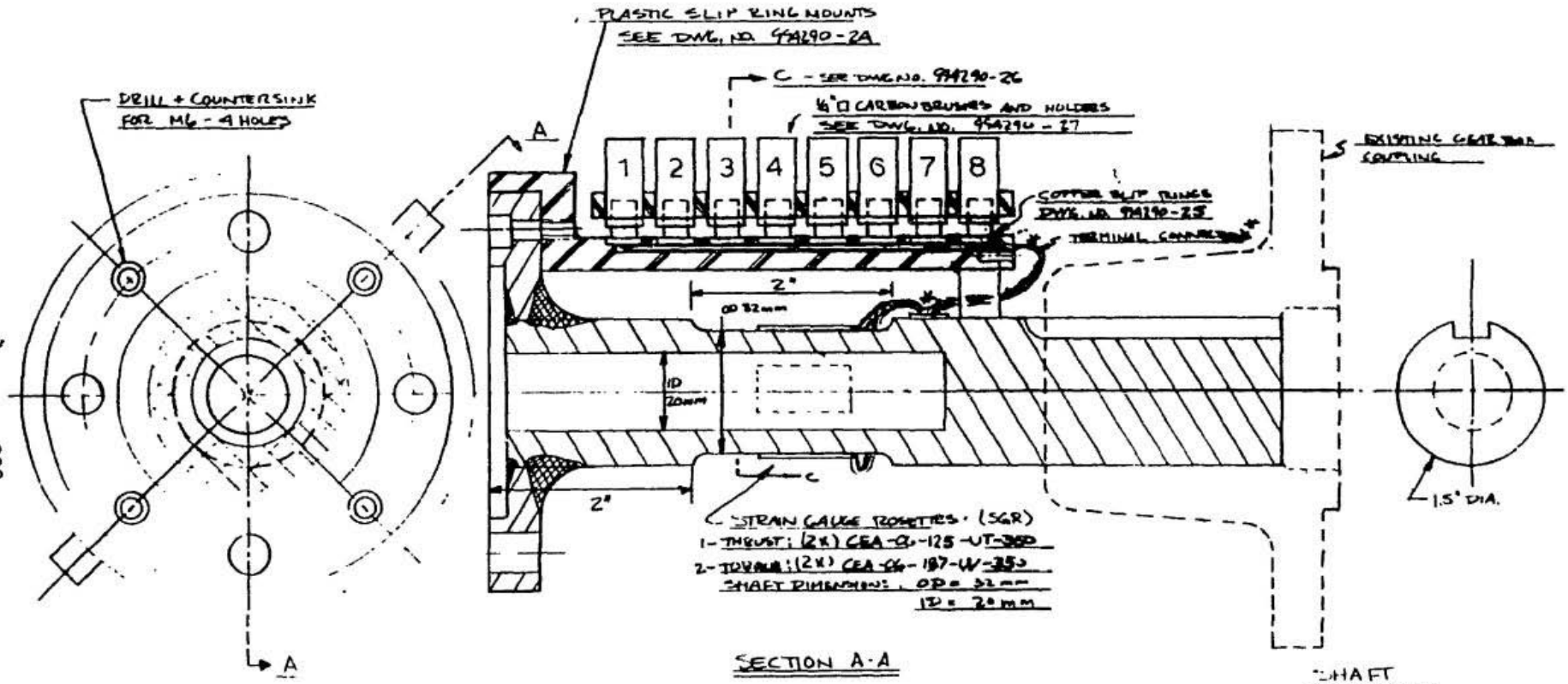

SECTION A-A

FOR MACHINING DETAILS OF SHAFT FLANGE, COUPLING FIT ETC. SEE STUB SHAFT DWG. NO. 994290-22

SHAFT

MATERIAL: 316 S/S

QUANTITY: 1- ONLY

INSTRUMENTED STUB SHAFT ARRANGEMENT	MEMORIAL UNIVERSITY OF NEWFOUNDLAND FACULTY OF ENGINEERING	DATE: APRIL 29, 91	SCALE: 1:1	DWG. NO. 994290-23

208

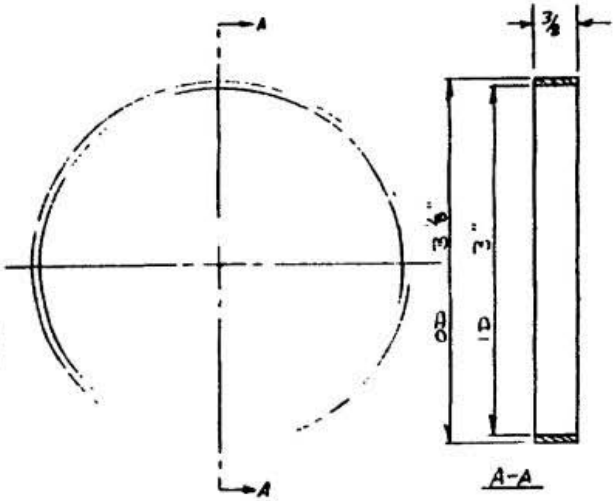

COPPER SLIP RINGS

8 - ONLY

CUT FROM 3" COPPER TUBE

MACHINE TRUE

"POLISH" OUTSIDE SURFACE

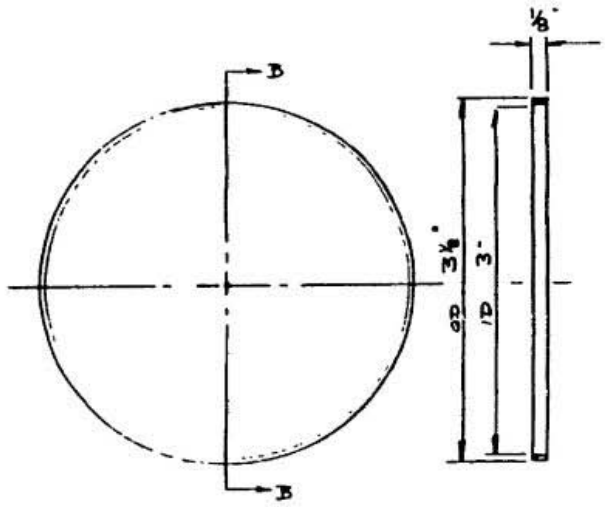

PLASTIC INSULATING RINGS

17 - ONLY

CUT FROM 1" PLASTIC PIPE

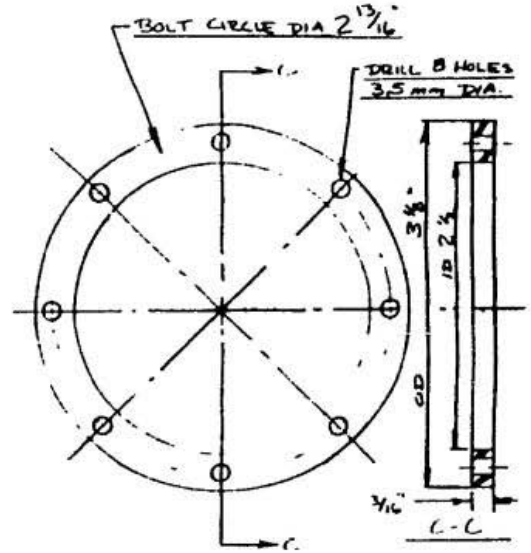

PLASTIC RETAINING RING

1 - ONLY

MACHINING DETAILS SLIP, INSULATING, RETAINING RINGS	MEMORIAL UNIVERSITY OF NEWFOUNDLAND FACULTY OF ENGINEERING	DATE: APRIL 29, '91	SCALE 1:1	[illegible] - 28

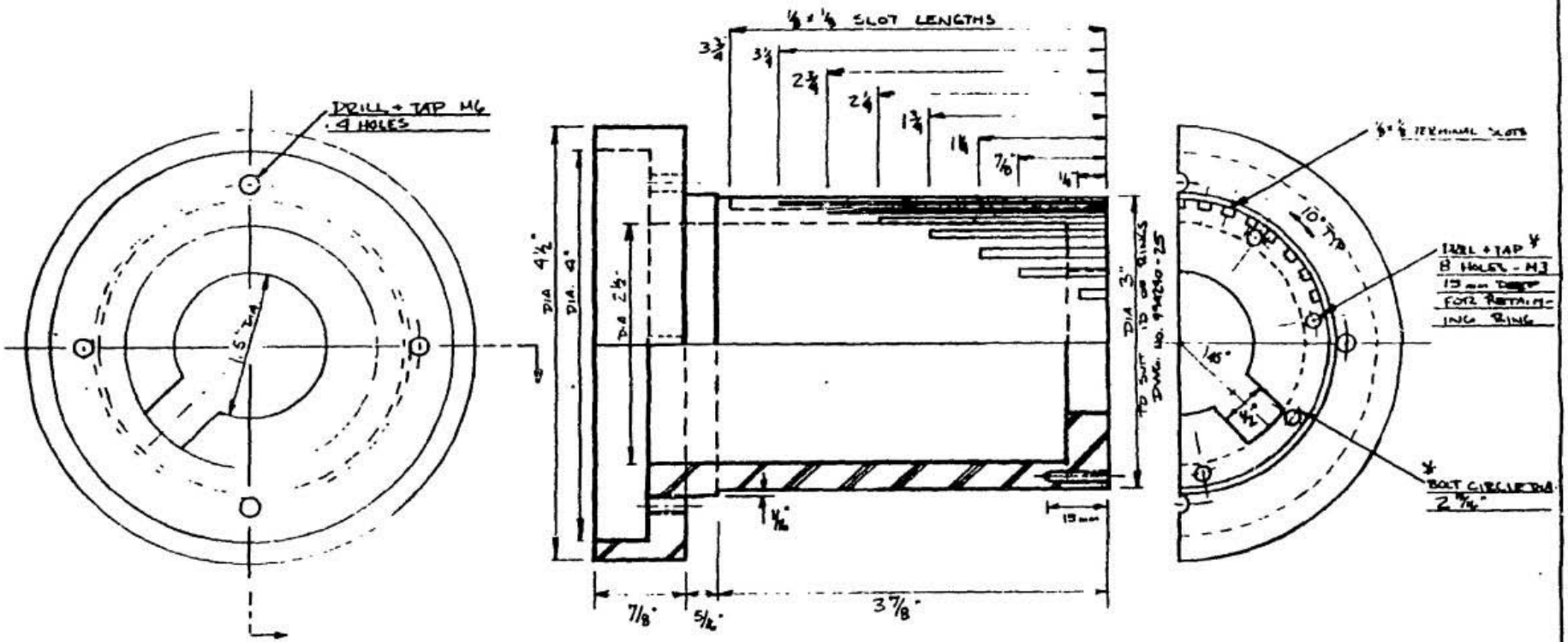

MATERIAL : PLASTIC
QUANTITY : 1- ONLY

MACHINING DETAILS SLIP RING MOUNTING SLEEVE	MEMORIAL UNIVERSITY OF NEWFOUNDLAND FACULTY OF ENGINEERING	DRN APRIL 29, '91	SCALE

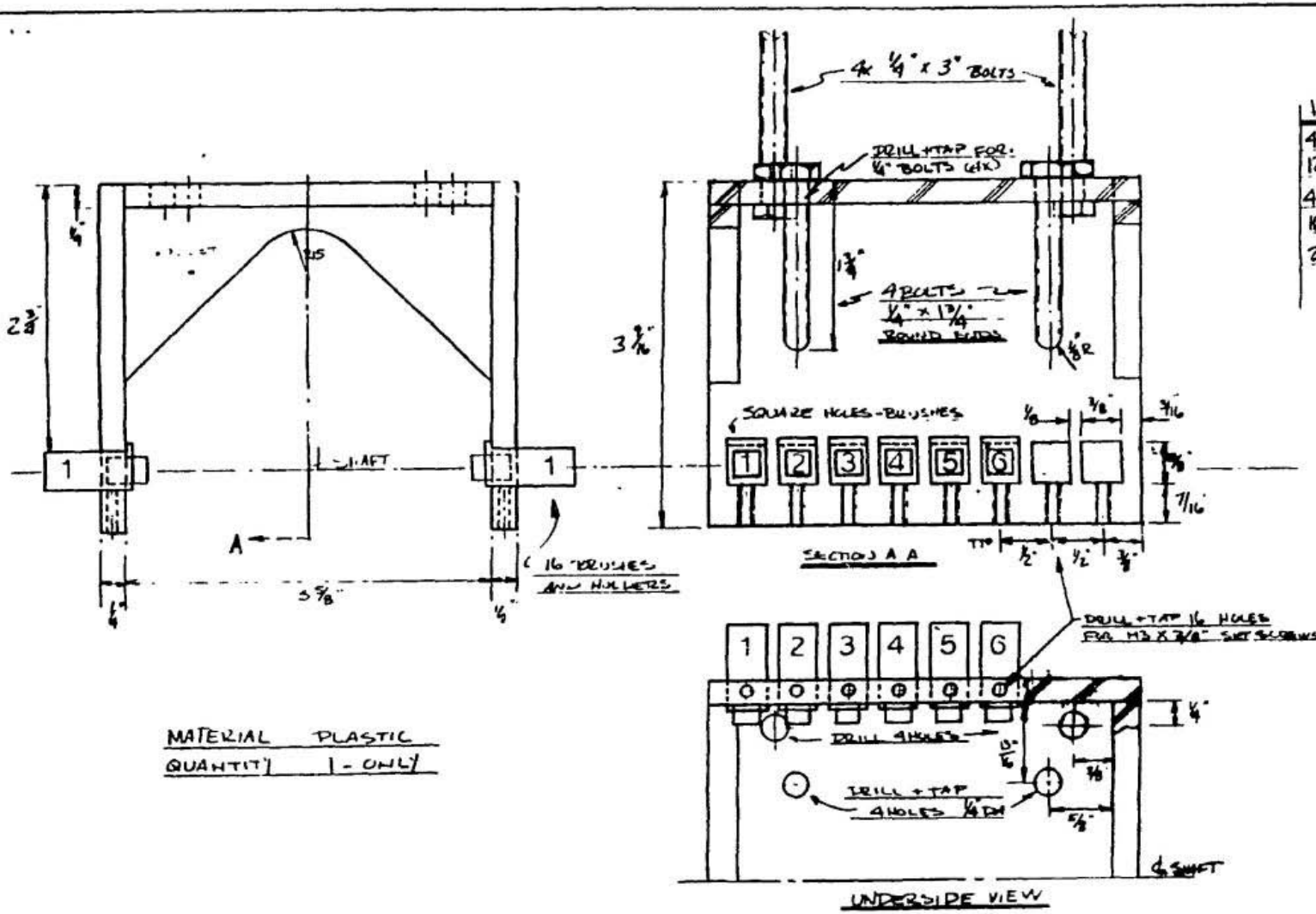

HARDWARE REQ'D:
4x 1/4" x 3" BOLTS
12x 1/4" NUTS
4x 1/4" x 1 3/4" BOLTS ROUND END
16x M3 x 10 SET SCREWS
2x ANGLE BAR
1 x 1 x 3/16 OA x 36"

INSTRUMENTED STUB SHAFT BRUSH HOLDER ASSEMBLY	MEMORIAL UNIVERSITY OF NEWFOUNDLAND FACULTY OF ENGINEERING	MAY 1, 1991	111

211

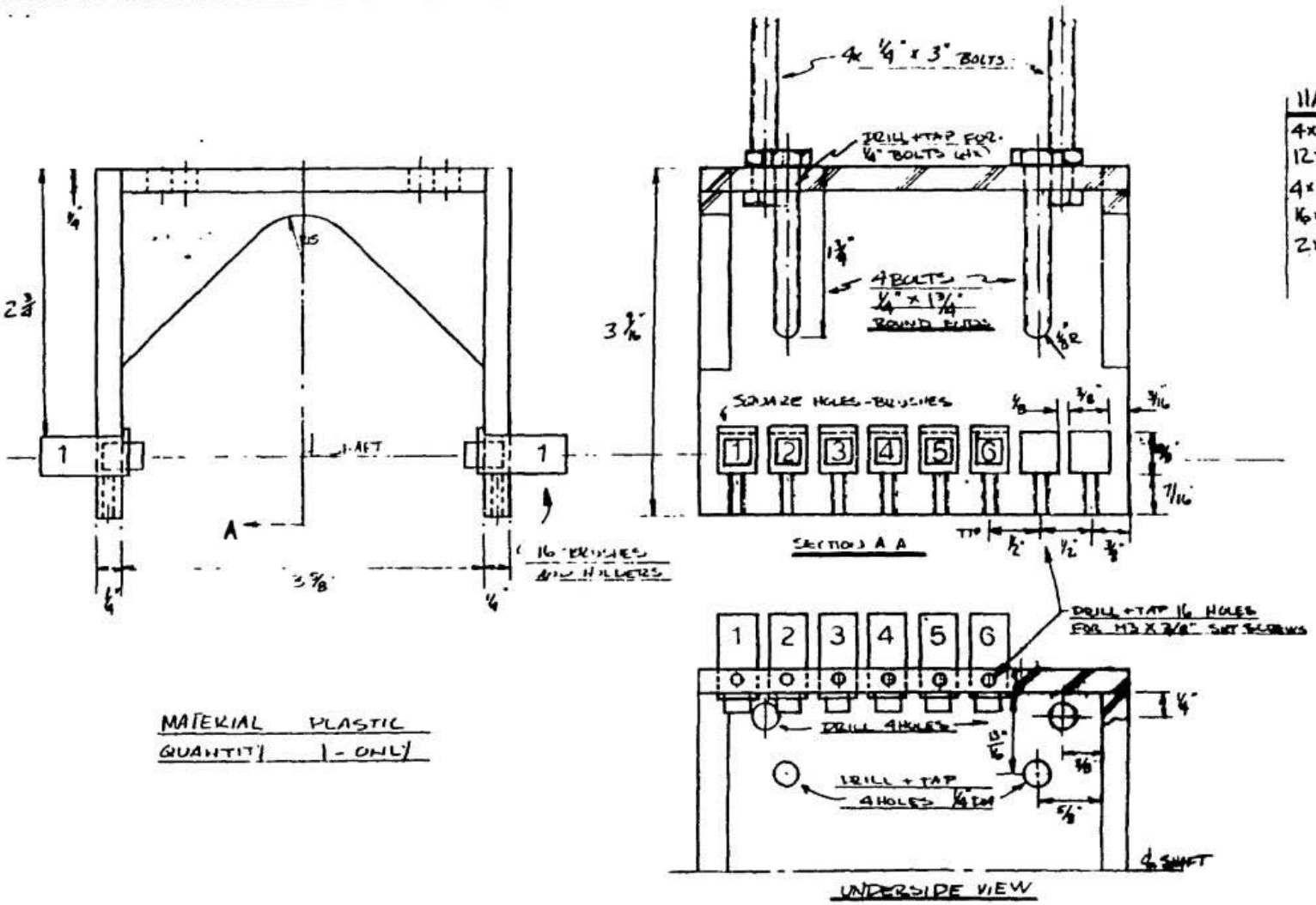

HARDWARE REQ'D:
4x 1/4" x 3" BOLTS
12x 1/4" NUTS
4x 1/4" x 1 3/4" BOLTS ROUND END
16x M3 x 10 SET SCREWS
2x ANGLE BAR 1 x 1 x 3/16 OA x 36"

MATERIAL PLASTIC

QUANTITY 1 - ONLY

INSTRUMENTED STUB SHAFT BRUSH HOLDER ASSEMBLY	MEMORIAL UNIVERSITY OF NEWFOUNDLAND FACULTY OF ENGINEERING	DATE MAY 1, 1991	SCALE: 1:1	DRAWN

212

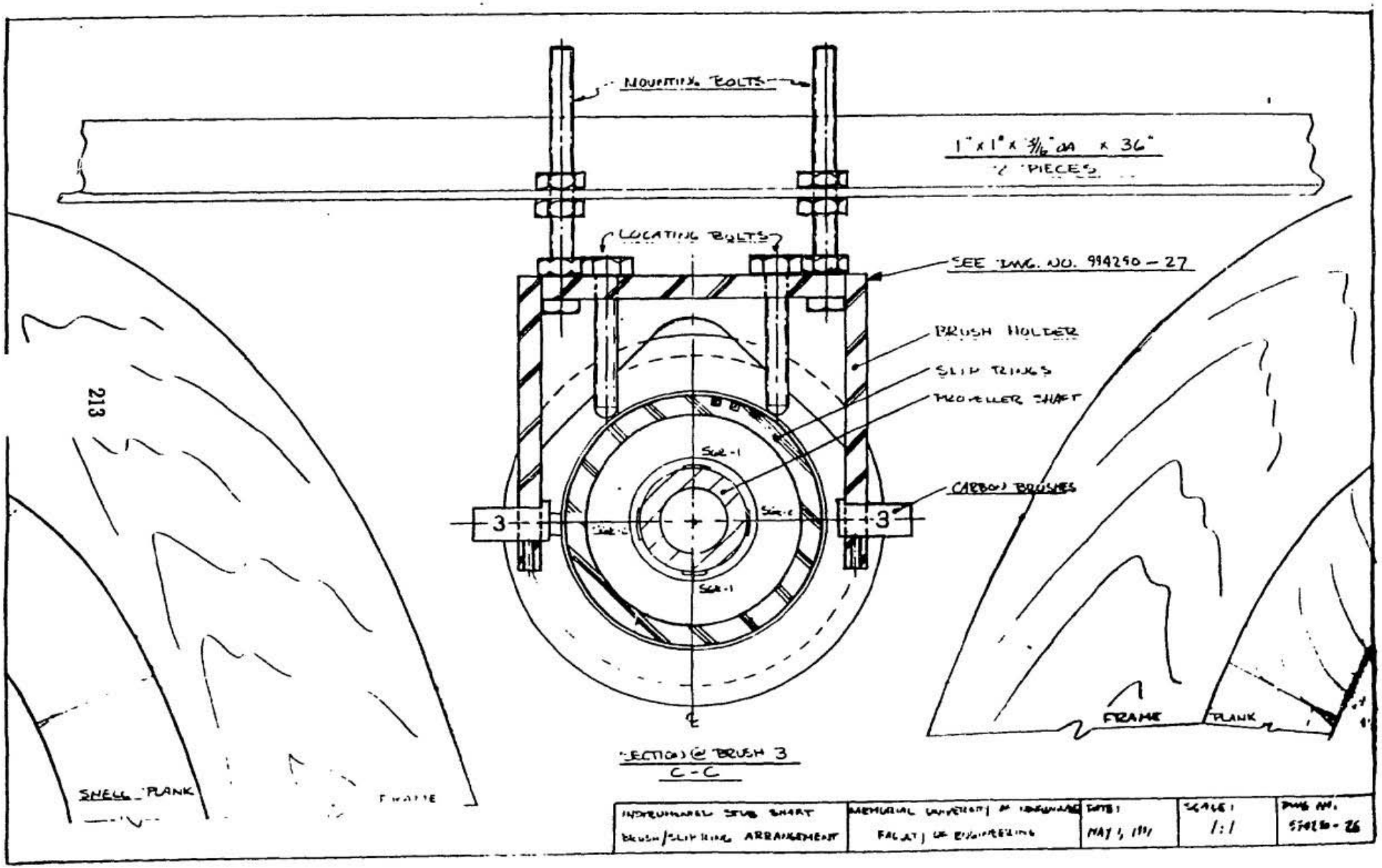

INSTRUMENTATION LAB SHAFT BRUSH/SLIP RING ARRANGEMENT	MEMORIAL UNIVERSITY OF NEWFOUNDLAND FACULTY OF ENGINEERING	DATE: MAY 1, 1991	SCALE: 1:1	DWG NO. 994250-26

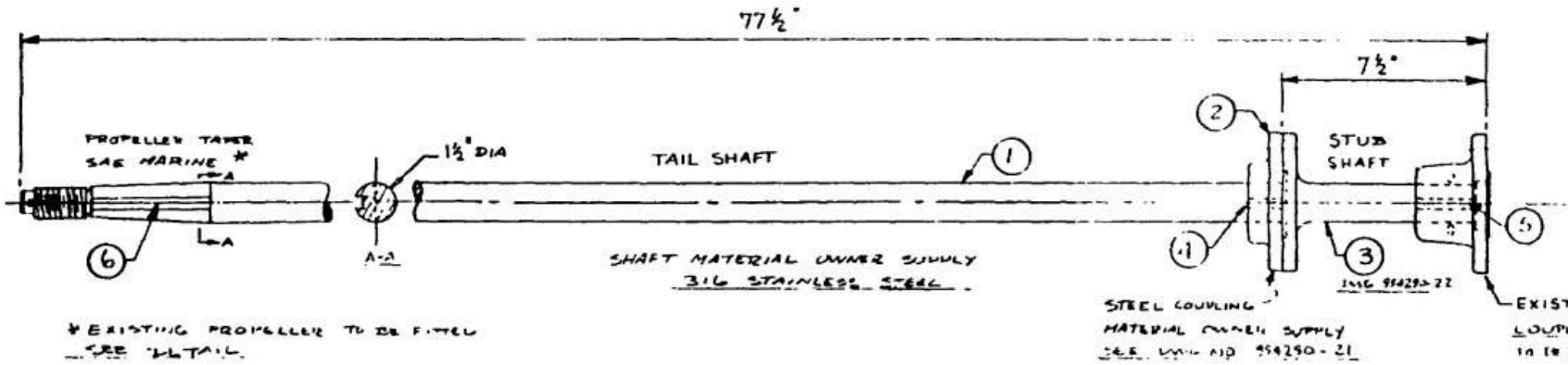

* EXISTING PROPELLER TO BE FITTED
SEE DETAIL

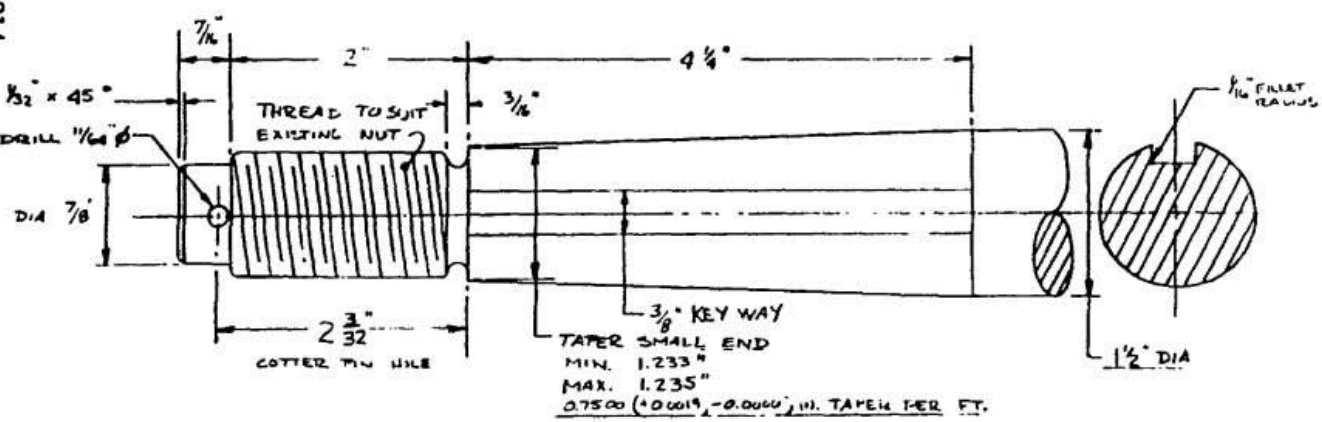

DETAIL: PROPELLER SHAFT TAPER

NO.	QTY	DESCRIPTION
1	1	TAILSHAFT 316 S/S
2	1	COUPLING STEEL
3	1	STUB SHAFT/FLANGE S/S
4	2	KEY 3/8 x 1¼" STEEL
5	1	KEY 3/8" x 1¾" STEEL
6	1	KEY 3/16" x 3½" MILAN.
7	1	COTTER PIN 1/32" x 1½" S/S
8	4	* FLANGE BOLTS 5/8"-24 x 1½"
9	1	* SET SCREW ½"-13, DOG PT

* GRADE 8 BOLTS.

"M.V. SUGAR" PROPELLER SHAFT ASSEMBLY	FACULTY OF ENGINEERING MEMORIAL UNIVERSITY OF NEWFOUNDLAND	DATE MARCH 27, 19	SCALE 3"=1'0 ; 1:1	DWG. NO. 99430

214

Appendix E

Description of vessels

Table E.1: Principal particulars of *MV SUGAR*

Property	*Description*
length overall	35'-1.375"
lenght waterline	33.33'
moulded bredth	10.92'
moulded draught	3.5'
displacment volume	200.53 ft^3
midship area	18.96'
waterplane area	150.76 ft^2
draught forward	3.25'
draught aft	3.25'
half angle of inflow	45 degrees
Powering:	
main engine	KUBOTA S2800-B
no. of cylinders	6 inline
four stroke	
horse power	45.5
RPM	2600 max.
reduction gear ratio	1.96:1
shaft rpm	1326.5
Propeller:	
no. of blades	3
diameter	22 in
' pitch	10 in
expanded blade area ratio	0.55
Afterbody details:	
height of shaft above baseline	1.917'
angle of shaft inclination	1.5 deg
skeg thickness	8 in
head of water above shaft centreline	17.5 in
Hull details:	
wetted surface area	272.22 ft^2
rudder area	10.0 ft^2
block coefficient	0.1571
prismatic coefficient	0.3171
midship area coefficient	0.4953
waterplane area coefficient	0.4141

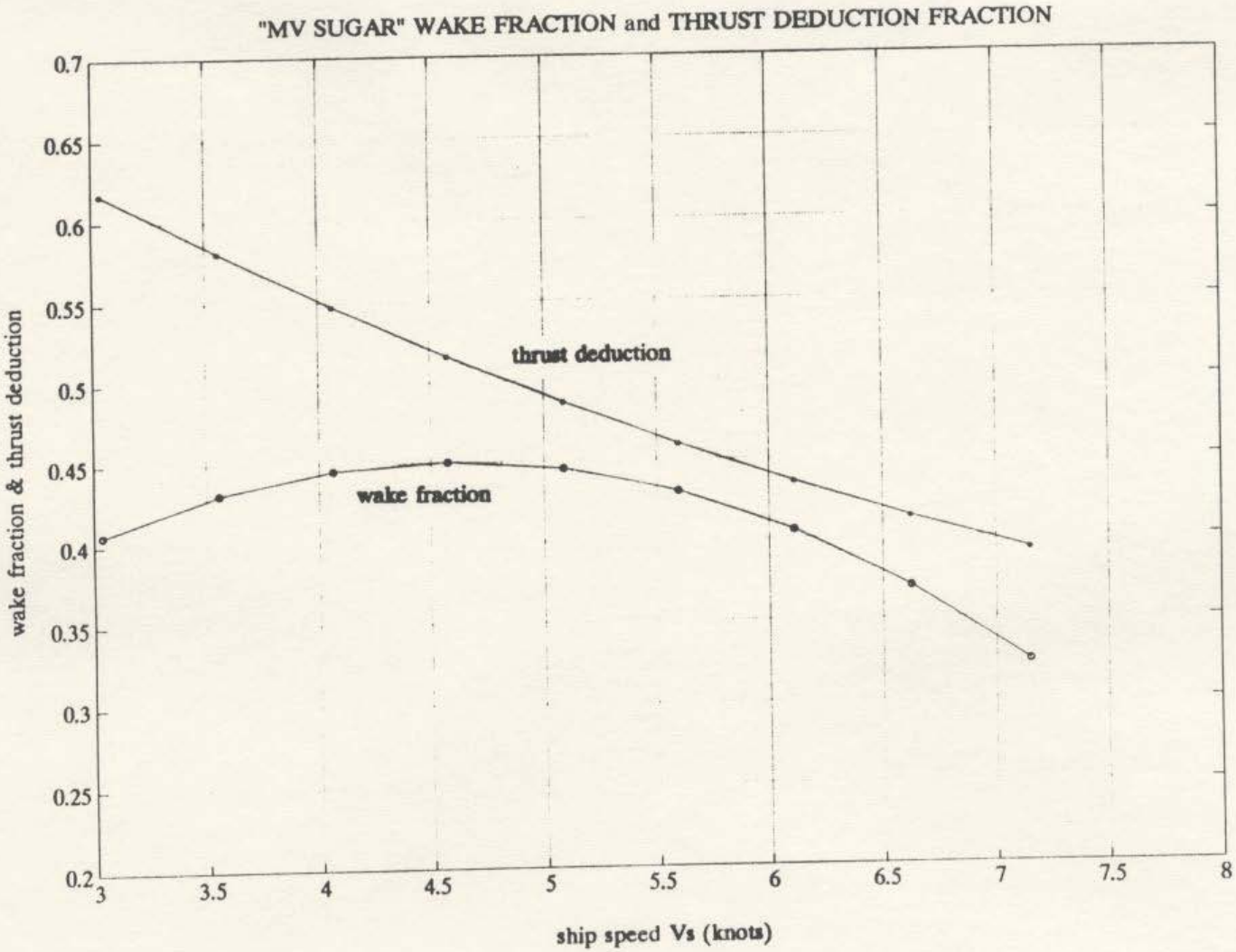
"MV SUGAR" WAKE FRACTION and THRUST DEDUCTION FRACTION
wake fraction & thrust deduction
ship speed Vs (knots)
thrust deduction
wake fraction
0.7
0.65
0.6
0.55
0.5
0.45
0.4
0.35
0.3
0.25
0.2
3
3.5
4
4.5
5
5.5
6
6.5
7
7.5
8

Table E.2: Principal particulars of *MV BECKY A.*

Property	Description
length overall	35'-0"
moulded bredth	12'-0"
moulded draught	4'6"
cargo capacity	25,000 lbs
draught forward	4'-0"'
draught aft	5'-0"
material	wood
builder	Henry Vokey, Trinity, Newfoundland
Powering:	
main engine	Ford Senator model 254
no. of cylinders	4 inline
four stroke	
horse power	80 hp
RPM	2500 max.
reduction gear ratio	2:1
shaft rpm	1250
Propeller:	
no. of blades	3
diameter	20 in
' pitch	16 in
expanded blade area ratio	n/a

Appendix F

Existing propeller data

Table F.1: Existing propeller section characteristics: *MV SUGAR.*

R	c/D	t/D	m/c	P/D
0.3	0.0960	0.103	0.0540	0.624
0.4	0.0850	0.073	0.0430	0.570
0.5	0.0738	0.051	0.0340	0.495
0.6	0.0628	0.038	0.0300	0.470
0.7	0.0518	0.029	0.0276	0.447
0.8	0.0407	0.022	0.0265	0.443
0.9	0.0285	0.016	0.0280	0.410

The following pages contain the blade section outlines drawn from measurements of the existing propeller.

0.3 R (D = 165)

pitch angle (θ) : 33.5°
chord length (C): 158.5
max. thickness (T): 17
camber (M): 8.5

P/D = 0.624
C/D = 0.960
T/D = 0.103
M/C = 0.054

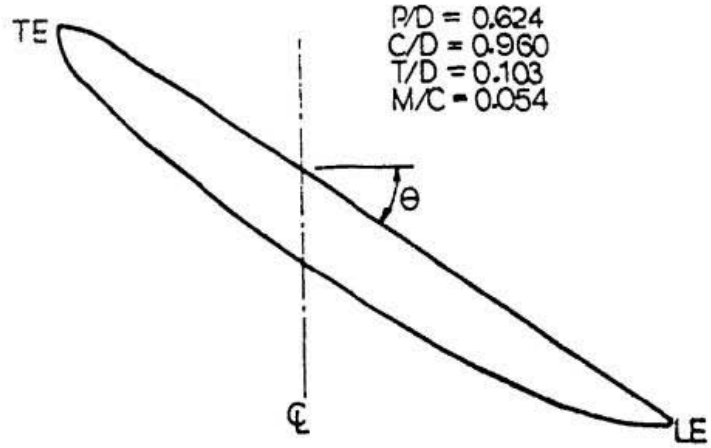

0.4 R (D=220)

pitch angle (θ): 24.4°
chord length (C): 187
max. thickness (T): 16
camber (M): 8

P/D = 0.570
C/D = 0.850
T/D = 0.073
M/C = 0.043

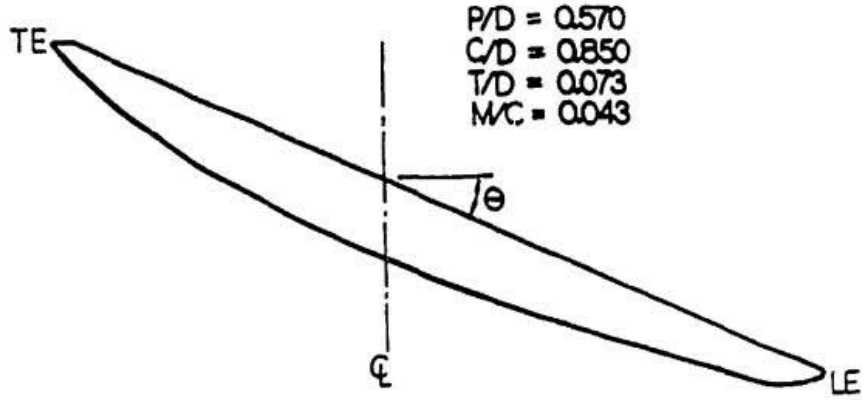

0.5 R (D=275)

pitch angle (θ): 17.5°
chord length (C): 203
max thickness (T): 14
camber (M): 7

P/D = 0.495
C/D = 0.738
T/D = 0.051
M/C = 0.039

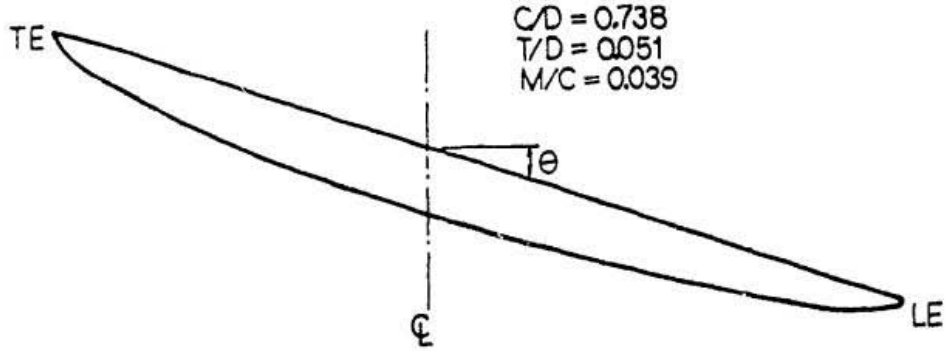

0.6 R (D=330)

pitch angle (θ): 14°
chord length (C): 207.5
max. thickness (T): 12.5
camber (M): 6.25

P/D = 0.470
C/D = 0.628
T/D = 0.038
M/C = 0.030

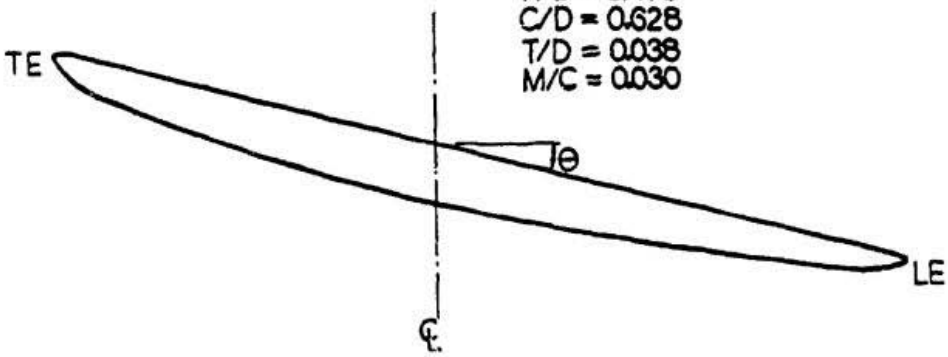

0.7 R (D=385)

pitch angle (Θ): 11.5°
chord length (C): 199.5
max thickness (T): 11
camber (M): 5.5

P/D=0.447
C/D = 0.518
T/D = 0.029
M/C = 0.028

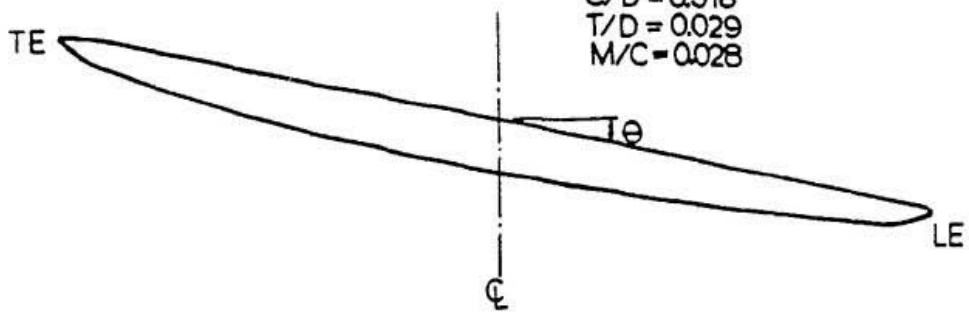

0.8 R (D=440)

pitch angle (Θ): 10°
chord length (C): 179
max thickness (T): 9.5
camber (M): 4.75

P/D = 0.443
C/D = 0.407
T/D = 0.022
M/C = 0.027

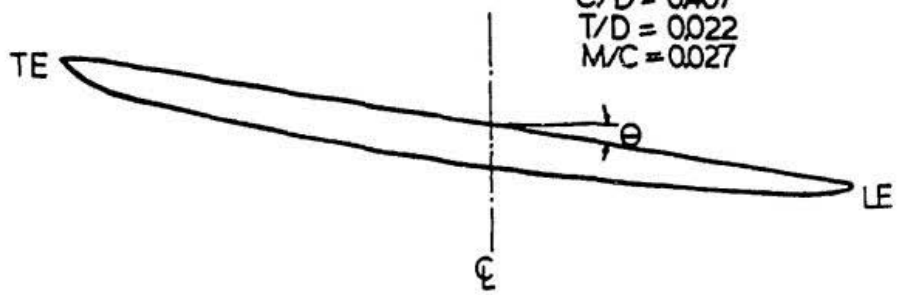

0.9R (D=495)

pitch angle (θ): 8.25°
chord length (C): 141
max thickness (T): 8
camber (M): 4

P/D = 0.410
C/D = 0.285
T/D = 0.016
M/C = 0.028

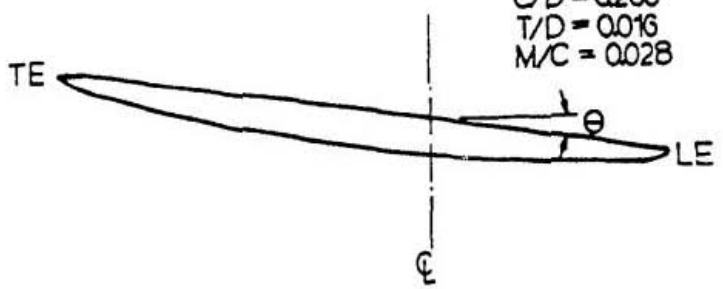

Appendix G

Assembly drawing strickle gear

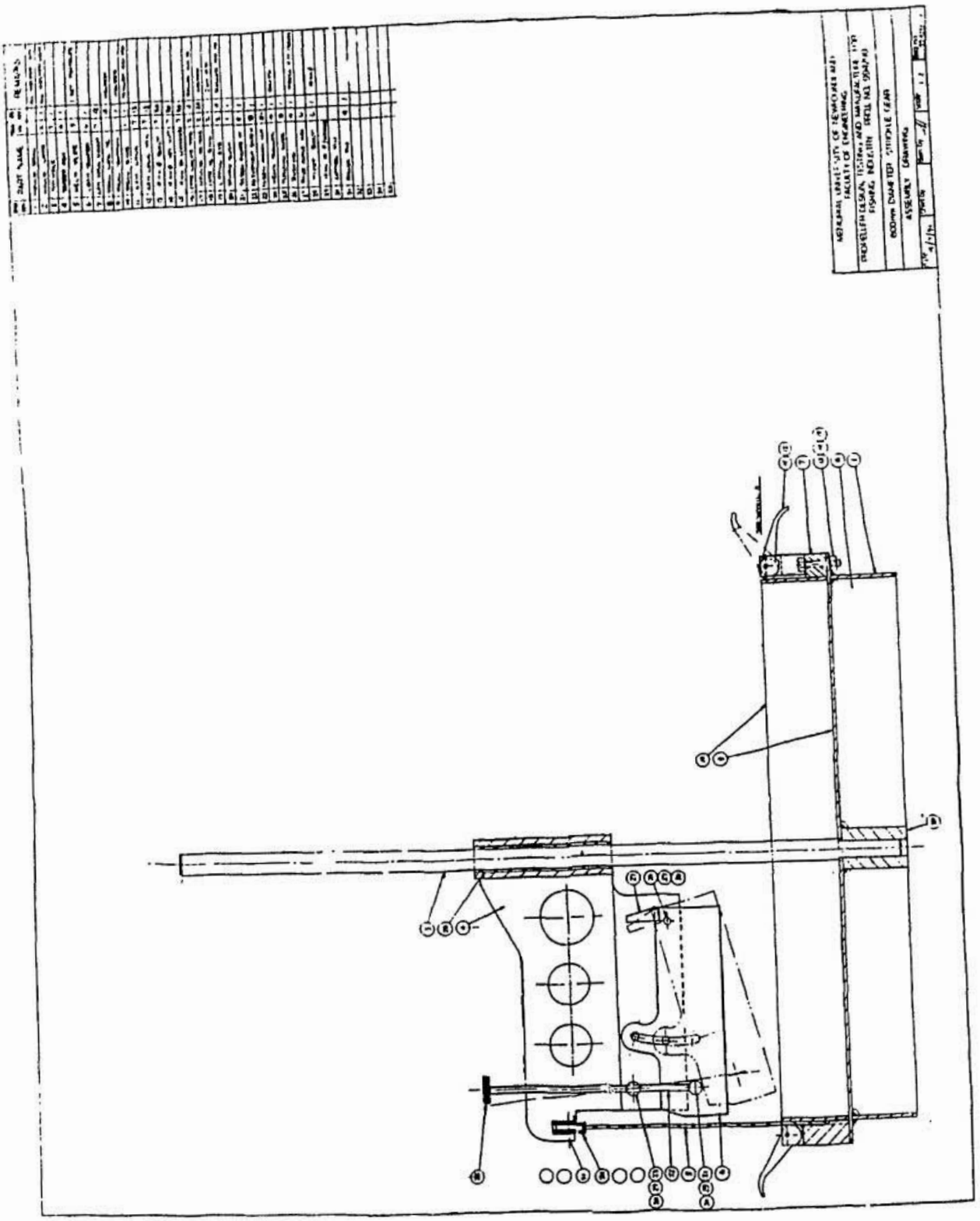

Appendix H

B-series propeller analysis results

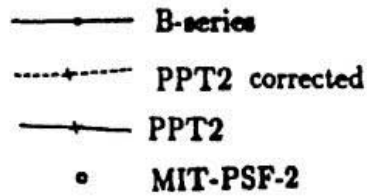

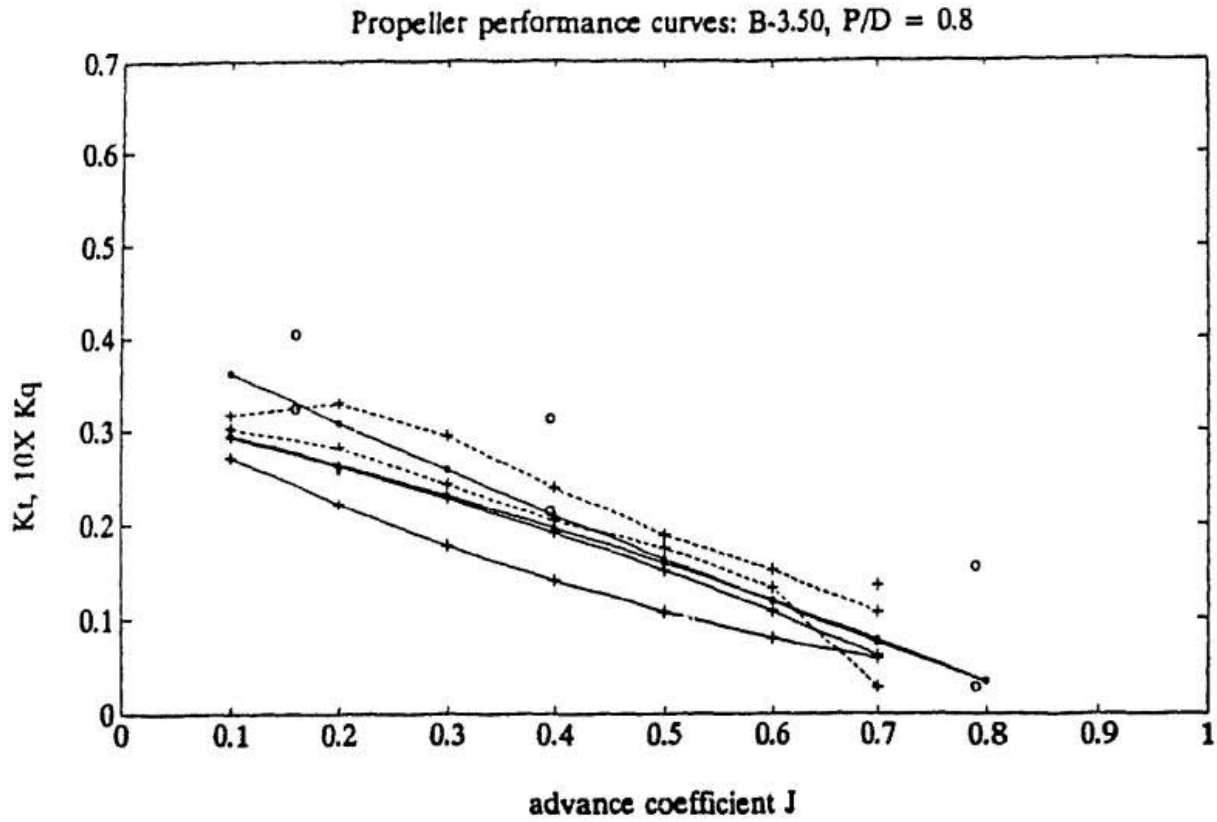
Propeller performance curves: B-3.50, P/D = 0.8
Kt, 10X Kq
advance coefficient J
0
0.1
0.2
0.3
0.4
0.5
0.6
0.7
0.8
0.9
1

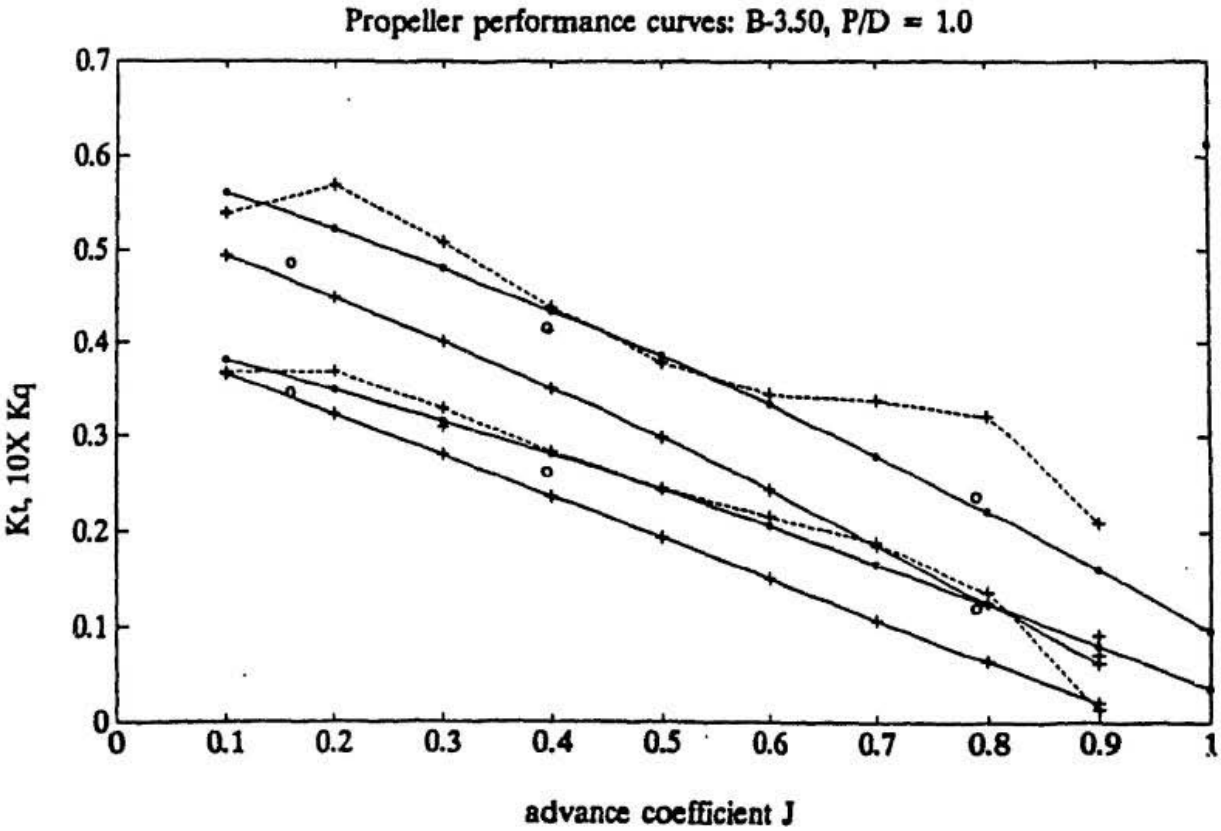
Propeller performance curves: B-3.50, P/D = 1.0
Kt, 10X Kq
advance coefficient J
0
0.1
0.2
0.3
0.4
0.5
0.6
0.7
0.8
0.9
1

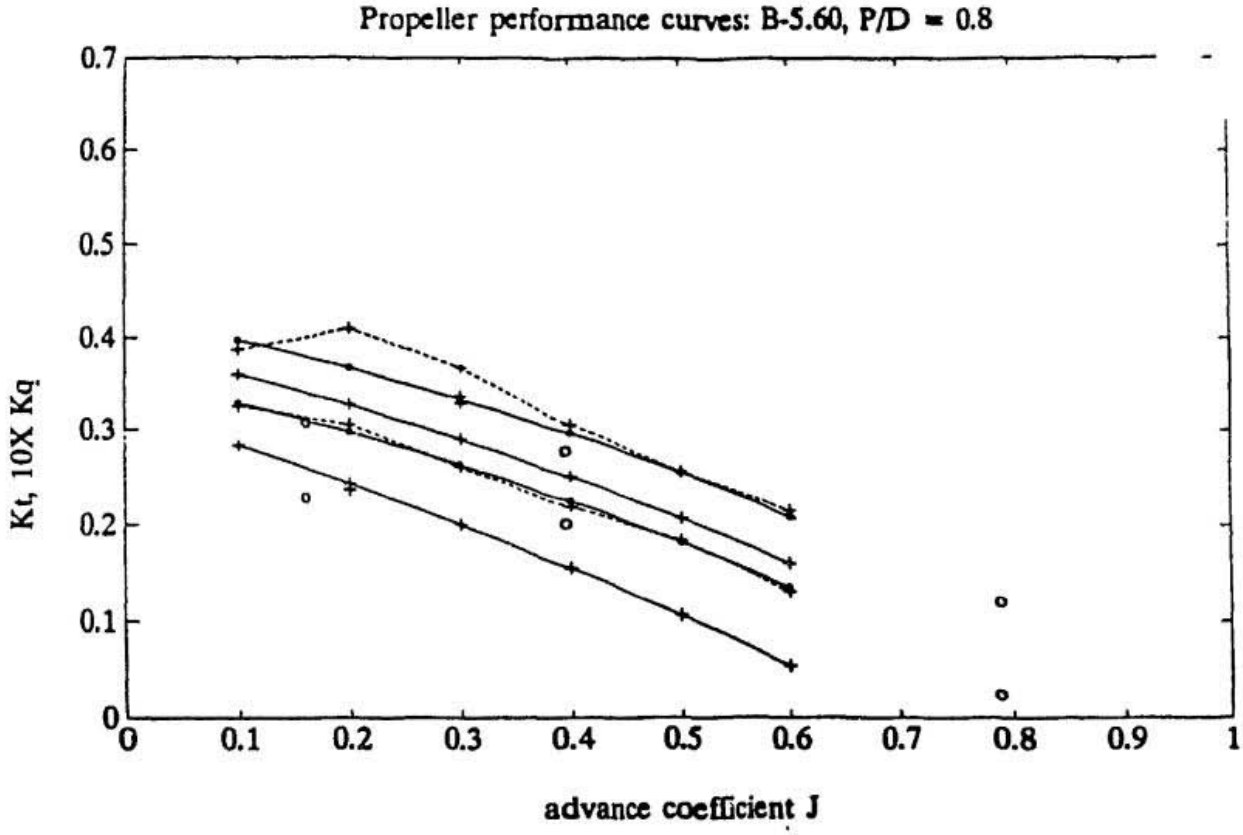
Propeller performance curves: B-5.60, P/D = 0.8
Kt, 10X Kq
advance coefficient J
0
0.1
0.2
0.3
0.4
0.5
0.6
0.7
0.8
0.9
1

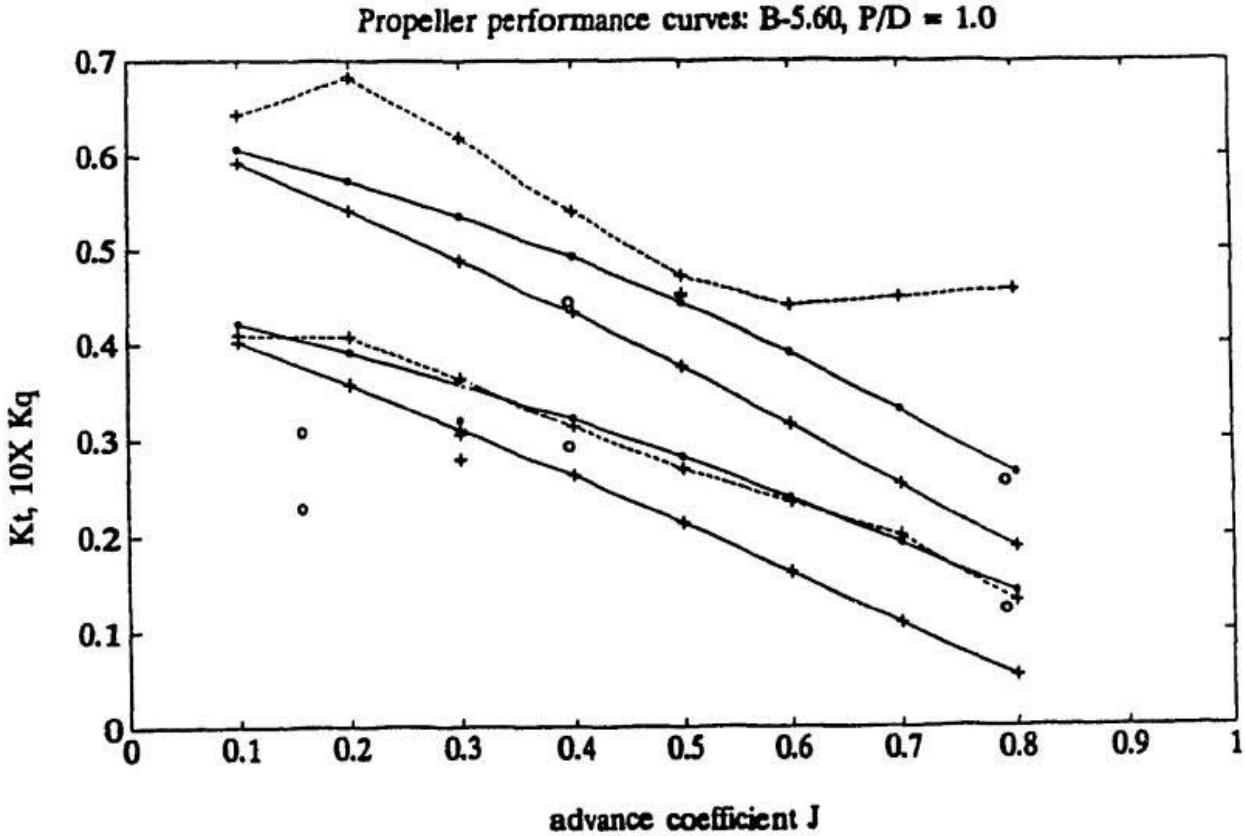
Propeller performance curves: B-5.60, P/D = 1.0
Kt, 10X Kq
advance coefficient J
0
0.1
0.2
0.3
0.4
0.5
0.6
0.7
0.8
0.9
1

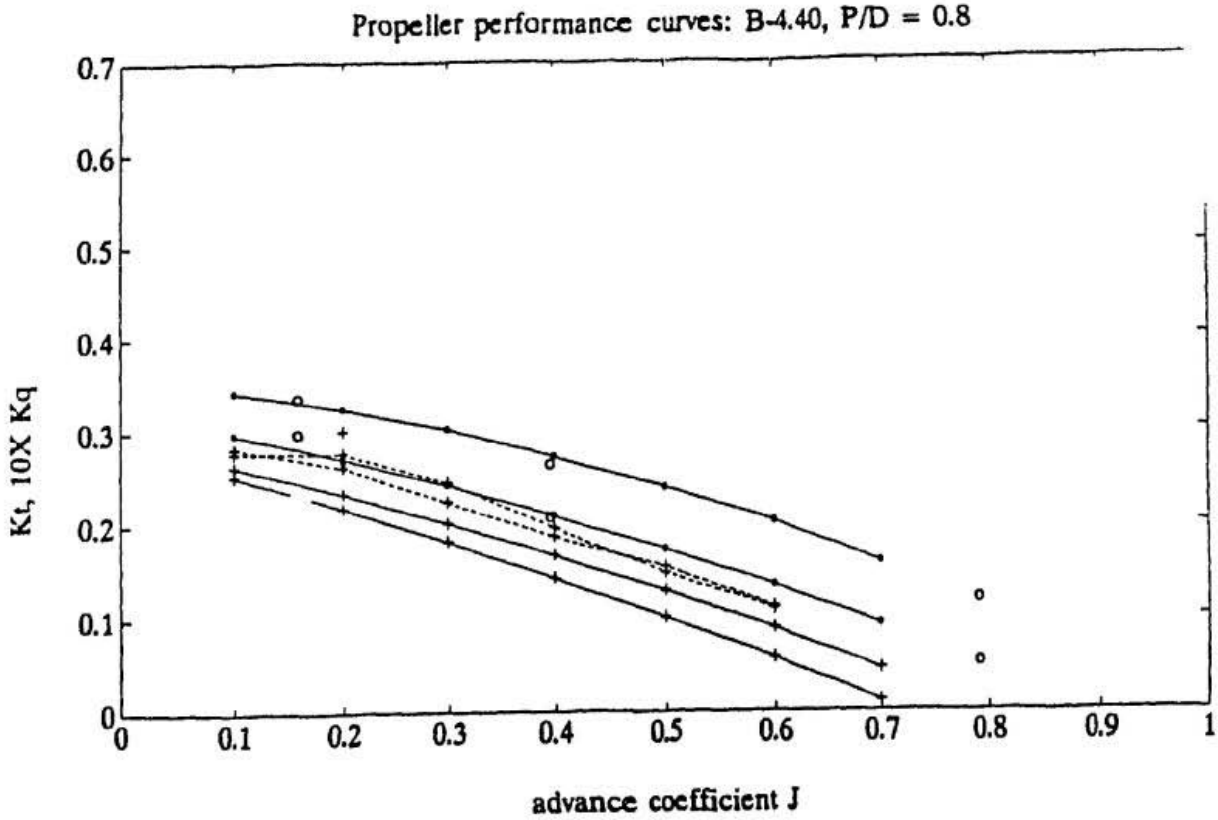
Propeller performance curves: B-4.40, P/D = 0.8
Kt, 10X Kq
advance coefficient J
0
0.1
0.2
0.3
0.4
0.5
0.6
0.7
0.8
0.9
1

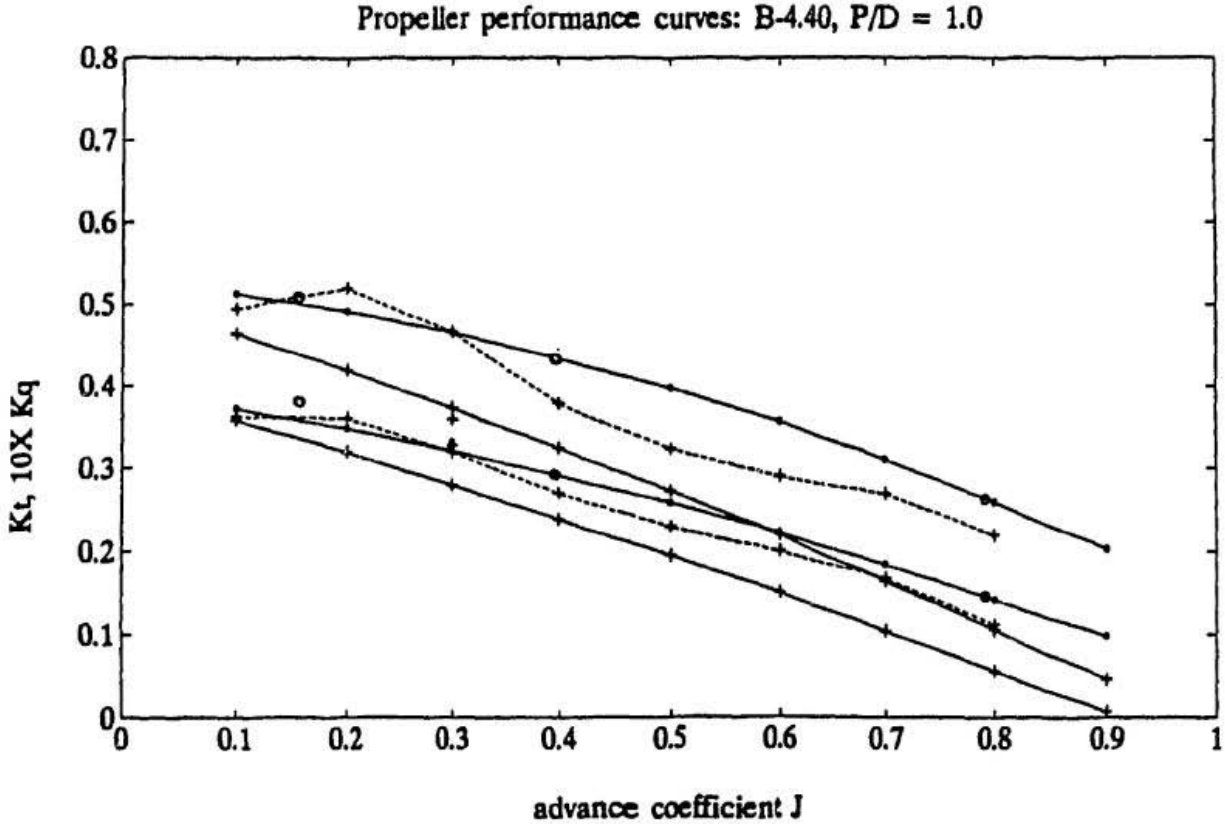
Propeller performance curves: B-4.40, P/D = 1.0
Kt, 10X Kq
advance coefficient J
0
0.1
0.2
0.3
0.4
0.5
0.6
0.7
0.8
0.9
1